1983

The Theory and Synthesis of [2.2.2] Propellane

Theodore Mark Prociv
The Graduate Center, City University of New York

INFORMATION TO USERS

This reproduction was made from a copy of a document sent to us for microfilming. While the most advanced technology has been used to photograph and reproduce this document, the quality of the reproduction is heavily dependent upon the quality of the material submitted.

The following explanation of techniques is provided to help clarify markings or notations which may appear on this reproduction.

1. The sign or "target" for pages apparently lacking from the document photographed is "Missing Page(s)". If it was possible to obtain the missing page(s) or section, they are spliced into the film along with adjacent pages. This may have necessitated cutting through an image and duplicating adjacent pages to assure complete continuity.

2. When an image on the film is obliterated with a round black mark, it is an indication of either blurred copy because of movement during exposure, duplicate copy, or copyrighted materials that should not have been filmed. For blurred pages, a good image of the page can be found in the adjacent frame. If copyrighted materials were deleted, a target note will appear listing the pages in the adjacent frame.

3. When a map, drawing or chart, etc., is part of the material being photographed, a definite method of "sectioning" the material has been followed. It is customary to begin filming at the upper left hand corner of a large sheet and to continue from left to right in equal sections with small overlaps. If necessary, sectioning is continued again—beginning below the first row and continuing on until complete.

4. For illustrations that cannot be satisfactorily reproduced by xerographic means, photographic prints can be purchased at additional cost and inserted into your xerographic copy. These prints are available upon request from the Dissertations Customer Services Department.

5. Some pages in any document may have indistinct print. In all cases the best available copy has been filmed.

University Microfilms International
300 N. Zeeb Road
Ann Arbor, MI 48106

Prociv, Theodore Mark

THE THEORY AND SYNTHESIS OF (2.2.2) PROPELLANE

City University of New York PH.D. 1983

THE THEORY AND SYNTHESIS OF [2.2.2] PROPELLANE

BY

THEODORE M. PROCIV

A dissertation submitted to the Graduate Faculty in Chemistry in partial fulfillment of the requirements for the degree of Doctor of Philosophy, The City University of New York.

1982

This manuscript has been read and accepted for the Graduate Faculty in Chemistry in satisfaction of the dissertation requirement for the degree of Doctor of Philosophy.

[Signature]

20 Dec 1982
date

Chairman of Examining Committee

[Signature]

20 December 1982
date

Executive Officer

[Signature]

[Signature]

Supervisory Committee

The City University of New York

Abstract

THE THEORY AND SYNTHESIS OF [2.2.2] PROPELLANE

by

Theodore M. Prociv

Advisor: Professor Joseph J. Dannenberg

INDO calculations indicated that the triplet state of dimethylene cyclohexane could rearrange to gometrically relaxed triplets which should collapse preferentially to the ground state [2.2.2] Propellane. A mercury sensitized photolysis of the dimethylene cyclohexane did in fact result in detectable quantities of the propellane, trapped as 1,4 dibromobicyclo octane. Synthesis of 1,4 dibromobicyclo octane and 1,1,6,6 tetradeuterodimethylene-cyclohexane are presented in the dissertation. Included in the dissertation are the results of INDO calculations of various propellane isomers having nitrogens and borons in the bridgehead positions.

TABLE OF CONTENTS

TABLE OF CONTENTS
(Continued)

TABLE OF CONTENTS
(Continued)

LIST OF FIGURES

Page

LIST OF FIGURES

LIST OF FIGURES
(Continued)

LIST OF FIGURES
(Continued)

LIST OF TABLES

LIST OF TABLES

LIST OF TABLES
(Continued)

CHAPTER I

THEORETICAL APPROACH TO THE SYNTHESIS OF [2.2.2] PROPELLANE

Introduction

Many organic chemists today use molecular orbital (MO) theory as an additional tool in their arsenal of chemical verification methods. The experimental chemist will often use the theory to validate a reaction mechanism or structure and often include his calculations in a theoretical section of a publication as supporting evidence for his postuation. The theoreticians actively pursue new, improved methods of calculation which yield a better correlation with empirical data. Two different types of efforts are evident in the literature:

- To make theory fit experimental data more accurately, or
- To make a calculation less time consuming thus less costly.

In both cases, the goal is correlation of experimental and theoretical information.

Literature reflects a good fit between the empirical and theoretical models proposed. The methods have been improved to a level of sophistication where scientists can have confidence in the calculation. The question then can be posed, "Can these theoretical methods be used to predict the reactions and/or structures prior to laboratory experimentation?" It would be a tremendous advantage for an experimentalist to use the various calculations available as a "test tube", that is an experimental system where selected geometries can be introduced into his "test tube", mixed, and the emerging

energy values and optimized structures would have a utility in predicting an experiment related to the calculated molecules.

In this thesis, we have taken one case of an experimental system which has proven extremely challenging to the synthetic and mechanistic chemists and have treated that system with a semiempirical MO calculation. We have then interpreted the results of the calculation in light of predicting a reaction synthesis pathway and performed the suggested experiment in the laboratory.

The particular molecular system chosen for this study has been the source of various recent controversies dealing with the existence of compounds having an unusually strained structure described by 1. Throughout this study particular attention is devoted to a single member of this group, the symmetrical [2.2.2]propellane, 2.[1-4] This highly strained, tricyclic molecule

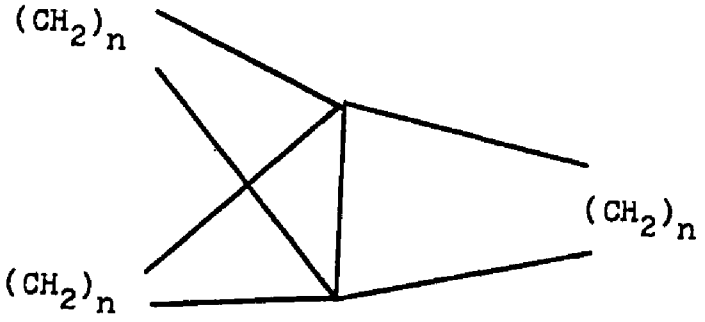

1

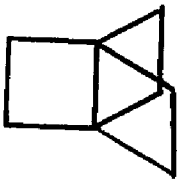

2

possesses an unusual potential energy surface reported to have two distinct energy minima.[5] This unprecedented observation, coupled with the realization that prior to this work every attempt at the synthesis of 2 ended in failure,

created enough of a mystery about the molecule to make 2 the subject of a substantive research investigation. If the suspicion that the unusual energy surface has a direct correlation to its synthetic elusiveness is correct, then this research presents an excellent opportunity to correlate theory with experiment.

However, unlike many previous studies where the theory was made to fit the experiment, this thesis attempts to conduct theoretical calculations on a variety of geometries and use the results of those calculations to predict an experimental pathway to actually synthesize the molecule, i.e., to use the calculation in a predictive manner. A successful correlation of the theoretical and experimental results would substantiate the worth of molecular orbital calculation as a "test tube" for proposing reaction pathways for the experimentalist to choose to perform the syntheses of selected organic molecules.

Description of Project

As mentioned earlier, this study concerns itself with the structure and reaction of a class of compounds known as "propellanes". The "propellane" nomenclature, first suggested by David Ginsburg, is useful to describe a class of tricyclic compounds conjoined by a common edge, where each ring may contain any number of carbon atoms "n", 1.[1a] The symbol "n", used to denote the number of carbons per ring exclusive of the central bridgehead atoms. For example, if the molecule consisted of three cyclobutane rings with a common edge, "n" for each ring would be equal to 2; hence, the appropriate nomenclature would be [2.2.2] propellane. (The two carbon atoms in the common bond are excluded.) This same compound, in the IUPAC system, would require

the cumbersome name of "tricyclo [2.2.2.$0^{1,4}$] octane". As described later, "n" can be any number of carbon atoms from one to infinity and each ring can have any number "n", i.e., n_1 does not necessarily have to equal n_2 or n_3.

[2.2.2]Propellane, 2, described above is the primary subject of this thesis, although other propellanes are discussed in subsequent sections. The structure of 2 implies that the tetracoordinate center of the bridgehead carbons is so strained that three of the orbitals might be forced into a trigonal sp^2 configuration, thus leaving the remaining p-orbital to form a pure p-σ bond with the other bridgehead carbon. The strain energy of such a molecule coupled with the unusual electronic configuration should make this molecule highly unstable and subject to some interesting reactions. In addition, it may be possible that there are two different ground states; one with a bond between the bridgehead carbons, 2, and one with a radical site at each of these carbons, 3.[5] If the molecule can be described by a different electronic configuration at each of its apparent minima, then it is likely to undergo a different set of chemical reactions depending on the source configuration (see later discussion). For instance, it may be likely that 3 was the source of the 1,4-dimethylenecyclohexane, 4, discovered in some unsuccessful attempts to synthesize 2.[2]

3

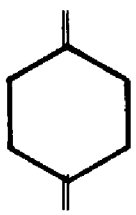

4

The challenge is to synthesize 2 and subsequently understand its stability and reactivity. The use of the molecular orbital calculations to predict an experiment to synthesize a new molecule has made this effort doubly valuable. Thus, we joined a distinguished group of investigators in studying this molecule from both a theoretical and experimental standpoint with an optimistic goal of synthesizing 2.[1-5]

Experimental History Related to the Propellanes

As is evident in references 1-5, the [2.2.2]propellane had already been the subject of considerable synthetic and theoretical study; however, at the outset of this project no one had reported a successful synthesis of the molecule. David Ginsburg reported the first synthesis of a purely hydrocarbon propellane, [4.4.4]propellane, 5.[1b] The synthesis consisted of a number of reaction steps (Figure 1) with a final Wolff-Kichner reduction to form 5. (This reduction mechanism suggested access to a variety of other propellanes in future research.) Looking toward the potential synthesis of 2, a ring contraction, decarbonylation reaction of the cyclopentanone rings on the tricyclic-ketone 6 to cyclobutane rings was also attempted.[1] A mercury photosensitized decarbonylation of 6 at low temperature did not yield any detectable 2 (Figure 2). It was, however, reported that three moles of CO_2 were liberated and a polymeric material was recovered from the reaction. Ring contraction attempts using 7 and 8 as precursors were similarly unsuccessful.

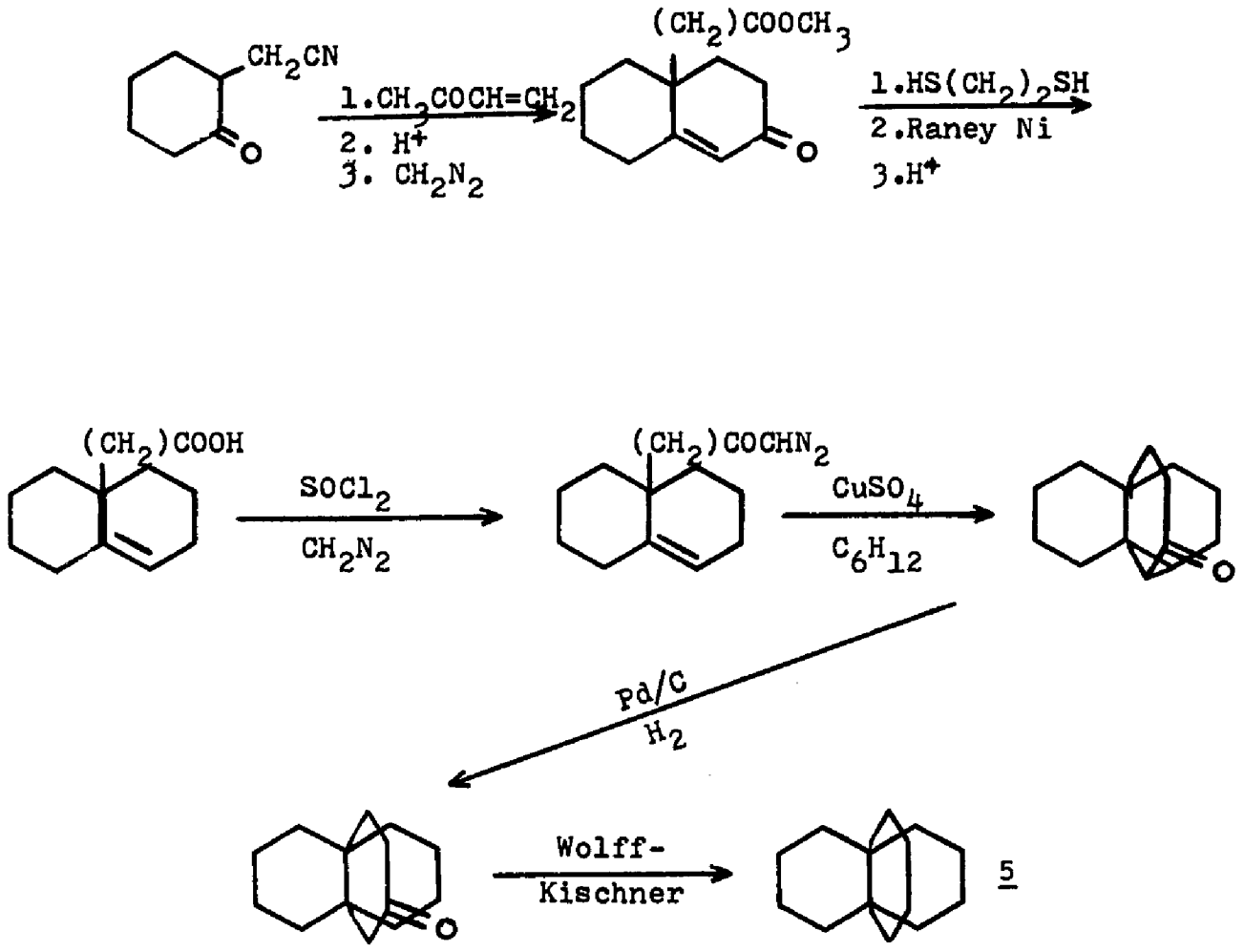

FIGURE 1. THE SYNTHESIS OF [4.4.4]PROPELLANE (Reference 8)

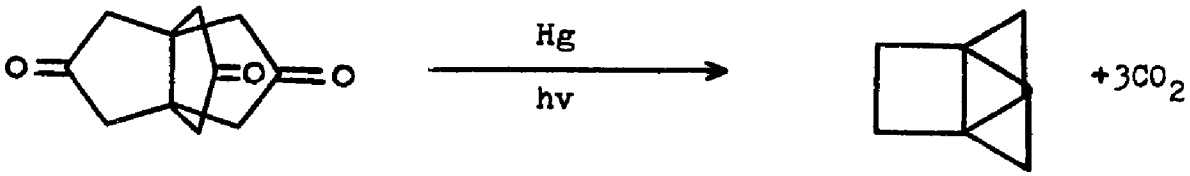

6 2

FIGURE 2. ATTEMPTED CONTRACTION OF CYCLOPENTANONE RINGS THROUGH PHOTOLYTIC DECARBONYLATION (Reference 1)

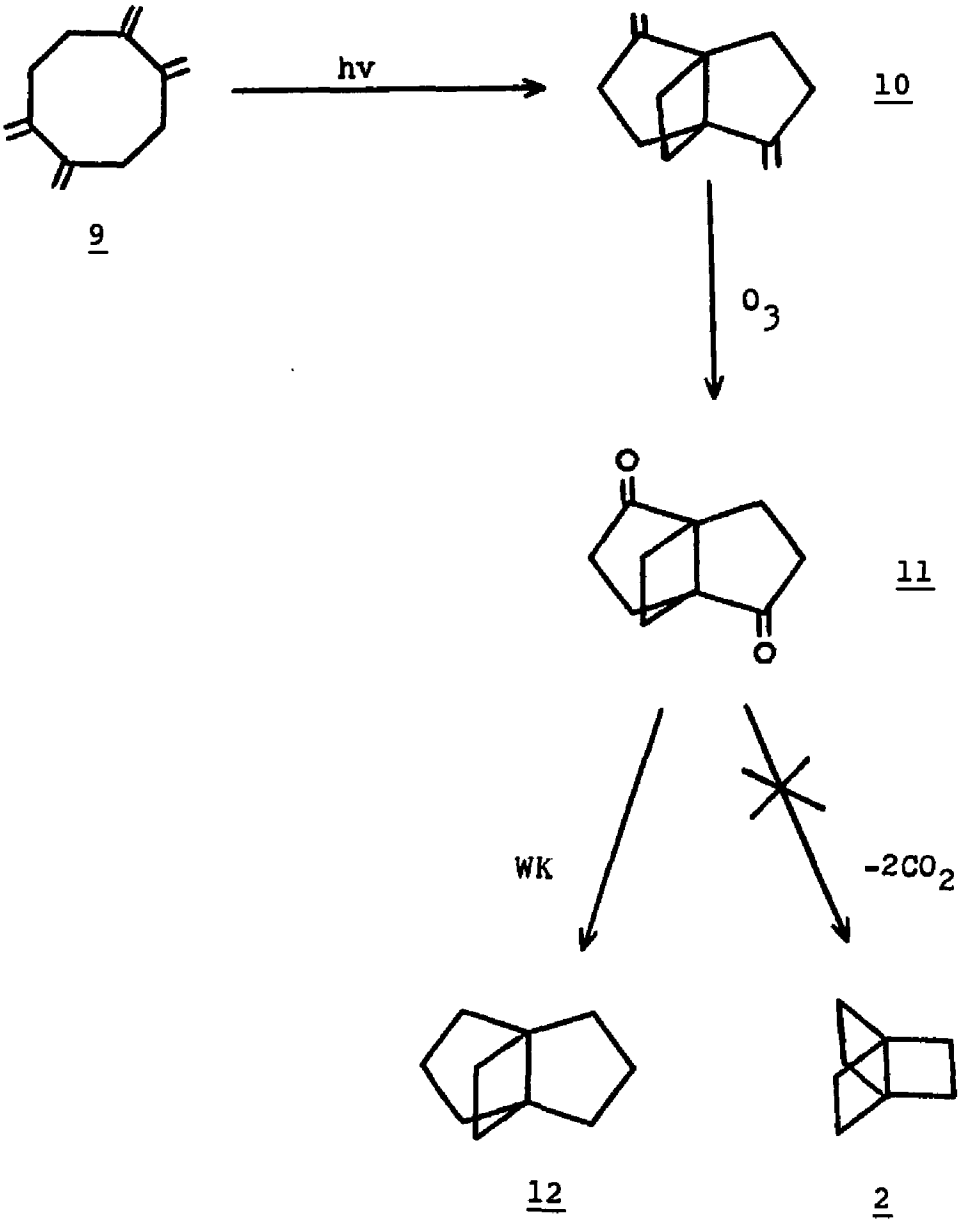

FIGURE 3. ATTEMPTED SYNTHESIS OF [2.2.2]PROPELLANE

Borden and co-workers started with 11, synthesized through a photolytic 1,5 transanular cycloaddition of 1,2,5,6-tetramethylene cyclooctane, 9 to yield 10.[6] Ozonolysis produced 11, yet attempts at a decarbonylation reaction to yield 2 did not meet with success (Figure 3). Wolff-Kichner reduction, however, did yield [3.3.2]propellane, 12. A similar attempt in the 2+2 cycloaddition of 13 to yield 14 failed (Figure 4).

P. Eaton discovered synthetic pathways to [4.2.2]propellane, 15 and [3.2.2]propellane, 16.[7] Both molecules were generated from the same intermediate 17 (Figure 5).

K. B. Wiberg added another molecule to the growing list of propellanes, [3.2.1]propellane, 18. This isomer of 2 possessed a similar inverted

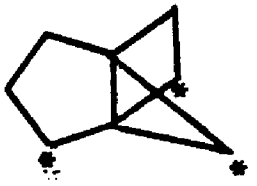

18

tetrahedron configuration at the bridgehead carbons. Through electron diffraction and x-ray crystallography evaluation of 18, it was discovered that all three methylene carbons and a bridgehead carbon on each face of the molecule lay on the same plane, thus approximately the sp^2 configuration at the bridgehead carbon of 2.

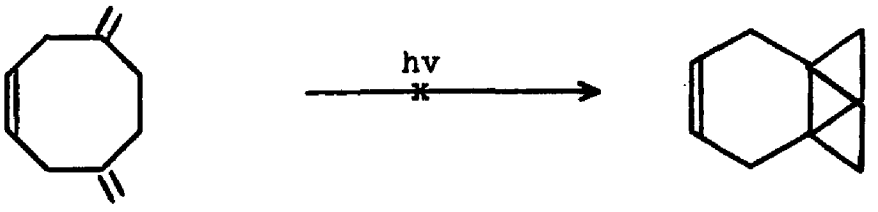

13 14

FIGURE 4. ATTEMPTED 2 + 2 CYCLOADDITION TO FORM A PROPELLANE

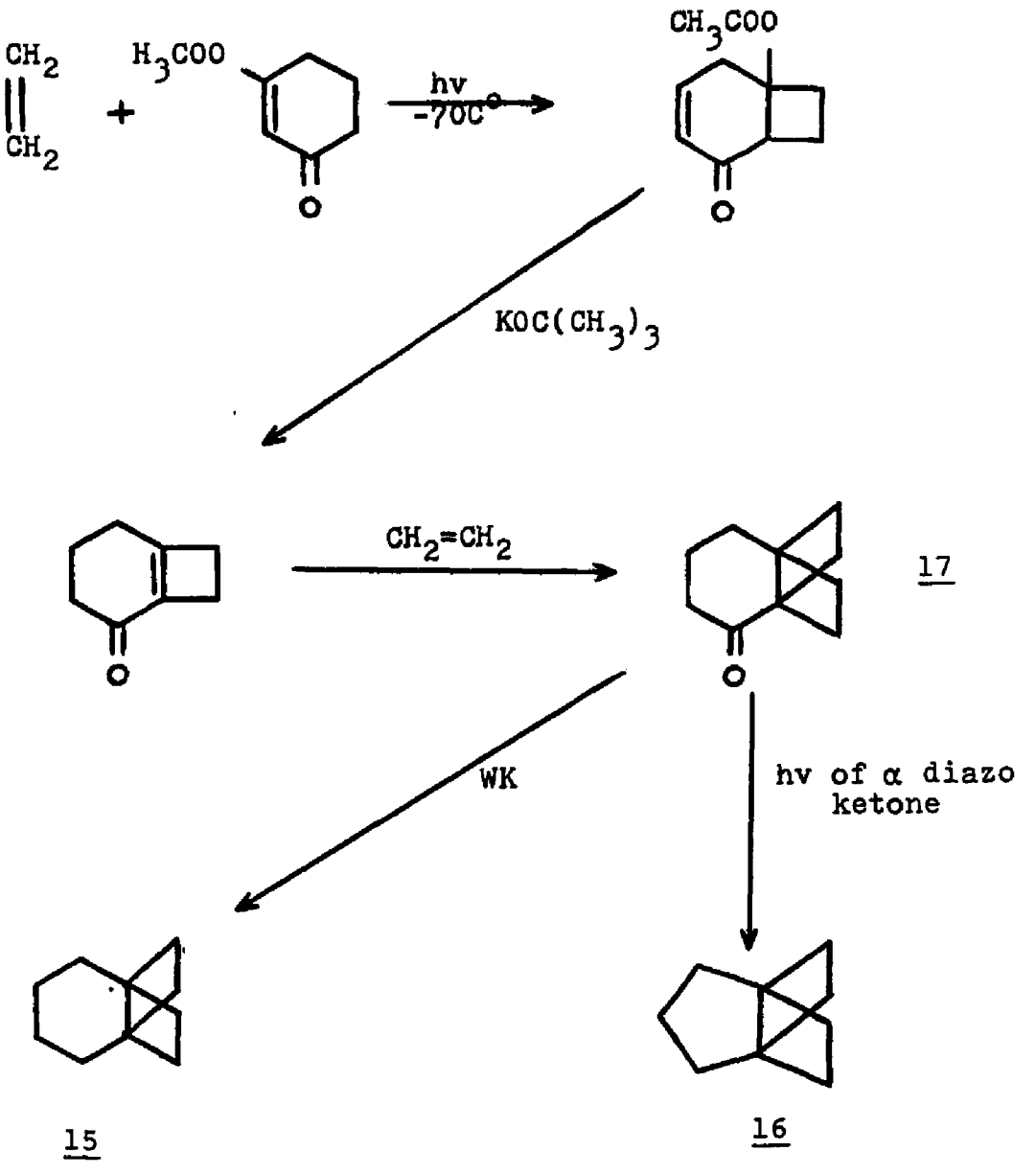

FIGURE 5. SYNTHESIS OF [4.2.2]PROPELLANE AND [3.2.2]PROPELLANE-BOTH MOLECULES ARE GENERATED FROM THE SAME PRECURSOR

Theoretical History Related to Propellanes

Numerous calculations have been performed relative to the dual minima energy surface of 2. This section attempts to deal with the significant work performed to date and interprets the results as to their impact on the synthesis of 2.

EH Calculation

Initial interest in the electronic structures of [2.2.2] propellane was generated by Hoffmann and Stohrer when they reported the orbital requirements for a chemical species exhibiting a double-well on a potential energy surface.[5] Using Extended Huckel (EH) calculations to measure the energy changes resulting from the stretching of the 1-4 bond($r_{1,4}$) of 2, accompanied by angular adjustments at the bridging carbons, a projection of the potential energy surface reproduced in Figure 6 was generated. The same calculation compared the energy changes of the highest occupied (HOMO) and lowest unoccupied (LUMO) molecular orbitals across the range of 1.5 to 2.8 angstroms(Å), showed that the orbitals crossed at r = 2.25 Å.

The double-well surface is "unusual" in that it describes two ground state electronic structures for the same molecule. The lower energy structure of the two is likely to be a diradical isomer of 2 and 3 corresponds to an approximate $r_{1,4}$ carbon-carbon distance of 2.52 Å. The higher energy molecule has an interatomic distance of about 1.5 Å. The higher energy molecule configuration approximates the geometry of 2. The authors remark that prior to this Extended Huckel (EH) study, it was not generally recognized that simply moving two atoms closer together could result in anything different than a single energy minimum.

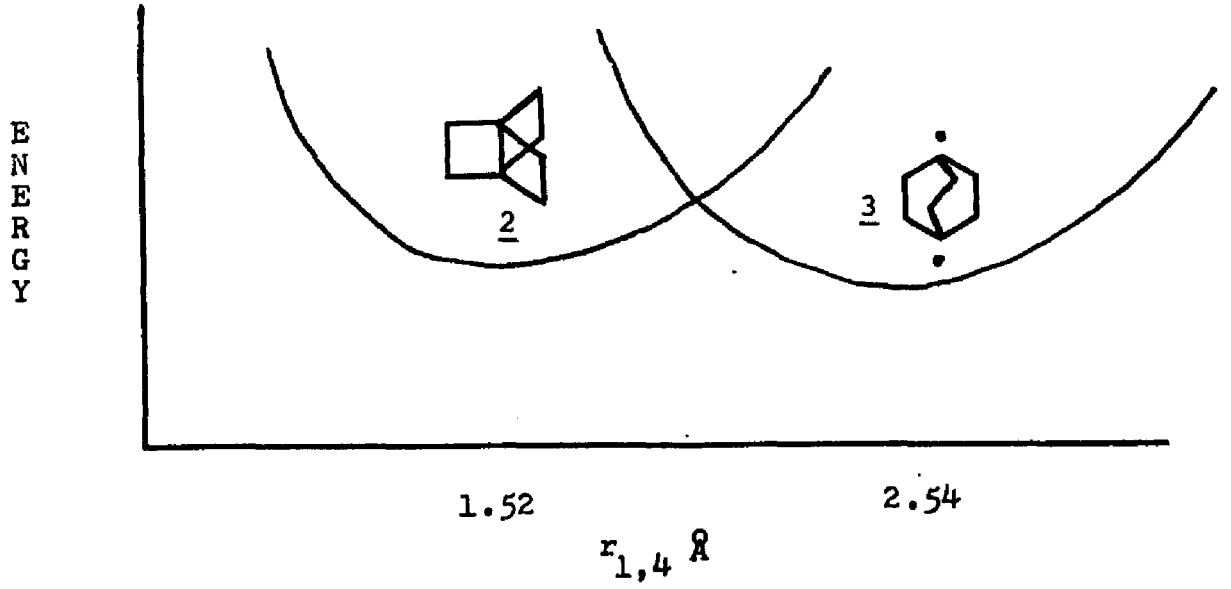

FIGURE 6. ENERGY SURFACE DERIVED FROM STRETCHING OF THE 1,4 BOND DISTANCE USING AN EH CALCULATION

Hoffmann suggests that the source of the double ground state indication for a single compound may be a combination of "throughspace" and "throughbond" coupling. Orbitals containing two lone pairs or radical centers, separated by three sigma bonds can be constructed and mixed as in Figure 7. Symmetry conditions are classified with respect to the rotation about an axis passing through the 2-3 bond and interchanging the bridgehead orbitals. Only the orbitals of like symmetry can interact with each other and as a result there is a destabilization into a low and high energy configuration. These configurations (left side of Figure 7) can be ranged using the generalization that the lower the number of nodes, the lower the resulting energy. Thus, n_1+n_2 mixes with σ (both S states) producing an S state with zero nodes and an S state with two nodes. When n_1-n_2 are mixed with σ^*, the resulting low energy state emerges with one node and a higher energy A state with three nodes. This lower energy structure is a good example of stabilization of a molecule using the "throughbond" coupling argument. This somewhat qualitative interpretation places the n_1+n_2 state at a higher energy than the n_1-n_2 state after orbital mixing (left side of Figure 7). The result is a HOMO-LUMO crossing as $r_{1,4}$ is changed.[7] Figure 7 demonstrates Hoffmann's argument that as the bridgehead orbitals come together ($r_{1,4}$ is decreasing), the corresponding orbitals exhibit a HOMO-LUMO crossing and, therefore indicates a forbidden transition.

Note that in the absence of any 1-4 orbital interaction n_1+n_2 and n_1-n_2 are degenerate. Due to the Jahn-Teller effect, the molecule will attempt to distort into a higher and lower energy configuration to remove the degeneracy (right side of Figure 7). The lower energy configuration would result in the molecule having a 1-4 "throughspace" coupling.

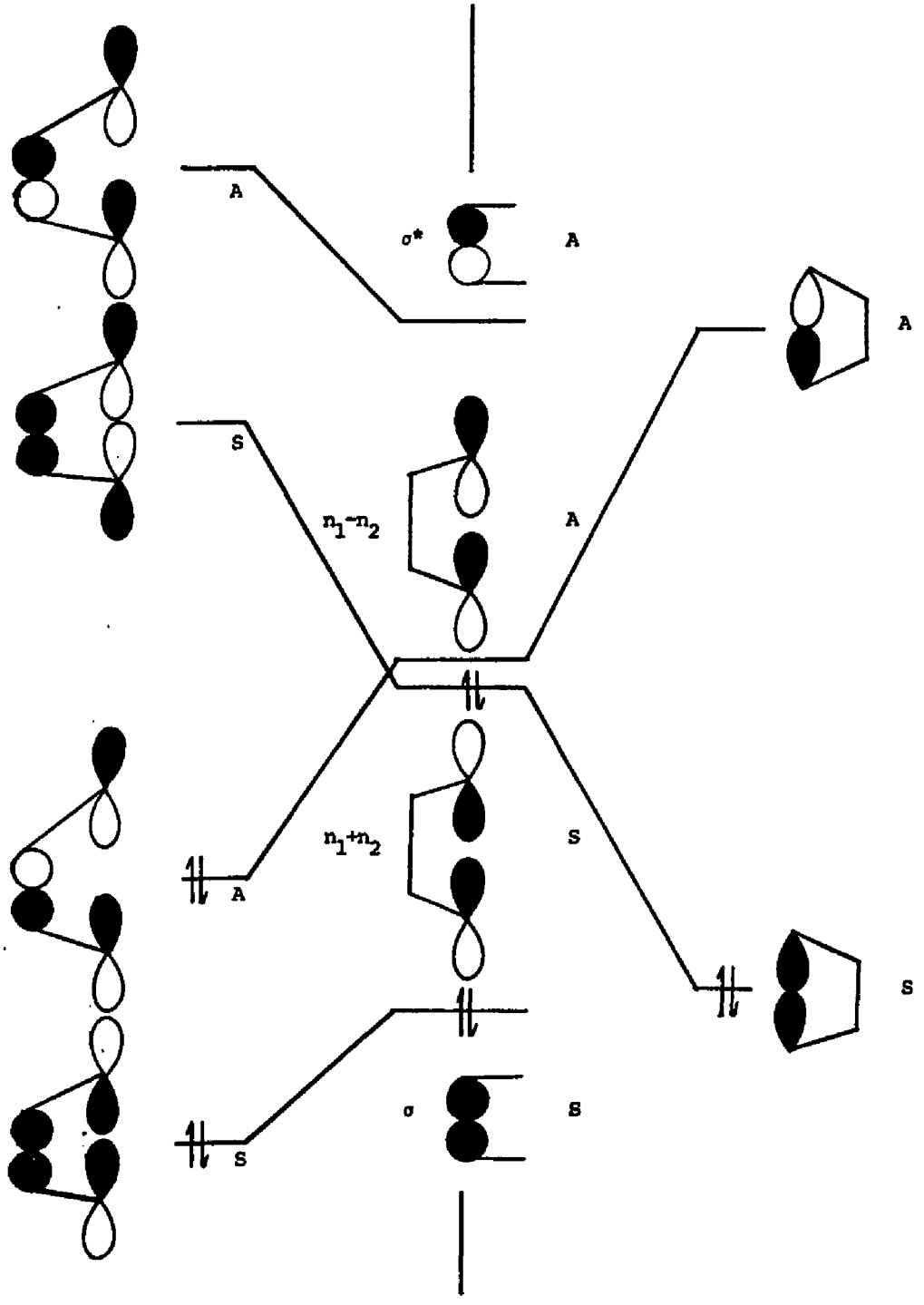

FIGURE 7. INTERACTION DIAGRAM BETWEEN THE TERMINAL ORBITALS AND THE 2,3 σ DIAGRAM

Ab-Initio SCF/CI

During the course of our investigation, a parallel effort was underway to further characterize the energy surface of 2.[8] In addition to confirming the double well projection of the energy surface, the investigation sought to estimate the true positions of the minima and as a result, estimate the magnitude of the intervening energy barrier. Using the STO-3G minimal contracted Gaussian basis set approximation with ab-initio SCF (self-consistent field) and CI (configuration interaction) wave functions, various geometries of the energy surface were calculated. The $r_{1,4}$ bond distances of 1.49 and 2.9 Å and values inclusive were calculated within the framework of 2, followed by the imposition of configuration interaction (averaging of covalent and ionic character).

Their results verified the existence of the double-well energy profile and placed 2 as the lower energy species (see Figure 8). The barrier to interconversion was calculated to be approximately 29 kcal/mol and the resulting half-life was predicted to be on the order of a few hours at room temperature.

This calculation proved encouraging to this research project as it suggested that not only was 2 more stable than the isomeric diradical 3, but that 2 would also have a half-life amenable to isolation and characterization.

Geometrical Strain Consideration

The hope for successful synthesis of 2 is strengthened by the ab-initio/CI calculations mentioned in the previous section. However, a consideration of the geometrical requirements of the propellane suggests a

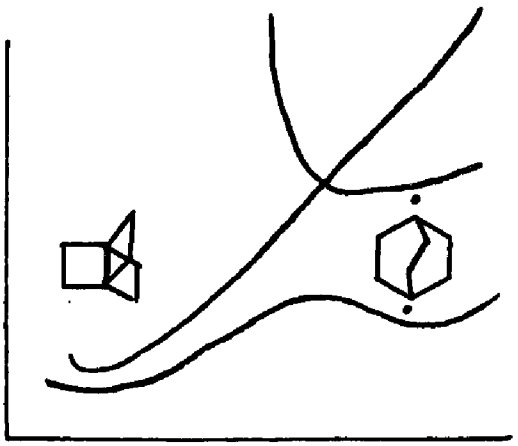

FIGURE 8. NEWTON-SCHULMAN CALCULATION AB-INITIO SCF and CI WAVE EQUATIONS

highly strained structure. To form the structural skeleton of 2 requires that the orbitals of the bridgehead carbons be sp^2 in order for a p-orbital to be available for forming an internal p-σ bond. The bridgehead angle is then constrained closer to 90° and all of the electron bonds are forced to locate on only one side (hemisphere) of the bridgehead carbon. The combination of the above geometrical constraints make it likely that this molecule is extremely unstable thermodynamically. Calculating the resulting energy in two ways, from the fusion of three cyclobutane rings $3(25 \pm 4)$; and from the calculated ΔH of the hypothetical reaction, 2, 2 ethanes = 3 cyclobutanes using known heats of formation of ethane and cyclobutane yielded similar results: 87 kcal/mol and 90 kcal/mol respectively.[8] Using Franklin equivalents the [3.2.1] propellane, 18, was estimated to have a strain energy of 60 kcal/mol and possessed a measured half-life of 20 hours at 195° C.[2] The same authors calculated the strain energy for 2 to be 86 kcal/mol.

Competition With the Cope Rearrangement

The synthesis of 2, formed through an intramolecular recombination of the bridgehead diradical, has been suggested.[2,4] The ab-initio/CI treatment of the corresponding geometries suggests that the energy required for interconversion is approximately 29 kcal/mol.[8] The interconversion of 2 and 3 would be difficult although possible. The strain energy of the diradical 3 should be much less than 2 and the interconversion may be favored. However, the propensity for reactivity or alternate intramolecular rearrangement of any radical species should make its existence relatively short lived.

It is useful here to remember that the 1,4-dimethylene cyclohexane, 4, has been discovered during unsuccessful attempts at the synthesis of 2.

Although it is not expected that 2 will rearrange to 4 by a thermal 2+2 retro-addition, since such a process is symmetry forbidden, nonetheless, compound 4 has been observed in unsuccessful attempts to synthesize 2.[2] Hoffmann has suggested that compound 2 might possibly rearrange to 4 through a diradical intermediate 3.[4,5] (See Figure 9.) This process is likely, provided enough energy is available to overcome the calculated barrier.

An important aspect to consider about the diradical is that it appears to be identical to the transition state of a competing reaction on the same energy surface.[10] The ground state energy represented by the minima for 3 on the propellane surface likely corresponds to a high energy barrier on a segment of the energy surface representing the Cope rearrangement of 4. The similarity can best be described as a "saddle point" contact on two slices of the hypersurface shown perpendicular to each other in Figure 10. With this surface in mind, the emergence of 4 should be no surprise since this diene can originate from both successful and unsuccessful syntheses of 2. A successful synthesis could yield 4 from thermal decomposition of 2 through 3, whereas an unsuccessful attempt may result in formation of the diradical 3 directly. This diradical should be recognized as merely a "short lived" transition state and expected to geometrically relax to form 4.

Using the arguments of orbital isomerism and the effects of a Jahn-Teller distortion, Dewar argues that the certain transitions requiring activation energy can proceed in a concerted manner.[11] Since a biradical can be thought of as a species with two degenerate orbitals occupied by two

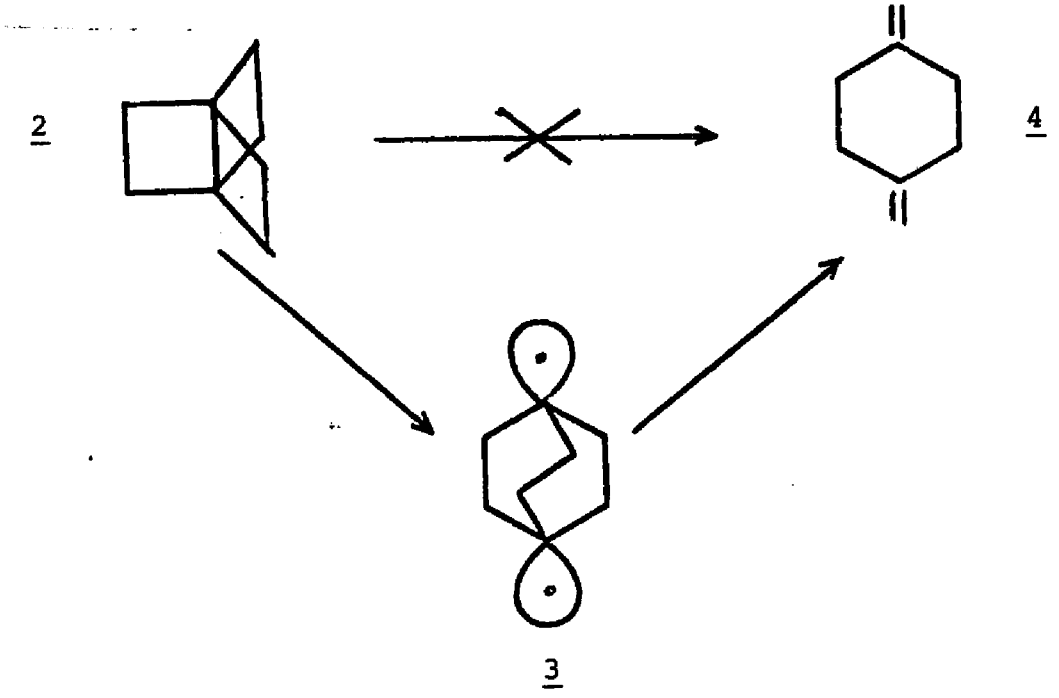

FIGURE 9. THE RELATIONSHIP OF [2.2.2] PROPELLANE TO 1,4-DIMETHYLENECYCLOHEXANE

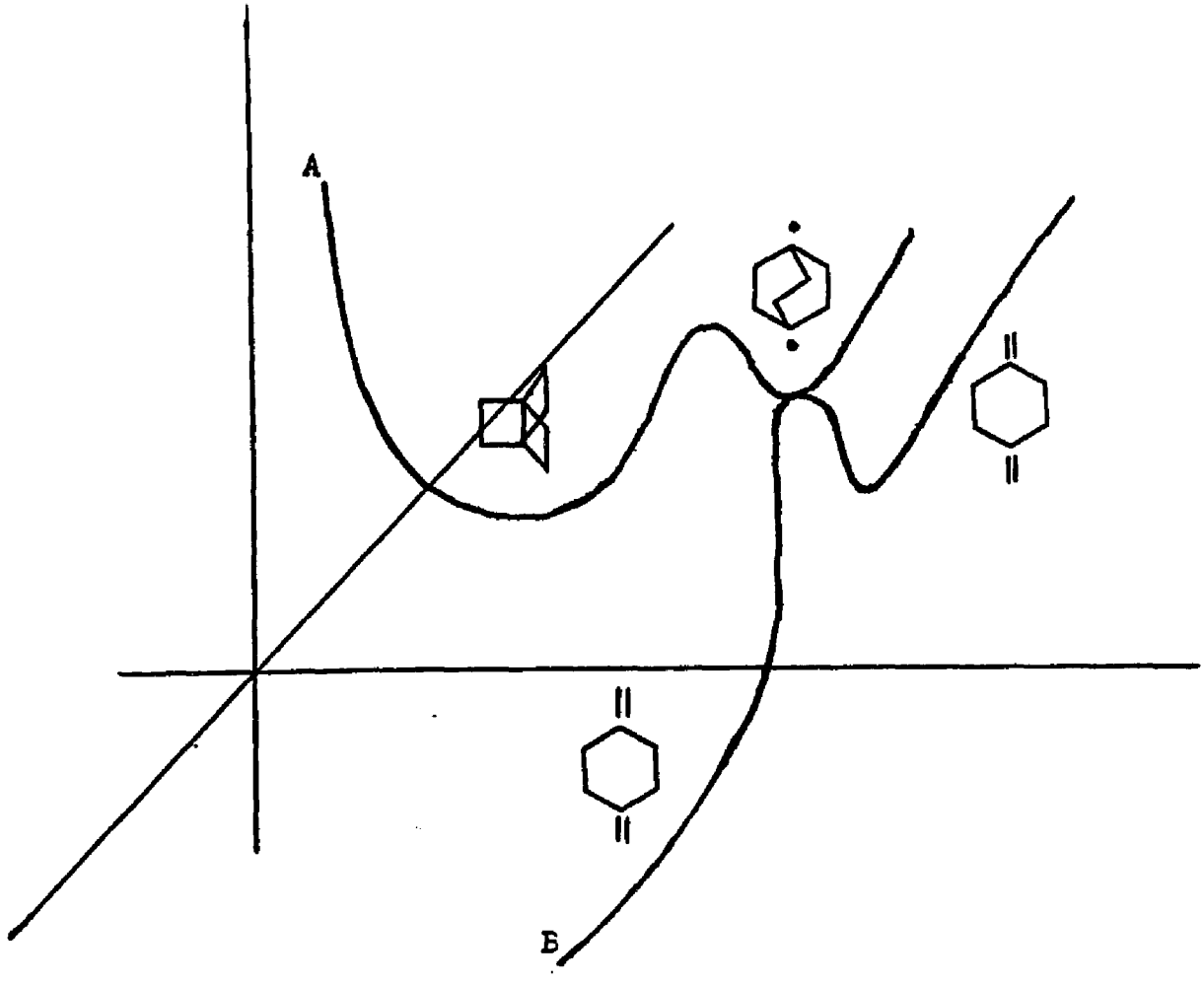

FIGURE 10. THE INTERACTION OF TWO SURFACES TO PRODUCE A "SADDLE POINT". SURFACE A REPRESENTS THE PROPELLANE ENERGIES, SURFACE B REPRESENTS A DEGENERATE COPE REARRANGEMENT FOR XIX.

electrons of opposite spins, this system should generally be unstable and undergoes a Jahn-Teller distortion to a more favorable species. The position in which an orbital crossing is observed in both the EH and the ab-initio calculations meets the criteria for the degeneracy of the two orbitals.** At this crossing, the molecule will attempt to remove the degeneracy by distorting to some more stable species. By this argument, the biradical is a highly transient species and rapidly decays to one of two possible geometries via a concerted pathway. It can best be described as a transition state for the interconversion of two isoelectronic, more stable structures.

Summary and Justification

In all of the investigations cited in the introduction, evidence was presented for the potential existence of a highly strained hydrocarbon, [2.2.2]propellane. Two questions exist which have not been answered adequately:

- The molecule 2 has not yet been synthesized. Is it stable enough as predicted by theory to have a finite lifetime?
- Molecular orbital calculations can predict geometries. Can these geometries and the resultant potential energy surfaces be useful in predicting pathways to the synthesis of the molecules in question?

This thesis attempts to answer both of the above questions.

**It is recognized that "avoided crossing" may result from imposition of CI. For the sake of simplicity only the term "crossing" will be used in this thesis.

CHAPTER I

REFERENCES

(1a) Ginsberg, D. Accts. Chem. Res. 1972, 5, 249.

(1b) Ginsberg, D. Accts. Chem. Res. 1969, 2, 121.

(1c) Altman, J.; Babad, E.; Itzchaki, J.; Ginsburg, D. Tetrahedron Suppl. 1966, Part 1, 8, 279.

(1d) Castaneda, F. F. Ph.D Thesis, University of California, Berkeley, 1970.

(2) Wiberg, K. B.; Burgmaier, G. J. J. Amer. Chem. Soc. 1976, 94, 7396, Wiberg, K. B.; Burgmaier, G. J. Tet. Letters 1969, 317.

(3a) Hoffman, R. Accts. Chem. Res. 1971, 4, 1.

(3b) Hoffman, R.; Swaminathan, B.; Odell, G.; and Gleiter, R. J. Amer. Chem. Soc. 1970, 92, 7091.

(4) Hoffman, R.; Stohrer, W. J. Amer. Chem. Soc. 1972, 94, 779.

(5) R. Hoffmann and W. Stohrer, XXIII International Congress of Pure and Applied Chemistry, Special Lecture; Butterworth, London.

(6) Borden, W. T.; Reich, I. L.; Sharpe, L. A.; Reich, H. J. J. Amer. Chem. Soc. 1970, 92, 3808.

(7) Eaton, P. E. 155th National Meeting of the American Chemical Society, San Francisco, CA, April, 1968, p. 1.

(8) Newton, M. D.; Schulman, J. M. J. Amer. Chem. Soc. 1972, 94, 4391.

(9) Franklin, J. L. Ind. Eng. Chem. 1949, 41, 1070.

(10) Gajewsky, J. J.; Hoffman, L. K.; Shih, C. N. J. Amer. Chem. Soc. 1974, 96, 3705, and personal communications.

(10a) Dewar, M.J.S.; Wade, L. E. Ibid. 1973, 95, 5121.

(10b) Goldstein, M. J.; Benzon, M. S. Ibid. 1972, 94, 5119; 1972, 94, 7147

CHAPTER II

MOLECULAR ORBITAL TREATMENT OF [2.2.2]PROPELLANE ENERGY SURFACE

Method of Calculation for this Thesis

As with any experiment, the choice of "tools" is critical to the success of an operation. The choice of a theoretical method appropriate to the system and the experimental plan are discussed in this section.

Selection of Method

The arsenal of molecular orbital (MO) calculations can range from the simple Huckel Theory to large basis set ab-initio calculations with correlation correction. The literature is replete with reports of significant correlation of the MO method to some empirical measurement. Likewise, there are reports exposing the weaknesses or detriments of various methods. The choice for an organic chemist is not always straightforward. In order for an MO calculation to be an effective tool or, as described earlier, a "test tube", it first must be within the range of quality for the given experiments. Secondly, the cost of the calculation cannot be prohibitively expensive. If the cost to "operate" the calculation exceeds the experimentalist's expenses in "trial and error" bench experiments, then the calculation can be only considered as a luxury. To be a useful "test tube" the selected MO method should have a demonstrated reliability for the important parameter to be measured, and be inexpensive enough to use to justify its predictive value.

Considering the above recommendations, in 1972 we looked at the choice of MO systems on hand and selected the Intermediate Neglect of Differential Overlap (INDO) method for our study.

INDO Method

It is our intention to calculate a triplet state geometry. Therefore, a calculation which has demonstrated an ability to treat an "open shell" system would be appropriate for this study. Pople and Dobosh introduced the method of INDO as an improvement on Complete Neglect of Differential Overlap (CNDO).[12] INDO is particularly suited for this study of radicals and triplet states. It is capable of calculating molecular geometries, spin densities, and hyperfine coupling constants of hydrocarbons and other organic compounds containing heteroatoms, nitrogen, oxygen, and fluorine. However, the method has a drawback in that there was a tendency to overestimate the stability of strained ring structures such as 2; a point to keep in mind when interpreting the relative configuration energies of 2 and its isomers.[13]

Two INDO programs are used in this research. The preliminary calculations were performed with a program belonging to Professor David Beveridge of Hunter College, City University of New York. The second, more current version of the program was purchased from the Quantum Chemistry Program Exchange (QCPE #144). The two programs produced slightly different energy values for the closed shell calculations. All the values presented in this paper were calculated using the latter program and are relative to each other in geometry and energy.

Theoretical Approach

A D_{3h} symmetry is assumed for all configurations of the propellanes. Optimized geometries, bond orders, and total configurational energies were calculated for each geometry studied. The geometry optimization resulted from calculating the total energy of a molecule and changing one of four variables: 1,4 and 1,2 bond distances; angle 123; and the CH bond length in that order. Variations in the bond distances were 0.0005 angstroms, and 0.05 degrees in all angles. Bond length 2,3 is generated by the calculation. When a low energy configuration was identified, a minimum of two points on either side of the minimum geometry was calculated for verification before changing to the next variable.

The geometries calculated were similar to the Hoffmann EH calculation mentioned earlier. Two singlet state combinations can be visualized from inspecting the molecular orbitals along the C_1C_4 bond axis. One of these is symmetric (S), 19, and the other antisymmetric (A), 20, with respect to the mirror plane perpendicular to the threefold axis (see Figure 11). In addition to the two lowest energy singlet states calculated by Hoffman, the lowest triplet state (T), 21, combination was also calculated.

Bond orders were also calculated corresponding to the p-σ overlap of the C_1 and C_4 carbon atoms. Positive values for the result of the calculation indicate a bonding interaction, negative values suggest repulsion and zero values are nonbonding.

Character tables were extracted from the eigenvalues for the optimized singlet and triplet molecules and are presented as an Appendix. A D_{3h} symmetry table was used to identify point symmetry groups.

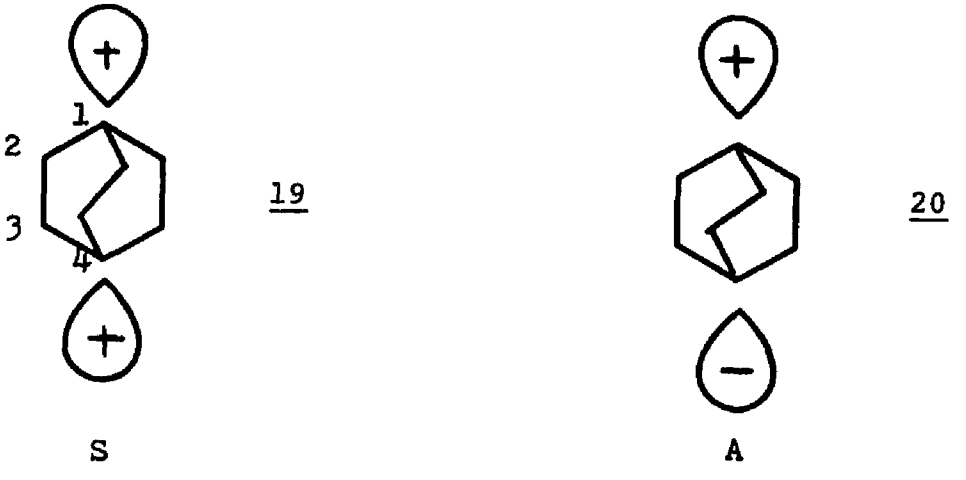

FIGURE 11. A DEPICTION OF THE TWO POSSIBLE ELECTRONIC CONFIGURATIONS OF PROPELLANE, SYMMETRIC (S) AND ANTISYMMETRIC (A)

Results: Optimization of Geometries

Significant optimized energy values are extracted from the calculations and are presented in Table 1 with associated bond order values.[14] The optimized geometries of three electronic configurations of the propellane hydrocarbon: the singlet symmetric 2, the antisymmetric 3 orbital geometries (Figure 11), and the lowest energy triplet state structure 21, are given in Table 2. As in the Schulman calculations, 2 is lower in energy than its isoelectronic 3. The difference in energy, approximately 115 kcal/mol, is considerably greater than the value calculated by the ab-initio method and, as mentioned earlier, this high value results from the propensity of the INDO method to overstablize small ring hydrocarbons. The triplet, 21, calculation proved most useful as it resulted in an intermediate configuration energy between the 2 and 3 states (~ 75 kcal/mol) and was also found to have an intermediate $r_{1,4}$ bond distance (2.09 Å) greater than 2 (1.56 Å) but shorter than 3 (2.45 Å). An inspection of the bond order implies that a "nonbonding" situation exists in the space between C_1 and C_4 for 21. A representation of segments of the two energy surfaces calculated for increasing $r_{1,4}$ and subsequently superimposed on each other is presented in Figure 12.[14]

The relative position of the triplet state minimum suggests that the associated geometry for 21 may be a viable intermediate for the synthesis of 2. The implications of this correlation are discussed in a subsequent section.

Symmetry tables for 2, 3, and 21 were assembled and are presented in total in Appendix A and summarized in Tables 3, 4, and 5. HOMO (orbital 22)

and LUMO (orbital 23) were found to interchange point symmetry groups A_1' to A_2' as $r_{1,4}$ increased. Likewise, the HOMO changed from a bonding (S) condition to an antibonding (A) state with increased r. In the triplet state calculation, the alpha spin case suggests a relative nonbonding^{1,4} condition.

TABLE 1. TOTAL ENERGY, BOND ORDER

State	INDO Total Energy (a.u.)	Relative Energies kcal/mol	Bond Order
2	-64.371624	0	.867
3	-64.185378	115	-.193
21	-64.249602	76	.009

TABLE 2. OPTIMIZED GEOMETRY FOR CALCULATED STATES

State	Interatomic Distance (A)				Bond Angle
	$r_{1,4}$	$r_{1,2}$	$r_{2,3}$	r_{C-H}	123
2	1.560	1.505	1.484	1.125	94.45
3	2.450	1.450	1.524	1.125	108.62
21	2.090	1.475	1.487	1.125	101.80

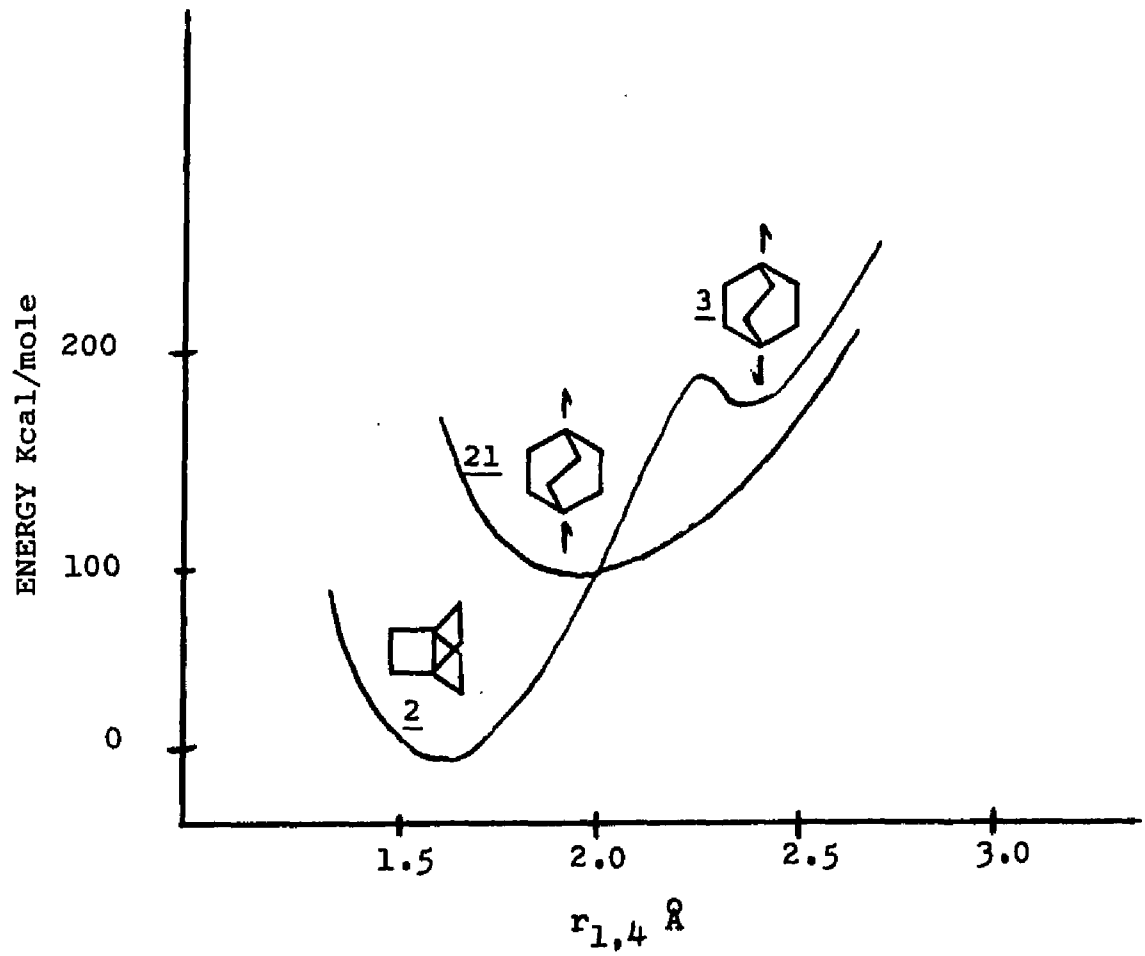

FIGURE 12. SUPERIMPOSITION OF THE ENERGY SURFACES FOR THE GROUND STATE SINGLET AND THE LOWEST TRIPLET STATES OF II

TABLE 3. ORBITAL SYMMETRY TABLE FOR 2

Orbital	E (a.u.)	σ_h	Point Symmetry
24	.2383	S	
23 (LUMO)	.2360	A	A_2''
22 (HOMO)	-.3226	S	A_1'
21	-.4279	A	
20	-.4279	A	
19	-.5461	A	A_1''
18	-.6103	S	
17	-.6103	S	
16	-.6532	A	
15	-.6532	A	
14	-.6998	A	A_2''
13	-.7470	S	
12	-.7470	S	
11	-.7567	S	A_2'
10	-.9031	S	A_1'

TABLE 4. ORBITAL SYMMETRY TABLE FOR 3

Orbital	E (a.u.)	σ_h	Point Symmetry
24	.2482	S	
23	-.0335	S	A_1''
22*	-.3053	A	A_2'
21	-.4493	A	
20	-.4493	A	
19	-.5325	A	A_1''
18	-.6139	S	
17	-.6139	S	
16	-.6320	S	
15	-.6320	S	
14	-.6723	A	
13	-.6723	S	
12	-.7259	S	A_2''
11	-.7359	A	A_2'
10	-.9509	S	A_1'

*HOMO

TABLE 5. ORBITAL SYMMETRY TABLE FOR 21

Orbital	Alpha Spin E (a.u.)	σ_h	Point Symmetry	Beta Spin E (a.u.)	σ_h	Point Symmetry
24	.2424	S		.2468	S	
23*	-.3207	S	A_1''	.1721	A	A_2'
22	-.3214	A	A_2''	.1090	S	A_1'
21	-.4574	A		-.4488	A	
20	-.4574	A		-.4488	A	
19	-.5404	A	A_1''	-.5358	A	A_1''
18	-.6318	S		-.6190	S	
17	-.6318	S		-.6190	S	
16	-.6667	A		-.6615	A	
15	-.6667	A		-.6615	A	
14	-.6871	S		-.6755	S	
13	-.6871	S		-.6755	S	
12	-.7257	A	A_2''	-.7007	A	A_2''
11	-.7503	S	A_2'	-.7471	S	A_2'
10	-.9753	S	A_1'	-.8843	S	A_1'

*HOMO

Discussion of Calculations

Singlet State Isomers

The double-well segment describing $r_{1,4}$ increasing for the singlet-energy surface survived intact when subjected to an INDO treatment. The symmetric isomer 2 was calculated to be of lower energy than the asymmetric 3 species by 115 kcal/mol. This value is probably excessive since the ab-initio treatment predicted a barrier to interconversion of only 29 kcal/mol. A comparison of the energy surfaces derived from EH, ab-initio, and the INDO method is presented graphically in Figure 13. Agreement in the 1,4 bond distances of optimized 2 and 3 geometries was good. A listing of the optimized 1,4 bond distances can be found in Table 6.

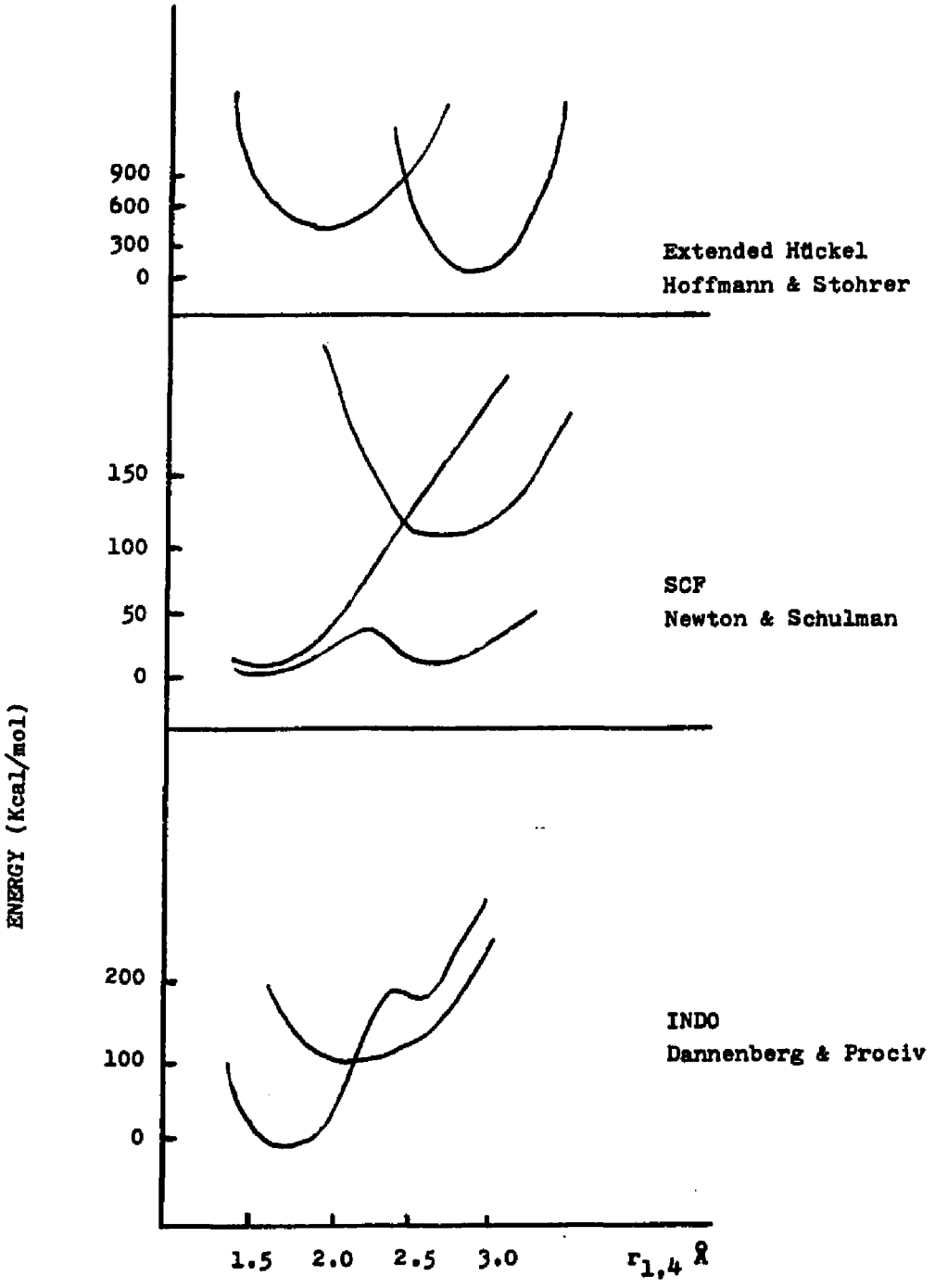

FIGURE 13. ENERGY SURFACES CALCULATED BY THREE INDEPENDENT GROUPS USING DIFFERENT LEVELS OF CALCULATIONS

TABLE 6. COMPARISON OF 1,4 BOND LENGTHS IN THE LISTED CONFIGURATIONS CALCULATED BY THREE DIFFERENT METHODS

r_{1-4} (A)	2	3	21
EH	1.54	2.47	....
SCF/CI	1.52	2.54	....
INDO	1.56	2.45	2.09

Evidence for the orbital reversal is derived from the symmetry tables presented in Tables 2 and 3. In 2 (Table 3), orbital number 22, the highest occupied molecular orbital (HOMO) is positive to symmetry operations σ_h, all C_2 operations and S operations of the D_{3h} symmetry group indicating considerable bonding character in the space between the 1,4 carbons. Orbital 23, the lowest unoccupied molecular orbital (LUMO), results in a negative number in the same operations indicating an antibonding condition. Extending the 1,4 carbon distance to the geometry of 3, however, yields an antibonding HOMO and a bonding LUMO under the same symmetry operations as indicated by the exchange of the symmetry point groups A_1' to A_2''. This is direct evidence of the exchange of S and A orbitals predicted in the Hoffmann work.[4]

The symmetry considerations applied above explain the existence of two different electronic species whose optimal geometries are governed by direct "throughspace" coupling of the 1,4 p-orbitals in the case of 2 and a "through-bond" coupling through the carbon framework of 3.[5]

The Triplet State

The triplet calculation is the key to suggesting a pathway to approaching the synthesis of 2. The INDO calculation places the 1,4 bond distance of the triplet state 21 (2.09 Å) intermediate to that of the 2 and 3 states. Likewise, the calculated energy for the optimized geometry of the 21 (75 kcal/mol) is greater than that of 2 yet lower than 3.

Orbitals 10-24 for 21, 2, and 3 are plotted on Figure 14 and populated with the appropriate electrons. Of note in this figure is the low-lying symmetric orbital which is expected to be the HOMO in the triplet alpha spin state. In comparison the triplet HOMO is only 1.2 kcal higher than the HOMO for 2 whereas the analagous orbital for 3 is 11 kcal higher in energy. The calculation suggests that the triplet state orbital should be easily populated.

Suggested Experimental Approach

The calculation results should still be treated cautiously since the MO method often does not take into account various electronic forces which may substantially change the actual energetic states of excited or transition state species. The calculation, however, is still indicative of a pathway to 2. The experiment to prove the calculation is designed around the simple idea that an intermediate or transition state of elevated energy should strive to achieve a more stable, lower energy configuration. In this case, that lower energy species is the [2.2.2]propellane, 2.

It was mistakenly suggested in some studies that any attempts to synthesize 2 could be complicated by the possibility of forming two different

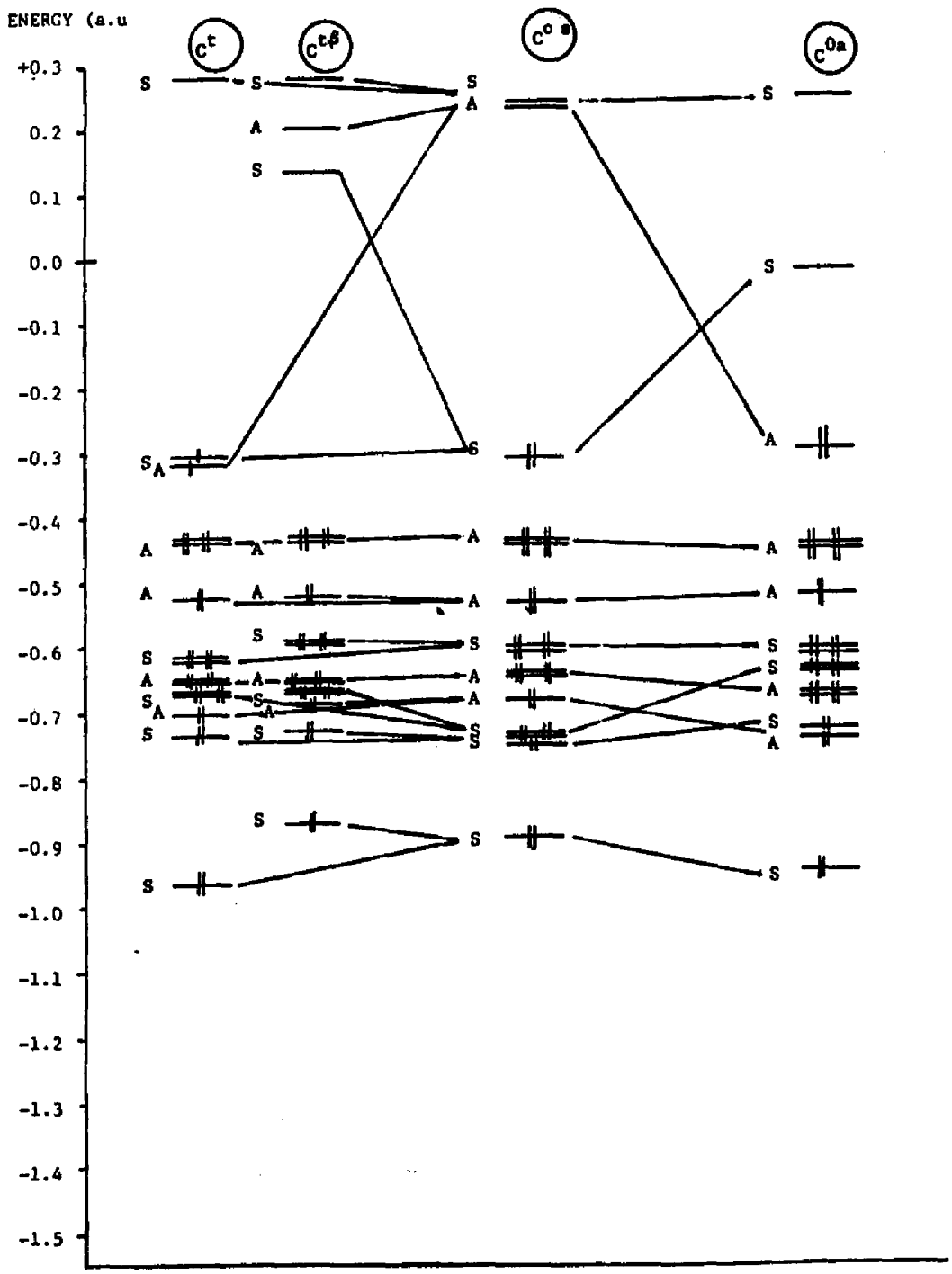

FIGURE 14. ORBITAL POPULATIONS FOR 21, 2, AND 3 AND THEIR COMPARISON

ground state species, 2 and 3.[1,3,4] Also suggested was that the most obvious approach to the synthesis of 2 could be to attempt the recombination of the two unpaired radicals in 3.[2] It is, however, shown in a previous section that 3 could not be a stable species as it is a transition state for another process participating in a very rapid mechanism on another surface, the Cope rearrangement (see Figure 10).

The choice of experiment suggested by the INDO calculations is to generate a triplet state isomer of 2. Any experiment that might populate an electronic state such as 21 should prove successful. This triplet might then be expected to decay to configuration 2, a reasonable fraction of time, by following a lower energy path on the surface. Compound 4, an isomer of 2, might be excited to a triplet state and geometrically relax to 21. If the triplet excited state 21 is higher in energy than calculated, entry into the right side energy well of Figure 12 is possible. This will yield 4 since 3 is the transition state of the degenerate Cope rearrangement (Figure 10). For this reason, the likelihood of 3 being available for reaction is negligible. Any reformation of 4 would not interfere with the reaction since the compound is merely recycled to starting material. In fact, the presence of 4, the expected product of this rearrangement, has been observed in earlier investigations where 4 was not a starting material for the reaction.[2]

If the energy surface is entered on the left side of Figure 12, the product expected is 2. The propellane is expected to be relatively unstable because of its highly strained geometry and would probably undergo decomposition to 4 also. This reaction will not, however, be concerted since it is a 2s+2s operation and is expressly forbidden by orbital symmetry postulates.

The transition from 2 to 3 is, however, allowed and has been recognized as a GROB fragmentation.[15]

Even though 2 is predicted to have a finite life, it is still expected to be short lived. The formation and trapping of a stable derivative is a likely approach to prove its existence initially. The likelihood of any diradical 3 interfering with the reaction has been eliminated since its existence is unlikely due to the reasons presented earlier.

We also noted earlier that the CNDO and INDO calculations have the propensity to overestimate the relative stability of small ring structures.[13] Thus, the ground state surface in Figure 12 may be artifically skewed in favor of 2. This fact, however, does not necessarily invalidate the predictive value of the calculations. Irrespective of the relative energy of 2, the surface predicts that the irradiation of 4 to a triplet state should allow entry on the side of the surface corresponding to 2. Those molecules which prefer to enter the diradical well will merely rearrange to 4, providing a recirculating supply of starting material. This dynamic system is ideal for maximizing the yield of 2.

In the next section, the worth of theoretical calculations will be challenged by a novel experiment suggested by the calculations. The INDO method has resulted in an energy diagram suggesting a synthesis pathway to the [2.2.2]propellane as yet untried by the synthetic chemist.

CHAPTER II

REGFERENCES

(12) Pople, J. A.; Beveridge, D. L.; Dobosch, P. A. J. Chem. Phys. 1967, 47, 2026.

(13) Snyder, E. I. J. Amer. Chem. Soc. 1970, 92, 7529.

(14) Dannenberg, J. J.; Prociv, T. M. J.C.S. Chem. Comm. 1973, 291.

(15) Grob, C. A.; Schiess, P. W. Angew Chem., 1967, 79, 1., Grob, C. A. Ibid. 1969, 81, 543.

CHAPTER III

SYNTHESIS OF [2.2.2]PROPELLANE

An Approach to the Synthesis of 2

Any practical approach to the synthesis of 2 must devise a manner of entering the energy surface on the left side of the diagram in Figure 12, therefore, avoiding entrapment in the diradical well. The triplet state, 21, suggests an accessibility to the surface from the left side. As described in Chapter II, the INDO calculation predicted that the calculated energy of 21 lies intermediate to 2 and 3. Therefore, if the triplet state of 4 could be achieved, it would have the same optimized geometry as 21 and should rearrange to a geometrically relaxed triplet by delocalizing the unpaired electrons. This triplet could then collapse preferentially to the ground state, 2. Based on this approach, it might be possible to excite 4 to its triplet state allowing it to relax to a ground state triplet, 21, and subsequently decay to 2.

Since the predicted half-life of this reaction is only about one-half hour at room temperature, the reaction should be run at low temperatures to maximize the yield.[8] The short half-life also suggests that a derivative reaction may be necessary to trap the elusive 2.

The information afforded by the INDO calculation discussed in the previous reaction encouraged the associated experiment for the synthesis of 2. In addition, suggestions were made related to the choice of starting material and the optimum conditions required for the reactant to be raised to its excited triplet state. It remains only to perform the synthesis to evaluate our predictions.

Choice of Starting Material

The 1,4-dimethylene cyclohexane, 4, was the best candidate for study as a precursor for 2. As part of this study, a quick geometrical optimization for both "boat" and "chair" structures were calculated using the INDO program discussed earlier for the propellanes (results shown in Table 7). By our calculations the "boat" configuration was favored over the "chair" by roughly 39 kcal/mol. This is in agreement with other experimental and theoretical observations although some authors have suggested the more preferred form would probably be a "twist" configuration.[16,17] Whether 4 prefers "boat" or "twist" is unimportant provided that the triplet state geometry is appropriate for the formation of 2.

TABLE 7. RESULTS OF INDO OPTIMIZATIONS FOR 1,4 DIMETHYLENECYCLOHEXANE, 4

	Chair	Boat
Energy (kcal/mol)	39	0
r_{C-C}	1.480	1.484
$r_{C=C}$	1.340	1.335
r_{C-H}	1.12	1.12
$r_{=C\ H}$	1.12	1.11

An inspection of the propellane surface in Figure 12 suggests that two possible products may result when irradiating 4. The excited triplet can be

formed and can choose to follow either the propellane route by decaying to the desired product or enter the diradical well and follow a secondary surface (see Figure 10) and rearrange to 4 via the Cope pathway. Thus, if the triplet state of 4 happens to be trapped on the undesirable portion of the energy surface it simply undergoes a rapid, concerted return to its original ground state and gets to "try again" as starting material. Compound 4 is a desirable precursor in that it purports to be recyclable in a dynamic sort of reaction.

Dibromo Derivative of 2

A conclusion was made earlier that the half-life of 2 is too short for simple isolation to be viable. Therefore, trapping to form a derivative was chosen--a derivative which would provide definitive evidence that 2 was its precursor.

Hoffmann pointed out that the "backsides" of the bridgehead carbons on 2 have a high accumulation of electron density and are most susceptible to external attack by an electron acceptor such as an acid or halogen.[4] Compound 2, therefore, should be extremely susceptible to halide attack and the derivatives of both the chloro and bromo adducts are stable and easily characterized. Bromination was chosen due to the relative ease of adding the bromine dissolved in an appropriate solvent to the cold, irradiated solution. The proposed reaction end product 1,4-dibromobicyclo[2.2.2]octane, 22, (see Figure 15) was synthesized by an independent pathway described later in the experimental section.

Some mention should be made here of the possibility of the diradical 3 entering into this reaction and forming the identical derivative, 22. In earlier sections we demonstrated that 3 is only the "transition state" of very

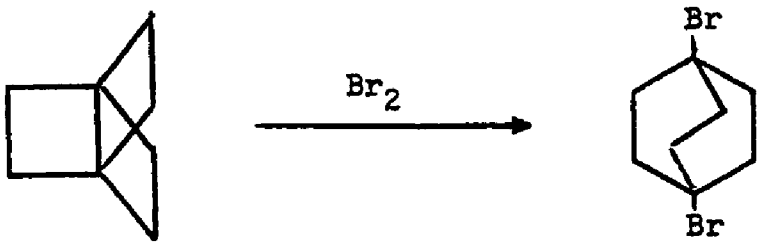

2 22

FIGURE 15. BROMINATION OF 2

rapid Cope rearrangement and, consequently, is not available for secondary reactions. Thus, we can be assured that no diradical will interfere with the derivatization process.

Experimental Approaches

Having determined a starting material and a method of trapping the product, 2, a number of laboratory approaches were devised. The specific irradiation experiments tried were:

A. 4 with $CuCl_2$ in ether

B. 4 in acetone as a triplet sensitizer

C. 4 with Hg in ether as a triplet sensitizer.

A general description of each set of experiments is provided in the subsequent section.

A. Photolysis of 1,4-Dimethylenecyclohexane Cuprous Chloride Complex

An attempt was made to "freeze" 4 into a complex having a geometry favorable for cyclization to 2. A similar complex was reported during the study of the photochemical transformations of 1,5-cyclooctadiene.[18] (See Figure 16a.) The reaction between 1,5-cyclooctadiene and a solution of cuprous chloride in hydrochloric acid gave a precipitate of the complex 23. Evidence of the above complex encouraged our attempts to form a similar complex using 4. The complex is expected to conform to a geometry, 24, suggested in Figure 16b. Complex 24 is, therefore,"frozen" in an ideal geometry for 2+2 cyclization to 2.

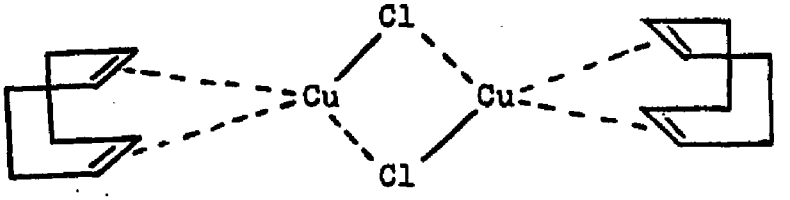

23

FIGURE 16a. CUPROUS CHLORIDE COMPLEX FORMED AS A PRECURSOR TO TRICYCLO[3.3.0.0.^{2,6}]OCTANE

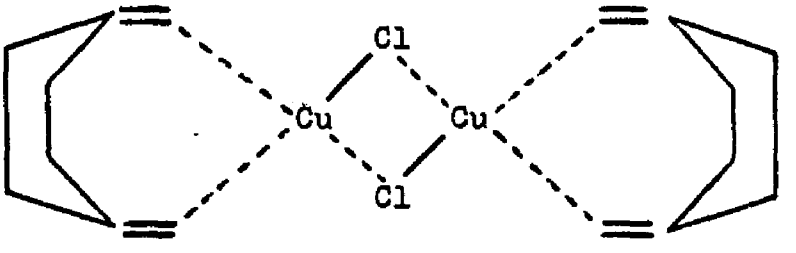

24

FIGURE 16b. CUPROUS CHLORIDE COMPLEX FORMED IN AN ATTEMPT TO SYNTHESIZE [2.2.2] PROPELLANE

B. Triplet Sensitization

The MO calculations suggested that a suitably populated triplet state of 4 should preferentially decay to 2. It is anticipated that the suggested precursor, 4, undergoes chemical reactions from both its lowest singlet state and its lowest triplet states to give different products. Possibly the irradiated molecule cannot absorb enough energy to reach either excited state. A suitable triplet sensitizer has often been used in such situation. A sensitizer would force the population of the triplet state through energy transfer and avoid the singlet reaction entirely. If 2 were formed in this experiment, the intermediacy of the triplet state would become more credible. The following sequence is predicted for the photosensitized formation of 2.

A sensitizer material absorbs enough energy (h) to reach an excited singlet state. It then undergoes "intersystem crossing" to its analogous triplet level. The triplet then encounters a receptor molecule, in this case 4, and imparts its energy to the receptor. The triplet of 4 is then expected to decay to 2. The energy source for our experiments was a custom "Hanovia" low-pressure UV lamp (254 nm). Similar combinations of UV light and triplet sensitizers were successfully demonstrated in experiments desiring photoisomerization of 1,5-cyclooctadiene.[18]

A reasonable experimental design would involve a solution of 4 in a solvent/sensitizer media. Acetone and d_6-acetone were selected as solvents for these experiments. Acetone is an identified triplet sensitizer having a measured triplet half-life (τ_D) of 4×10^7 seconds when irradiated at 320 nm.[19]

C. Mercury Sensitization

Mercury (Hg) has been reported as a useful triplet sensitizer when irradiated in a vapor phase mixture with the starting material.[18] A vapor phase reaction of the compound 4 at low pressure and low temperature was not attempted in this study. Hg was, however, introduced into solutions of 4 dissolved in diethyl ether. These samples were then evacuated at -69 C and sealed. The quartz tubes were then thawed to room temperature and shaken vigorously. Small droplets of Hg were visible on the glass walls of the tube above the liquid layer indicating the presence of an Hg vapor above the liquid also. Although the contact of vapor and liquid was limited, some triplet sensitization at the surface of the liquid was expected to occur.

Results of Syntheses

A. Results of CuCl Complex Irradiation

Bromination of the irradiated solution produced a white solid with a sharp melting point of 131-132°C as compared to the expected 248-249°C for 22. NMR and mass spectral analysis concluded that this solid was 1,4-bis(bromomethyl)-1,4-dibromocyclohexane, 25 (see Figure 17). The yield of this product was approximately 79 percent. No 22 was detected whatsoever by either GLC or NMR. Initial anlysis of NMR suggested the presence of a small peak at $\delta = 2.4$ which might possibly be 22. Addition of authentic 22, however, caused the peak to split with separation of only 1 cps (see Figure 18).

NMR spectra of unbrominated samples analyzed over the entire period indicated only starting materials present in the solution.

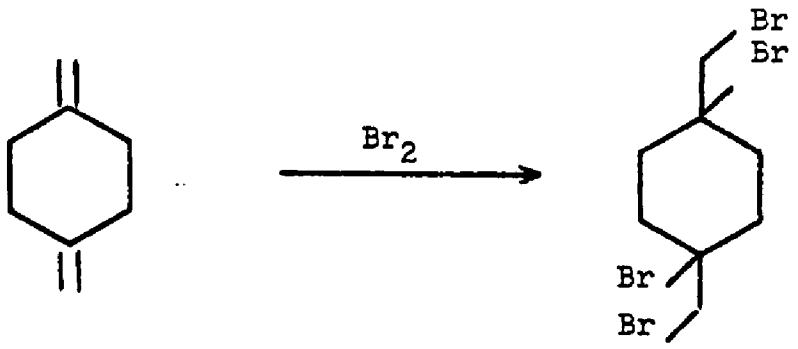

4 25

FIGURE 17. BROMINATION PRODUCT OF 4

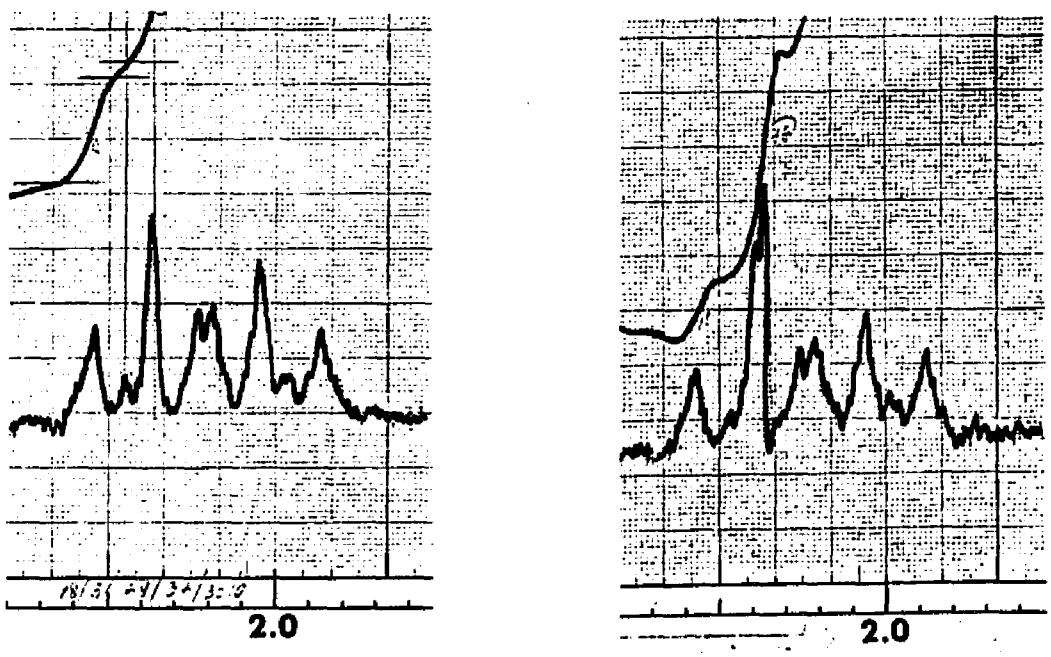

A B

FIGURE 18. A. SUSPECTED NMR DETECTION OF 22

B. AFTER ADDITION OF 22, NOTE DOUBLE PEAK

B. Results of Acetone Sensitization Experiments

Irradiation of 4 in acetone and acetone d_6 produced no evidence of 22 after bromination. An unusual NMR peak at approximately $\delta = 1.3$ was present after 22 hours of irradiation. A negative peak was observed as the sample was left to stand, indicative of a rapidly decaying species. Figure 19 depicts the undefined peak and negative absorption observed on three different samples within a 48 hour period.

Although the signal is located at a possible absorption position for 2 protons, no 22 was identified during the parallel bromination reactions. Therefore, it is not possible to identify 2 in these series of experiments. The identity of this signal can possibly be the subject of another study.

C. Results of Mercury Sensitization Experiments

The NMR spectra of the brominated irradiation product were compared and interpreted for the presence of 22. A singlet at $\delta = 2.41$ was discovered in the irradiation sample which was absent from the dark control. When authentic 1,4-dibromo[2.2.2]octane was added to the sample, the peak increased in intensity (Figure 20a-c).

Table 8 presents the calculated yield of dibromide from four independent irradiation experiments. The yield was observed to increase gradually with increased radiation time. Samples analyzed after 670 hrs demonstrated no further increase in the production of 22.

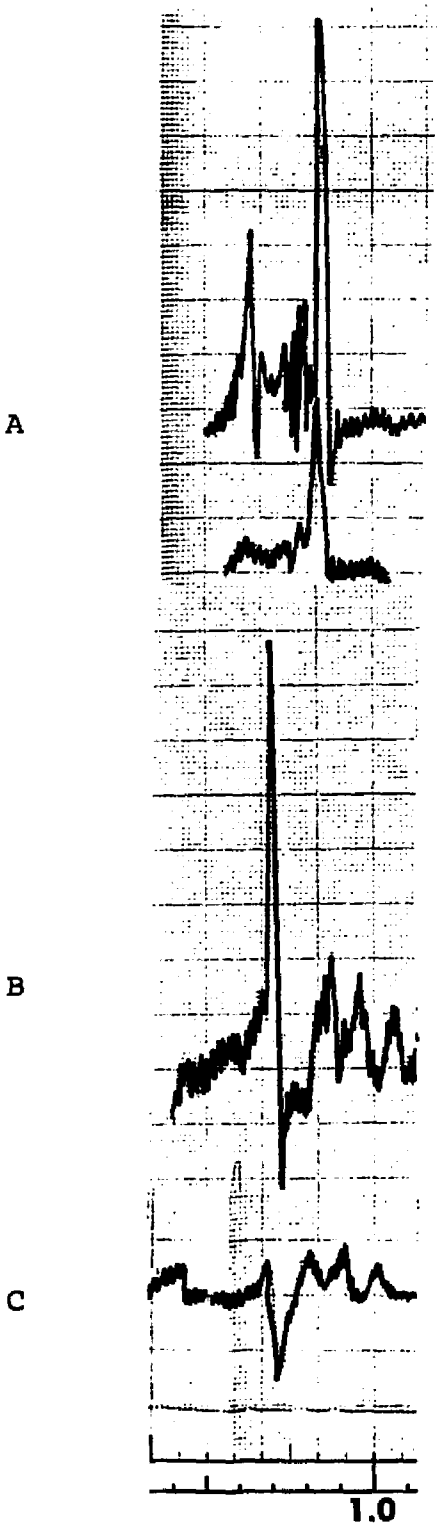

FIGURE 19. UNEXPLAINED BEHAVIOR AT δ = 1.3.
NOTE NEGATIVE PEAKS.

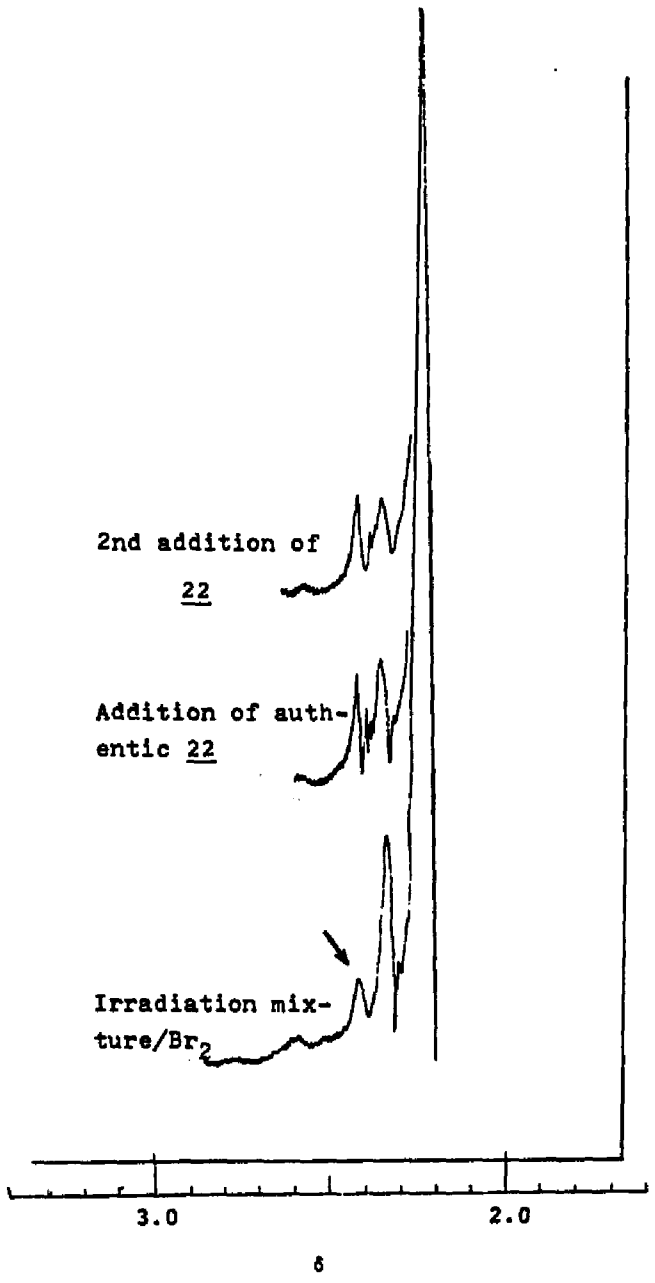

FIGURE 20a. DETECTION OF THE DIBROMIDE BY NMR SPECTROSCOPY. PEAK FOR 22 WAS FOUND AT 2.41 δ. ACTUAL NMR SPECTRA GIVEN IN FIGURES 20b-20c

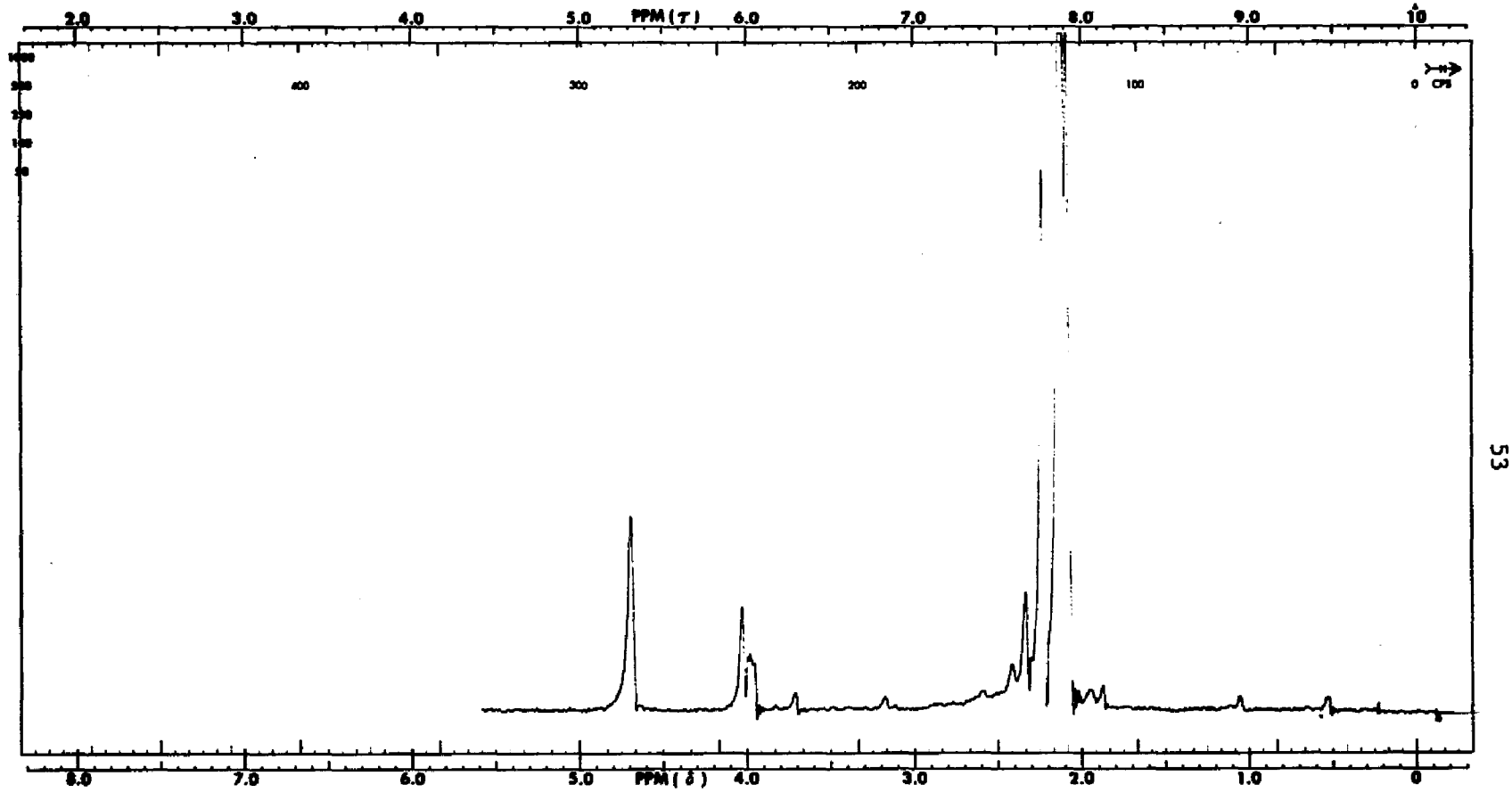

FIGURE 20b. BROMINATED REACTION MIXTURE WITH SUSPECTED PEAK FOR 22 AT ∿2.4 δ

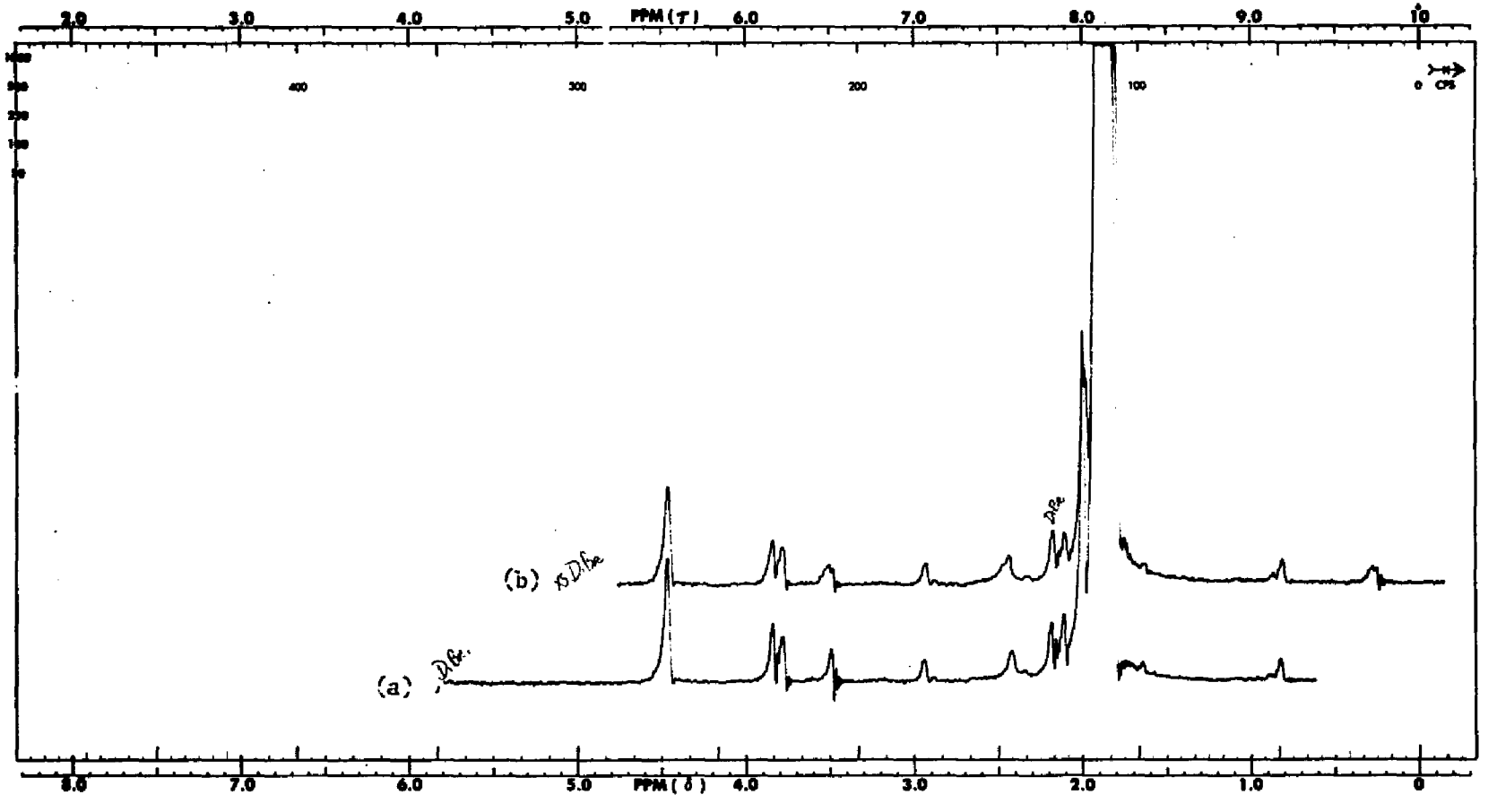

FIGURE 20c. SAME MIXTURE AS IN (b) WITH AUTHENTIC 22 ADDED,

(a) 1st addition of 22
(b) 2nd addition of 22

TABLE 8. YIELD OF 2 RELATIVE TO IRRADIATION TIME

Time of Irradiation	% Yield of 2*
68 hrs	1.40%
67 hrs	1.17%
120 hrs	2.20%
670 hrs	4.50%

*Yields determined by triangulation of NMR peaks for derivations 22.

Gas chromatography analyses were performed on the samples eluted from the column and compared to the authentic 22. With the conditions listed in Figure 21, the retention time for 22 was measured to be 27.5 minutes verifying the actual presence of the brominated derivative.

Mass spectral patterns consistent with a sequence expected for a molecule with two bromines attached. Major peaks were found at 265, 266, 267, 268, 269, and 270 and at 184, 185, 186, 187, and 188 (Figures 22a-b). This compares favorably with authentic 22 (Figure 22b, top).

Carbon-13 NMR spectra of authentic 22 produced a resonance at -61.5 and -36.5 ppm from TMS (Figure 23a). The first of these peaks was also present in the brominated reaction mixture. The second peak was difficult to identify and may be the -37.4 ppm peak (Figure 23b). When a small quantity of 22 was added (doped), both peaks increased in intensity slightly (Figure 23c). Table 9 allows the reader to make comparisons of the irradiated and doped signal intensities and integrals. It should be noted that these reported resonances agree with published spectra of similar compounds.[20]

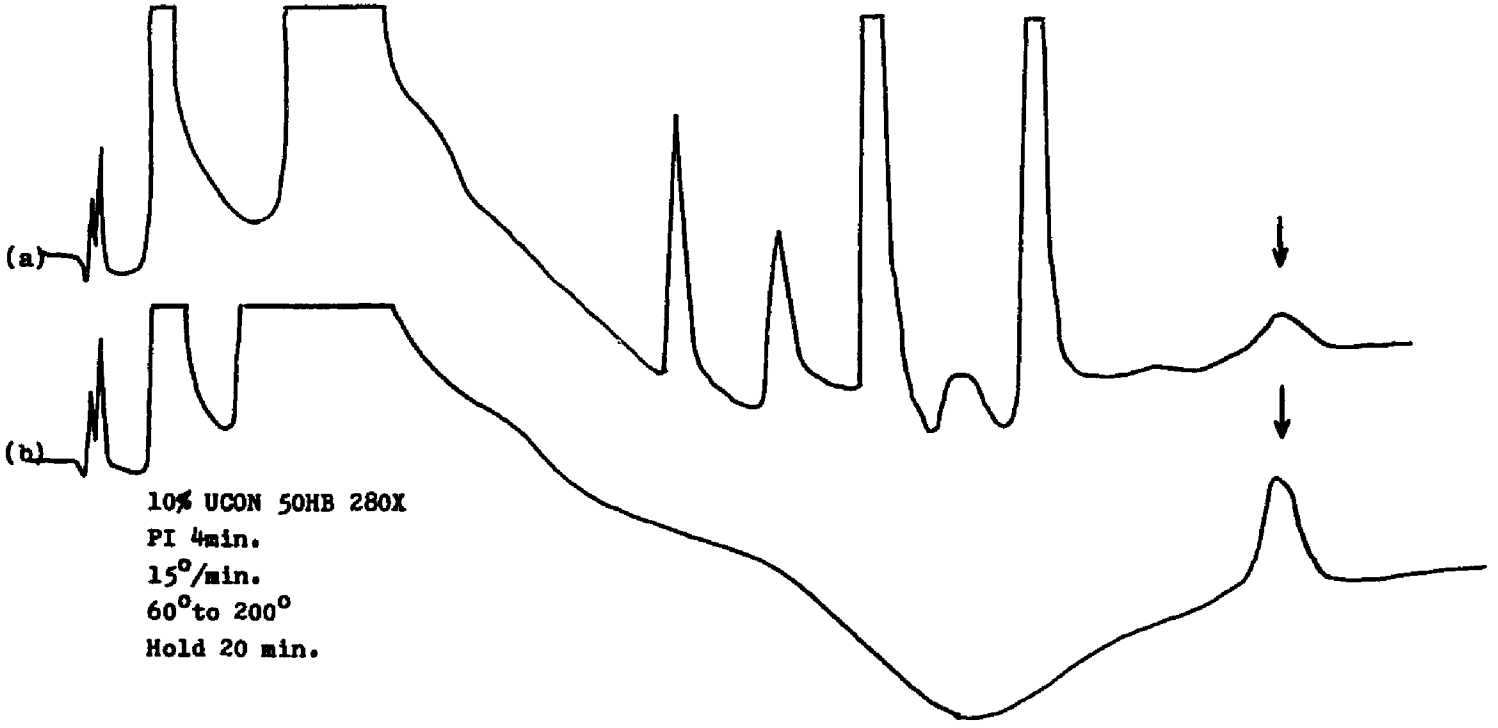

FIGURE 21. GC TRACE COMPARING (a) BROMINATED REACTION PRODUCT AND (b) AUTHENTIC 21, RETENTION TIME 27.5 MIN

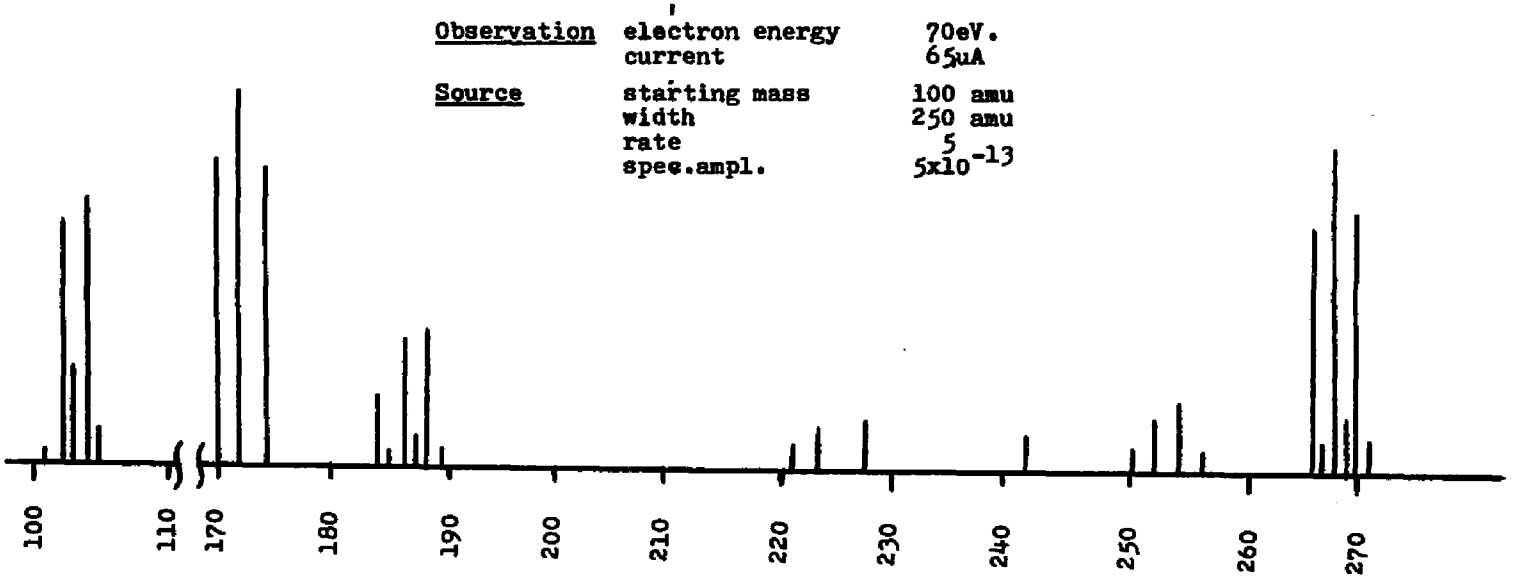

FIGURE 22a. MASS SPECTRUM OF 22 FROM GC SEPARATION. COMPLETE MS SCANS GIVEN IN FIGURE 22b.

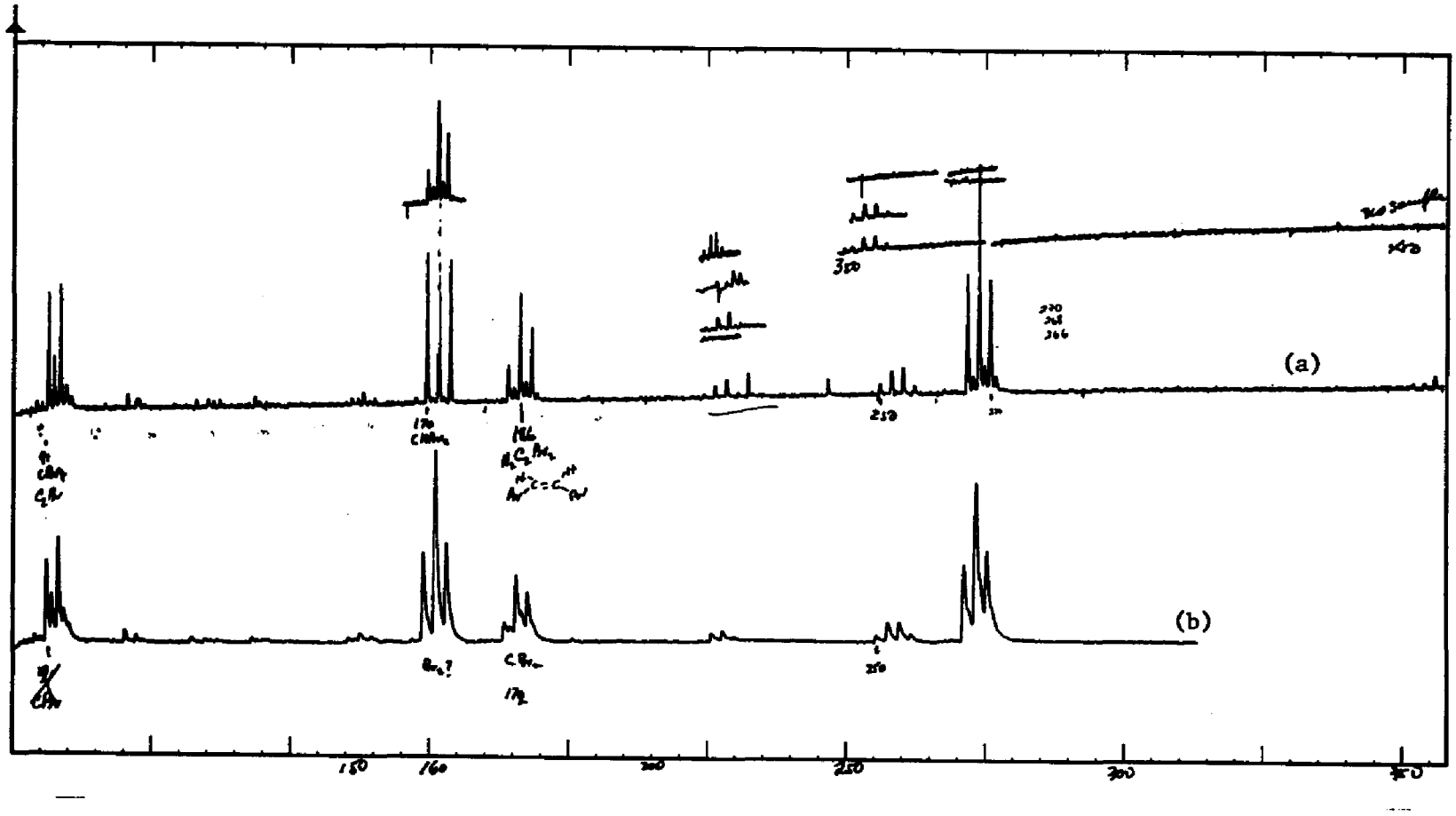

FIGURE 22b. ACTUAL MS SCAN, SAME AS (22a) INDICATING AUTHENTIC 22(a) AND IRRADIATION MIXTURES(b)

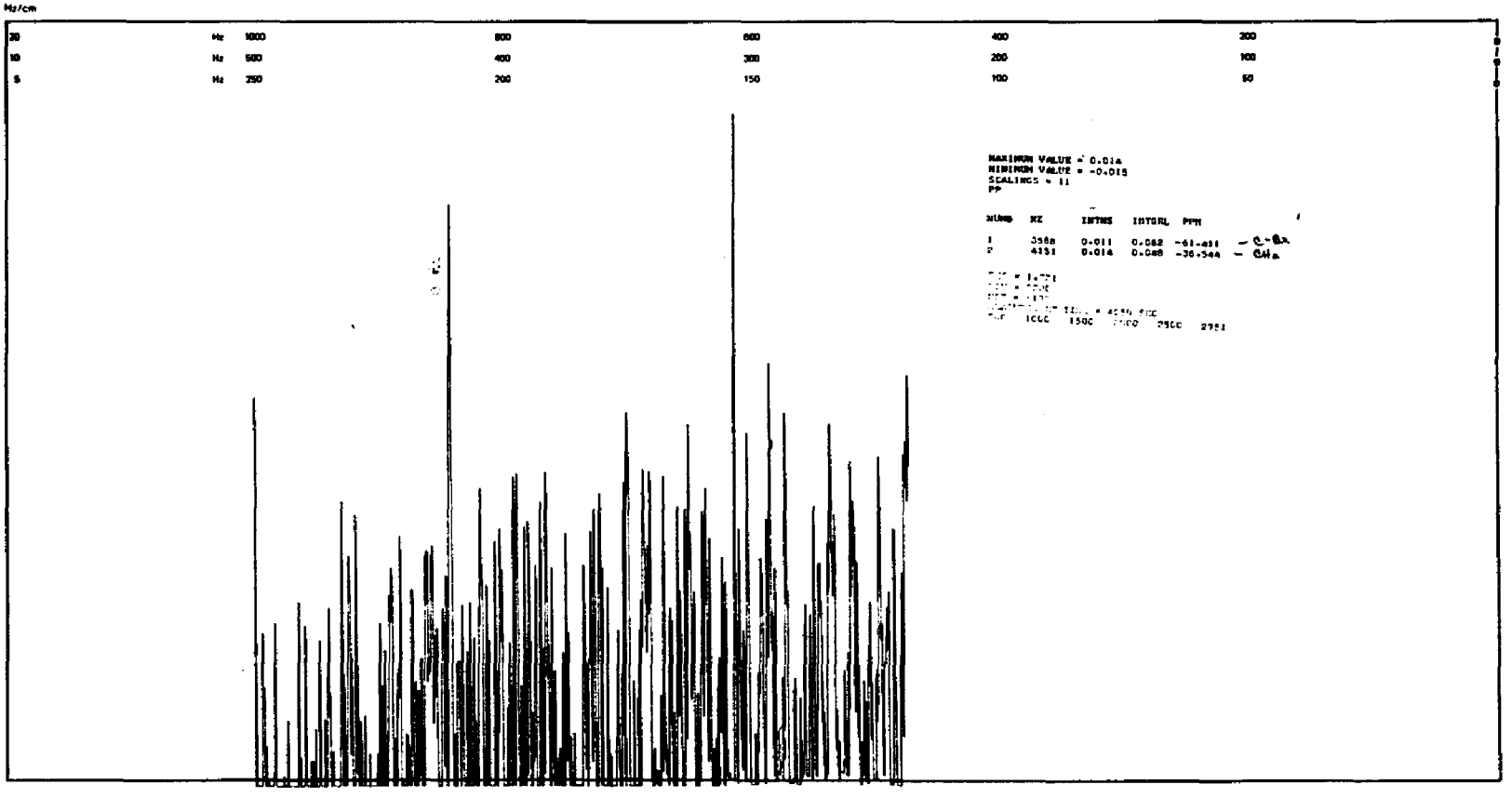

FIGURE 23a. C^{13} NMR, AUTHENTIC 22

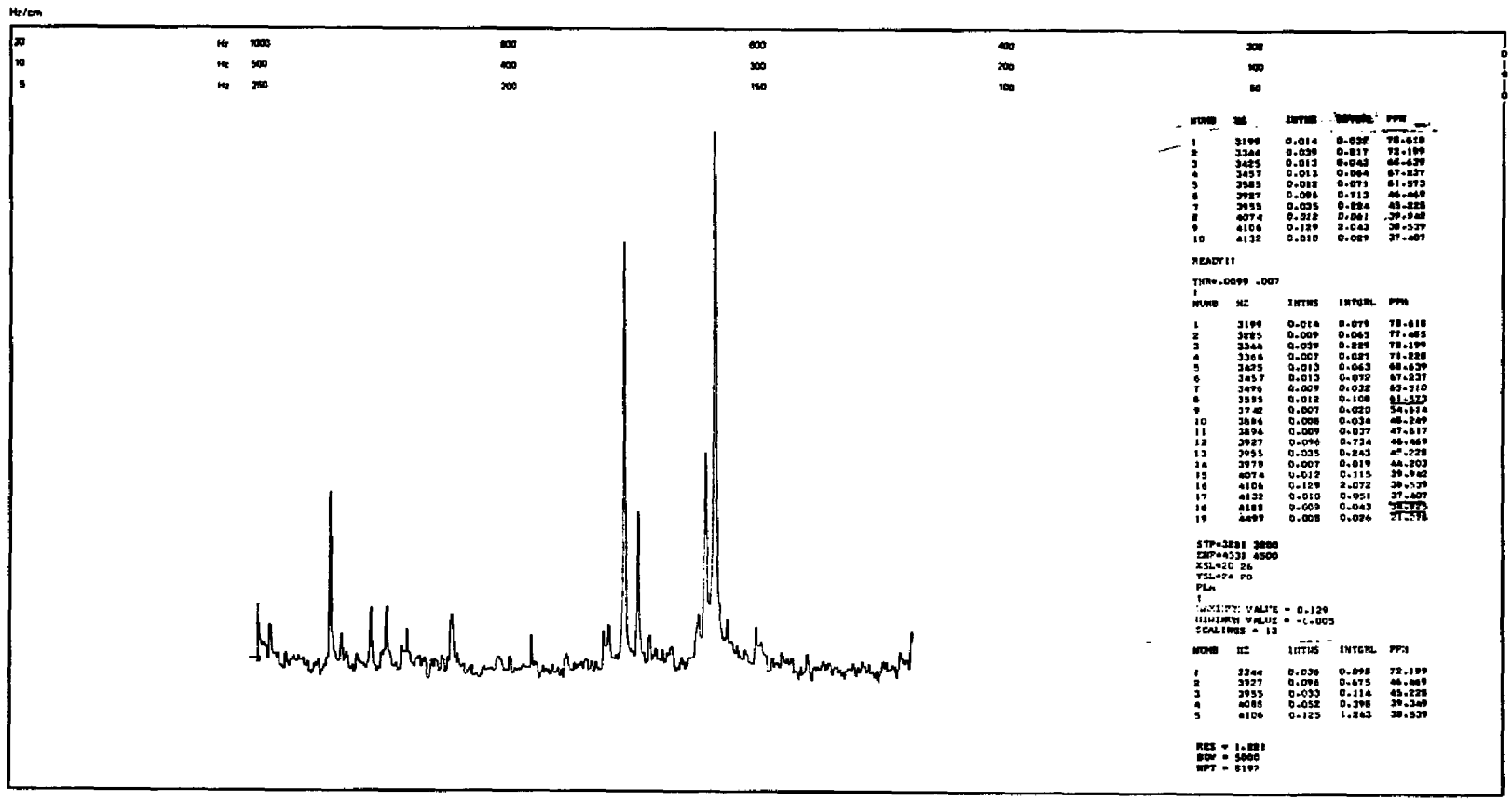

FIGURE 23b. BROMINATED IRRADIATION MIXTURES

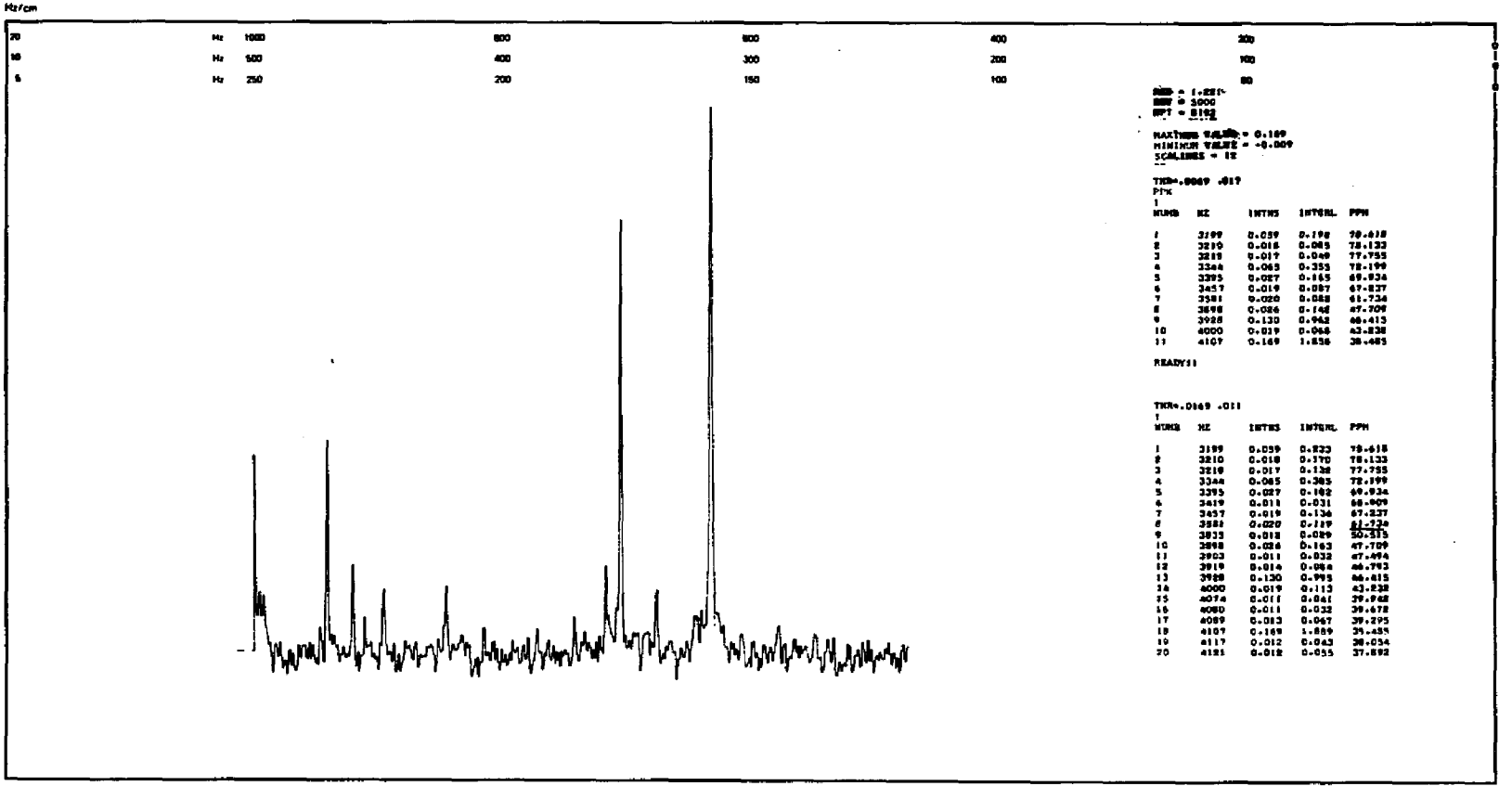

NUMB	HZ	INTNS	INTGRL	PPM
1	3199	0.039	0.198	78.618
2	3210	0.018	0.085	78.133
3	3218	0.017	0.049	77.755
4	3344	0.065	0.355	72.199
5	3395	0.027	0.165	69.934
6	3457	0.019	0.087	67.237
7	3581	0.020	0.088	61.734
8	3898	0.026	0.148	47.709
9	3928	0.120	0.942	46.415
10	4000	0.019	0.068	43.238
11	4107	0.169	1.858	38.485

NUMB	HZ	INTNS	INTGRL	PPM
1	3199	0.039	0.823	78.618
2	3210	0.018	0.370	78.133
3	3218	0.017	0.138	77.755
4	3344	0.065	0.385	72.199
5	3395	0.027	0.182	69.934
6	3419	0.011	0.031	68.909
7	3457	0.019	0.136	67.237
8	3581	0.020	0.119	61.734
9	3833	0.018	0.029	50.515
10	3898	0.026	0.163	47.709
11	3903	0.011	0.032	47.494
12	3919	0.016	0.084	46.793
13	3928	0.130	0.995	46.415
14	4000	0.019	0.113	43.238
15	4074	0.011	0.041	39.968
16	4080	0.011	0.032	39.678
17	4089	0.013	0.047	39.295
18	4107	0.169	1.869	38.485
19	4117	0.012	0.043	38.034
20	4121	0.012	0.055	37.892

FIGURE 23c. BROMINATED IRRADIATION MIXTURES WITH ADDED 22

TABLE 9. A COMPARISON OF INTENSITY AND INTEGRATION OF SIGNALS FROM C_{13} NMR OF IRRADIATED PRODUCT SOLUTIONS AND THE SAME SOLUTIONS DOPED WITH A SMALL QUANTITY OF 22

	Intensity		Peak Integration	
ppm	Irradiated	Doped	Irradiated	Doped
61.573	.012	.020	.108	.119
37.407	.010	.012	.051	.055

A low temperature proton NMR was taken of a sample immediately after irradiation. An absorption at $\delta = 1.98$ was sharp and exhibited a CIDNIP negative peak (Figure 24). A decay in the signal was observed after approximately 45 minutes. The sample was warmed to room temperature and recooled to -30 C with no return of the signal. For verification, the experiment was duplicated with similar results.

Discussion

The mercury sensitization reaction is a rather inefficient though successful method for synthesizing 2. The overall yield of the propellane was only 2 to 3 percent after 120 hours of irradiation and 4 to 5 percent after 600 hours as determined by integration of proton NMR spectra (see Table 9). The yield increased with increasing length of radiation time up to about 4.5% before leveling off, indicating that the precursor to the dibromide must have a considerable half-life at the low experimental temperatures. An NMR

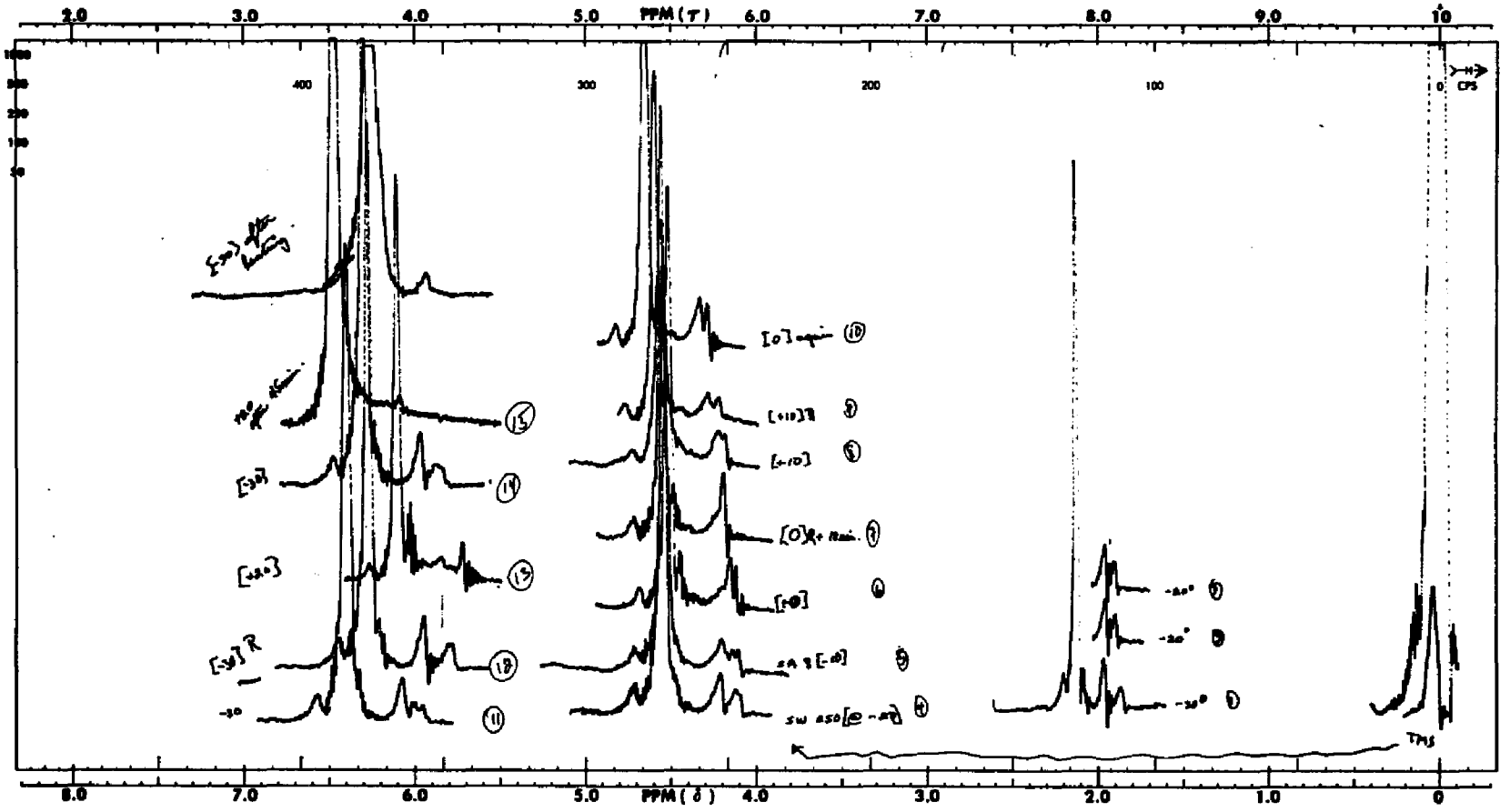

FIGURE 24. MONITORING OF CIDNIP SIGNAL AT ∿1.98 δ

absorption at δ = 1.98 is an acceptable position for a signal of a strained hydrocarbon such as 2.

Acetone sensitization was unsuccessful in producing 2 in a measurable quantity as was the copper complex experiment. In all cases, the solution always remained clear and colorless with no evidence of polymerization even after prolonged periods of irradiation. The polymerization would be present the reactions were operating free radical species which were subsequently polymerizing. Therefore, it is unlikely that the dibromide could result from bromination of a diradical such as 3.

Conclusion

A considerable amount of evidence was presented in the preceding section indicating the existence of 2 in the reaction mixture. Several experiments were repeated and the results were consistent. The trapping of the dibromide product, 22, was indicative of the presence of 2 in the reaction mixture. The evidence consists of the detection of a small yield of a derivative product 22 and a signal in the NMR region expected for 2. The presentation of the evidence is based on the interpretation of GLC, NMR and MS signals in the presence of strong responses from side products. No comparison of known spectral information of 2 could be made, and only a small quantity of 22 was available for characterization. The evidence is therefore interpreted for the presence of 2 although 2 itself has not been isolated.

The indication that 2 has been synthesized in this thesis work is supported by the consistency of the data resulting from repetitive and diverse experiments. The analysis of GLC, NMR, and MS data all yielded the same

results on repeated trials. This evidence is supported by NMR data suggesting the presence of 2 in the solution and observing its decomposition as predicted by theory.

The true value of this study has been the demonstration of the usefulness of a semiempirical calculation in the prediction of an experimental synthesis approach. The INDO calculations did indeed suggest a unique experimental approach for synthesis of 2. The approach of producing an intermediate having a triplet state configuration of 4 had not been tried in any of the numerous synthesis attempts prior to this study. Based on the evidence presented, this approach was successful in demonstrating that 2 was indeed synthesized.

Experimental

Apparatus

The light source was a custom Hanovia, low pressure mercury UV lamp in a coil configuration. Irradiations were performed in a wide-mouth dewar flask containing recirculating methanol at -20 C. The tubes and lamp were immersed in the methanol and irradiation was conducted for fixed time periods. Multiple tubes with identical contents were used to allow sampling at varying time periods in an attempt to optimize time for irradiation.

A custom-made, light shroud, fabricated of heavy duty dark green canvas was sewn over an aluminum frame and served as the reaction chamber. The shroud was designed to allow easy access to the sample tubes for shaking or withdrawing samples through a small opening, precluding the need to shut off the lamp unnecessarily. It also provided eye protection for other persons in the laboratory.

To insure maximum light transmission, experiments were typically run in quartz tubes. Also, solvents such as diethyl ether and carbon-tetrachloride were used due to their low absorption of UV. The quartz tubes containing the reactants were attached to a vacuum manifold, frozen, and pumped to 0.5 mm Hg vacuum. The process is best described as a series of "freeze, pump, thaw" steps. The tubes were then sealed with a torch while under vacuum prior to irradiation.

Authentic compound 4 was purchased from the Chemical Samples Company. The boiling point was measured at 121-122°C; melting point, -20.5 to -20°; n_D^{20}, 1.4721; d_{20}, 0.821.

A. Irradiation of 24

CuCl was prepared from the more common $CuCl_2$.[21] A saturated solution of $CuCl_2$ (500 ml) was placed in a three neck, round bottom flask containing copper foil. (Copper foil is much easier removed at the completion of the reaction than pellets or dust.) The flask was equipped with a nitrogen inlet tube and an exit oil bubbler. Without an inert atmosphere, a green impurity forms, presumably $CuCl_2$. The reaction mix was refluxed for 24 hours. Positive nitrogen pressure was maintained as water was slowly added to wash out the excess $CuCl_2$ without disrupting the white crystal. The solubility of the CuCl is 0.0062 g/100 ml, as compared to $CuCl_2$ which is 70.6 g/100 ml. The water is agitated to disperse the crystal and transferred to a separatory funnel where diethyl ether is added. The water is then removed and the ether/CuCl saturated solution is retained.

A solution containing 4.1 g (38 mmoles) of 4 in 300 ml of the CuCl saturated ether was prepared. Solutions were analyzed using a Carey UV

spectrophotometer. The complex 24 was detected by UV absorption at 285 nm. Absorptions for 2 at 250 nm and CuCl at 295 nm were also measured. The solutions were then sealed in quartz reaction tubes as described above and the tubes introduced into the methanol bath and allowed to equilibrate to -15 C.

The solutions of 4 dissolved in diethyl ether and saturated with cuprous chloride were irradiated for approximately 220 hours at -15 C. Reaction tubes were removed at 24, 47, 78, 110, 124, 198, and 214 hours. Ten milliliters of cold carbon tetrachloride was added and the ether was removed on a rotary evaporator at $0^{\circ}C$ and 5 mm Hg pressure. The cold carbon tetrachloride solutions were then decanted into chilled NMR tubes, immersed in a dry-ice acetone bath and sealed. These frozen tubes were then inserted into the probe of a Varian A60D, 60 MHz NMR spectrometer. Samples were allowed to return to room temperature in a controlled manner and spectra taken periodically over a 24 hour period. The resultant spectra showed only starting material, 4, present; NMR (CCl_4, 60 MHz) δ = 4.67 (4H, s), 2.2(8H, s).

To two samples, 198 and 214 hour irradiations, an equal volume of Br_2 in CCl_4 (chilled) was added immediately after irradiation. The samples were then prepared for analysis by evaporation of the solvent and excess Br_2 using a rotary evaporator at 5 mm pressure. The remaining residue was redissolved in $CDCl_3$ and decanted into an NMR tube.

The NMR spectra was analyzed for the presence of 22 unsuccessfully. Similar results were received by GLC analysis using a 5 ft, 10 percent UCON, 50 HB-280 X (60-80 mesh) column, programed at 15 /min. from 60 to 200, post injection delay of 4 minutes. The authentic peak for 22 was found to have a retention time of 27.5 minutes under the above conditions. No 22 was discovered by NMR or GLC.

The residue from the evaporation step was isolated by fractional crystallization from acetone: ether (1:1) by rotary evaporation and subsequent filtration. A white crystalline solid was separated having a melting point of 131°-132°C. This melting point compares favorably with the published value for 25, 1,4-bis(bromomethyl)1,4-dibromocyclohexane.[16b]

B. Acetone Sensitization

Acetone as a sensitizer seemed a good initial choice since both the triplet state energy and intersystem crossing efficiency are high. A solution containing 9.1 g (50 mmoles) of 4 in 100 ml of distilled acetone was irradiated as described above. A single tube was removed at 12 hour intervals, up to a maximum of 72 hours. The experiment was duplicated using acetone D_6. Each of the tubes were divided into two aliquots; one directly frozen in a dry-ice/acetone bath and slowly warmed as NMR spectra were run; the second was brominated with a cold bromine/ether solution and analyzed by both GLC and NMR. The experimental procedures were similar to those described above.

An NMR singlet was seen (δ = 2.41,s) in one case, which suggested the presence of 22. Addition of authentic 22, however, caused the signal to split with J=1 cps. An unusual signal at δ = 1.3 was observed, however, subsequent bromination could provide no evidence of 22.

C. Mercury Sensitized Photolysis of 4

In this series of experiments, concentrations ranging from .5 M to .74 M solutions of 4 in ether were sealed in evacuated quartz tubes with 0.5 grams of distilled mercury metal included as a triplet sensitizer. After shaking

the sample vigorously to get the mercury vapor above the liquid, the solution was irradiated at -20°C. Evidence for the mercury in the gas phase was seen as beads of mercury condensed on the glass walls. The total time for irradiation at 254 nm was 600 hours during which the tubes were removed twice a day and the solutions agitated by shaking for a few seconds to keep the mercury in the gas phase. After irradiation, the tubes were opened and the liquid portion decanted into a cold solution (0°C) containing bromine in diethyl ether. The ether layer was washed with a dilute solution of silver nitrate. The excess bromine was removed as AgBr, the organic residue was dried of solvent and a proton NMR spectrum was run in distilled chloroform. A control was established consisting of the identical components and concentrations found in the irradiated samples; however, not subjected to irradiation. The controls were processed in an identical manner.

Gas chromatography was used to verify the existence of the dibromide using a 10 percent UCON, 50 HB, 250 X column for the analysis. A temperature program from 60-200°C, a rate of 15 degrees/minute, preinjection time of 4 minutes, and a post injection time of 20 minutes was set for GLC operation. Under the above conditions, the retention time for authentic 22 was measured at 27.5 minutes. Small quantities of the dibromide were trapped from the GLC effluent using capillary tubes adapted for this purpose.[22] Chloroform was eluted through the capillary and dripped directly onto a hot, solid inlet of a mass spectrometer. Brominated samples were sealed in NMR tubes and sent to both the Stauffer Chemical Company for C_{13} NMR analysis and Columbia University for mass spectral analysis. C_{13} resonance for authentic 22 were found to be -61.4 cps, (-C-Br) and -36.5 (-C-H_2). Sample unknowns exhibited similar peaks at -61.6 and -37.4 cps. Mass spectral analysis yield peaks at m/e =

270, 269, 268, 267, 266, 265, and 188, 187, 186, 185, 184. Similar patterns were identified for the effluent collected from the GLC for the suspected 22.

D. Preparation of 1,4-Dibromobicyclooctane, 22

Authentic 22 was prepared in a multi-step process. Each step is described in detail below and depicted graphically on Figure 25.

1,4-Dicarbethoxy-2.5 Diketobicyclo [2.2.2] octane, 27.[23] Sodium hydride, (20 g, 0.83 mmole) dispersed 50 percent in mineral oil was suspended in 211 ml of monoglyme in a standard taper, three neck flask fitted with a condenser and additional funnel. The apparatus was purged with nitrogen gas at positive pressure. Distilled t-Butanol (1.3 g) was added and the temperature raised to 60°C. Diethyl succinate (160 g, 0.9 mmole) was added at a slow rate to control the evolution of hydrogen gas.[26] It was necessary to stir the reaction in an ice bath to prevent the temperature from exceeding 60°C. Stirring was continued for an additional hour at which time H_2 evolution ceased. An additional 200 ml of glyme was added, the nitrogen turned on, and the reaction was stirred at room temperature for 9 hours. Glyme and ethanol were distilled "in vacuo". The residue had a characteristic red color indicating the presence of the disodium salt of 27. Dry 1,2-dibromoethane (160 ml) and monoglyme (100 ml) were added to the flask and the temperature was raised to 80-90°C. The course of alkylation was followed by the determination of the pH of hydrolyzed samples. The reaction was complete in 72 hours. Dibromomethane and monoglyme were removed by steam distillation and the residue crystallized. Mineral oil was removed by washing with cyclohexane. The product was recrystallized from ethanol and washed with

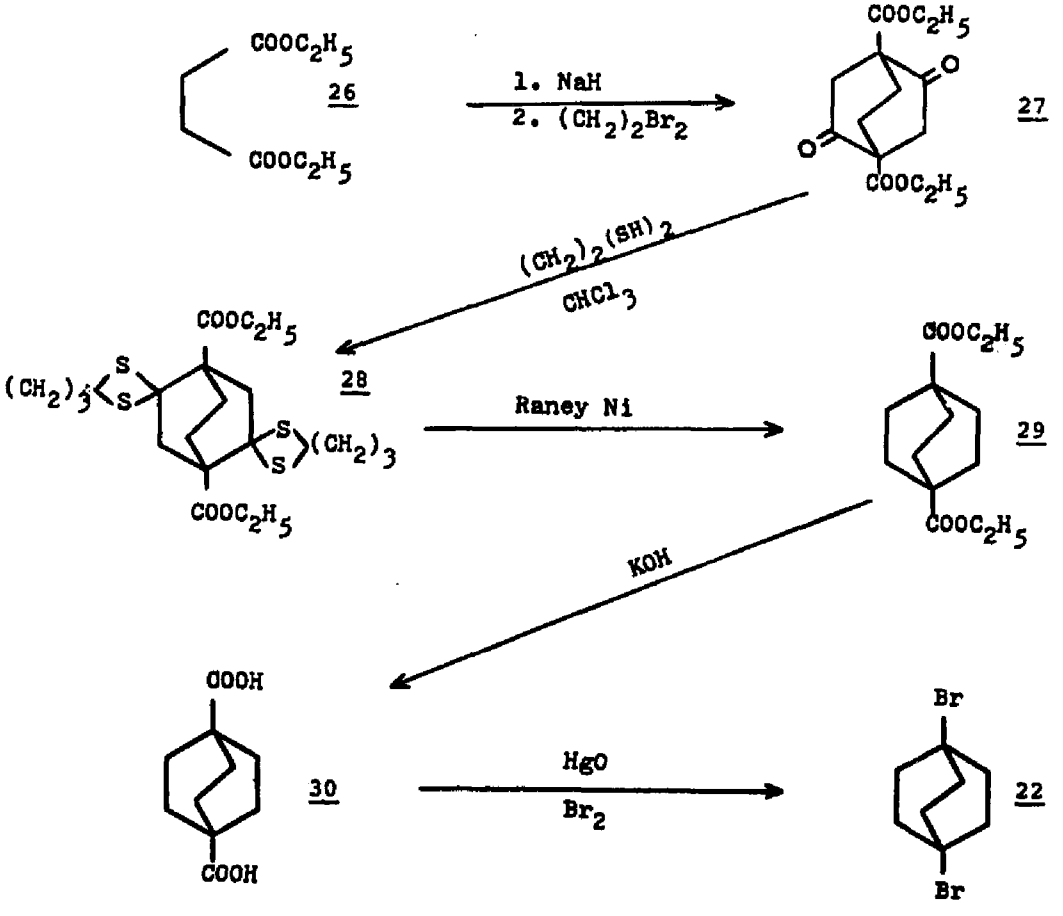

FIGURE 25. SYNTHESIS PATHWAY USED FOR THE 1,4 DIBROMOBICYCLO [2.2.2]OCTANE

dilute potassium hydroxide. A second recrystallization gave a product with m.p. = 107°C (lit 111-112°C). Sublimination at 100°C and 1 mm pressure gave 9.0 g (.032 mmole) of a white solid with a sharp m.p. of 112°C. Yield 10.6 percent.

Bis-(trimethylene)mercaptol of Dicarbethoxy-2.5 Diketo Bicyclo[2.2.2] octane, 28.[24] The diketoester 27 (7 g, 2.5 mmoles) was dissolved in a minimum amount of chloroform in a separatory funnel, propanedithiol (10.8 g, .010 mmole) was added and HCl gas was bubbled through the mixture for 7 hours at 0 C. The solution was washed with 25 ml portions of 2N sodium hydroxide solution until no further reaction occurred, then washed with water, dried over sodium sulfate, concentrated, and heated at 100°C, 20 mm for 1 hour. The resulting oil was dissolved in n-hexane and the mixture refluxed until a white solid appeared (6 days). The solution was filtered hot and air dried. 4.4 g (.009 mmole) of product was collected with m.p. 120°C. Yield 38 percent (lit 81 percent).

Diethyl Bicyclo[2.2.2]octane-1,4-Dicarboxylate, 29.[24] The mercaptol 28 (4 g, 8.7 mmoles) was refluxed for 48 hours with 60 g of Raney nickel in 50 ml of 95 percent ethanol. The nickel was filtered, the solvent removed through a 20 mm Vigreux column and the residue was removed by vacuum distillation yielding 1.36 g (b.p. 160° C at 5 mm). An additional 0.14 g of material was obtained by using a soxhlet extractor and an ether mixture with the filtered Raney nickel. Total yield was 1.50 g (6 mmole). Yield 68 percent (lit 70 percent).

Bicyclo [2.2.2] octane-1,4-Dicarboxylic Acid, 30.[25] A solution of potassium hydroxide (0.44 g, 8 mmoles), the dicarboxylate, 29 (1.50 g, 0.006 mmole), and 100 ml of ethanol was refluxed for 12 hours then cooled and diluted with 150 ml of water and acidified with 3 M HCl. The thick white product was collected and washed with ethanol and ether giving the dicarboxylic acid product, (0.453 g, 2.3 mmole). Yield 28 percent, m.p. 410-418°C (lit 422°C dec.).

1,4-Dibromobicyclo[2.2.2]octane, 22.[25,26] A solution of bromine (0.634 g) in 1,2-dibromoethane (4.8 ml) was added slowly through a microaddition funnel to a mixture of red mercuric oxide (0.612 g, 2.8 mmoles) and the dicarboxylic acid (0.4 g, 2.0 mmoles) in 14.4 ml of 1,2-dibromoethane at 75°C. Stirring at this temperature was continued for 12 hours. The mixture was filtered and the solid was washed with ether and benzene. The combined filtrates were washed with dilute sodium bisulfite, dilute sodium hydroxide, water, and dried over anhydrous sodium sulfate. Evaporation and sublimination (120°C, 5 mm) gave the desired product (0.2164 g, .8 mmole). Yield 40 percent, m.p. 246-249°C (lit 256-258°C). NMR spectrum in chloroform showed a singlet at δ = 2.40. Analysis: H = 2.81 percent, C = 17.2 percent, and Br = 28.96 percent by weight.

CHAPTER III

REFERENCES

(16a) Lambert, A. J. Amer. Chem. Soc. 1967, 89, 1836.

(16b) Lantenshlaeger, F., Wright, C F. C~n. J. Chem. 1963, 41, 1972.

(17) Allinger, N. L.; Freiberg, L. A. J. Amer. Chem. Soc. 1960, 82, 2393; 1966, 88, 2999.

(18) Srinivasan, R. J. Amer. Chem. Soc. 1964, 86, 3318.

(19) Turro, N. J. Molecular Photochemistry, W. A. Benjamin, Inc., New York, 1965, p. 119.

(20) Maciel, G. E.; Dorn, H. C. J. Amer. Chem. Soc. 1971, 93, 1268.

(21) Chatt, J.; Venazi, L. M. J. Chem. Soc. 1957, 4735.

(22) Bulkin, B. J.; Dill, K.; Dannenberg, J. J. Anal. Chem. 1971, 43, 974.

(23) Holtz, H. D.; Stock, L. M. J. Amer. Chem. Soc. 1963, 86, 5183.

(24) Roberts, J. D.; Moreland, W. T., Jr.; Frazer, W. Ibid. 1953, 75, 637.

(25) Dewar, M.J.S.; Gordberg, R. S. Ibid. 1970, 92, 1582.

(26) Baker, F. W.; Holtz, H. D.; Stock, L. M. J. Org. Chem. 1963, 28, 514.

CHAPTER IV

SYNTHESIS AND REACTION OF 2,2,3,3-TETRADEUTERO [2.2.2] PROPELLANE

Experimental Design

To prove the prediction of the INDO calculation that the triplet state isomer 21 was the source of 2, an experiment was devised which would measure the half-life of a deuterated version of the triplet, 31. The description of this experiment and the related synthesis of 1,1,6,6-tetradeuterodimethylenecylohexane, 32, are presented in this chapter.

The fragmentation of 2 can occur in any of three positions: C_2-C_3, C_5-C_6, or C_7-C_8 in the irradiation raction of 32. For 4, the ring protons produce an NMR singlet at $\delta = 2.14$ and the methylidine protons at $\delta = 4.70$. The latter resonance should be absent in 32. Any evidence of a signal at the 4.7 cps region of the NMR after irradiation would indicate that 31 had been present in the reaction and had thermally rearranged to 33 or that, in the least, we had passed through the Cope transition state under the conditions of irradiation. The products from this reaction were studied on the mass spectrometer specifically searching for the C_2D_2 fragment as evidence of rearrangement of 32 proceeding through 34 to form 33. The synthesis of 32 is given in the experimental section at the end of this chapter.

A graphic depiction of the possible mechanisms involved in the propellane reaction is presented in Figure 26. The selectively deuterated form of 4, 32, is used in this reaction scheme to demonstrate the ability to

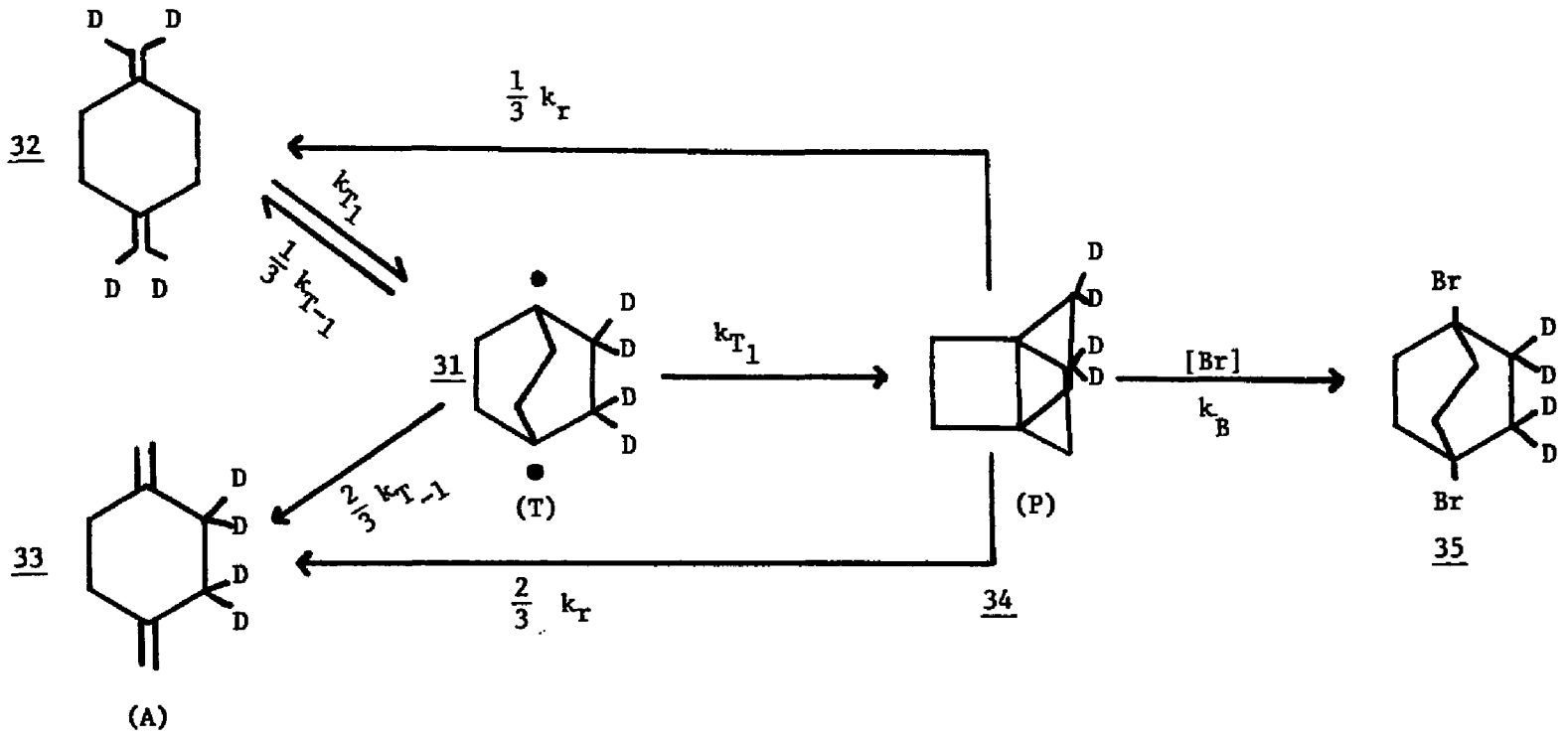

FIGURE 26. DECRIPTION OF THE POSSIBLE MECHANISM INVOLVED IN THE PROPELLANE SYNTHESIS AND TRAPPING

measure a half-life for the triplet intermediate, 31, directly by measuring the yield of Cope product 33. Once the concentration of 33 can be determined in a reaction such as described, this value can be used to determine the dependent rate of formation of 31.

Descriptions of Experiments

Synthesis of 32 by Wittig Reaction

Two modified Wittig reactions were attempted initially for the synthesis of 32 starting with 1,4-cyclohexane dione and deuterated methyl iodide. Although the desired product was achieved in good yield, in a 24 hour period, the molecule was observed to scramble deuterium atoms. The scrambling was identified by following the rapid growth of the associated NMR signal at 4.7 cps. Figure 27 depicts the reaction path expected in the synthesis.

Reverse Deuteration of 4

The possibility existed that deuterium exchange may be catalyzed by any one of a group of impurities involved in the Wittig synthesis. Possibly the same impurity could catalyze the reverse reaction, i.e., the deuteration of 4 in a deuterated solvent. The following solutions were prepared in the NMR sample tubes and their spectra recorded daily for 3 days and on the 8th day:

- 4 in d_6 DMSO (dimethyl sulfoxide)
- 4 in d_6 DMSO with triphenylphosphine
- 4 in d_6 DMSO with triphenylphosphine oxide
- 4 in d_6 DMSO with sodium metal (basic condition)
- 4 in d_6 DMSO with dilute d_2 sulfuric acid in D_2O.

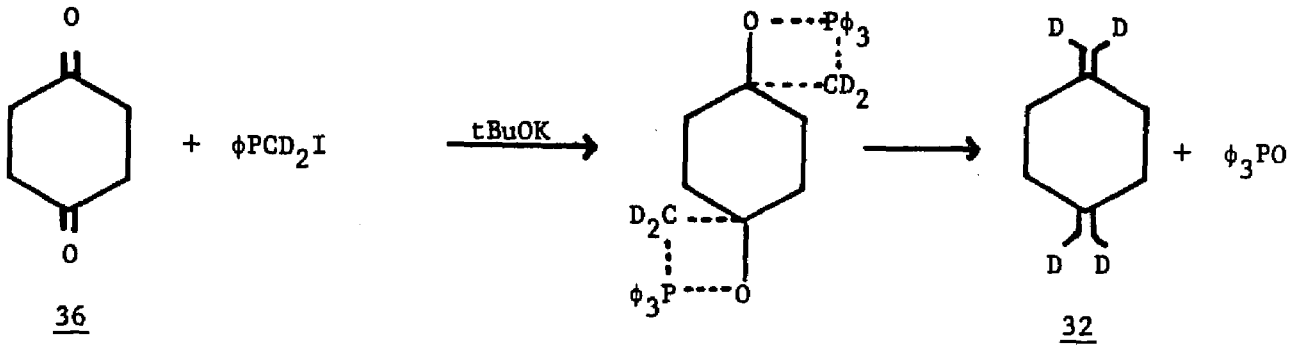

FIGURE 27. MODIFIED WITTIG REACTION FOR THE SYNTHESIS OF 32

Each sample was analyzed by NMR to determine if there was any change in the proton ratios of the exocyclic methylene protons versus the cyclic protons.

An Alternative Synthesis of 32

An alternative pathway (see Figure 28) was selected which required the reduction of the diester 37 to 1,4-dimethanol cyclohexane 38. Tosylation of 38 yields 40. Treatment with NaI in acetone and subsequent dehalogenation did yield 4 and in the final synthesis, 32. In an initial synthesis attempt, the dehydrobromination of 38 to 32 was effective, but the bromination of the dimethanol 38 could not be accomplished. Thus the recommended synthesis path was through the tosylate, 40, and iodide, 41, derivatives.

Irradiation of 32

An experiment identical to the irradiation of 4 (described in Chapter III) was performed using the newly synthesized 32. A number of sample tubes were prepared for comparison. These solutions consisted of:

Samples a. 4 stored cold and dark

b. 32 stored cold and dark

c. 32 stored in an evacuated tube, cold, 0.5 gms Hg, dark

d. 32 irradiated 15°C for approximately 216 hours, 0.5 gms Hg.

Results

Synthesis of 32

Yield of 32 by the Wittig reaction was 85 percent. Although the synthesis was successful, within 24 hours, scrambling of the deuterium was observed by NMR (peak at 4.7 cps).

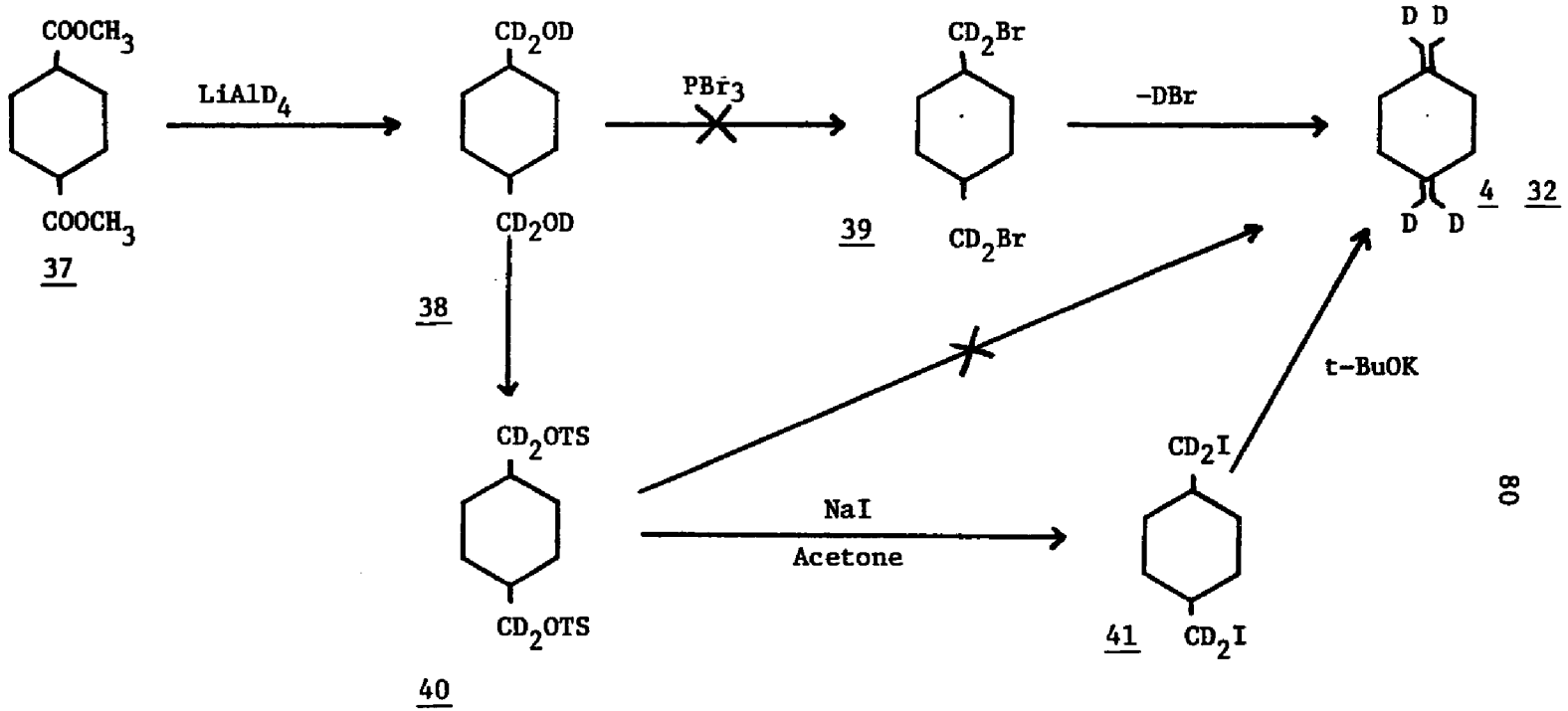

FIGURE 28. ALTERNATIVE SYNTHESIS OF 4 and 32

The subsequent experiment to attempt reverse deuteration of 4 by intervention of suspected impurities also failed. NMR analysis gave evidence for only starting material. The alternate synthesis path produced yields shown in Table 10.

TABLE 10. PERCENT YIELD FOR SYNTHESIS OF 32
(R IS 1,4 SUBSTITUENT)

Compound	R	% H Yield	% D Yield
37	$-COOCH_3$	-	-
38	$-CD_2OH$	36	78
40	$-CD_2OTS$	67	49
41	$-CD_2I$	92	84
32	$=CD_2$	42	75
Overall Yield		8.9	25

Irradiation of 32

The brominated irradiation product was analyzed for the presence of 35 by GLC as described earlier. A 5.56 percent yield was calculated by triangulation of the appropriate peak. The peak was absent from the dark control sample analyzed in an identical manner.

NMR of the unbrominated portion presented a roughly symmetric quartet at 272 Hz with J=7 Hz. The expected exocyclic methylene absorption is at 280 Hz (δ= 4.7) for the nondeuterated sample. The unirradiated control sample produced identical mass spectra to the unbrominated sample with no obvious effect of the mercury in the absence of light. A list of peaks is presented in Table 11.

TABLE 11. FRAGMENTATION PATTERN FOR 1,4 DIMETHYLENE CYCLONEXANE

Fragment	Group	4	32
C_8H_{12}	i	109-105	113-105
C_7H_{10}	ii	94-91	98-91
C_6H_8	iii	81-87	84-77
C_5H_8	iv	67-62	72-65
C_4H_6	v	55-50	57-50
C_3H_4	vi	42-38	43-39
C_2H_2	vii	30-27	32-27

Although the peaks at 58 and 44 seem to confirm the formation of the propellane as an intermediate, other peaks indicate a great amount of deuterium scrambling. For example, the peak at 113 which is normally attributed to the C^{13} species has a normal 5 percent intensity in samples a, b, and c; it reaches approximately 55 percent in d. Table 12 presents the interpretation of the fragment information, including suggestions for fragment structures.

TABLE 12. FRAGMENTATION PATTERN OF IRRADIATED 24

Group	m/e	Suspected Fragment
i	119	$C_8D_{11}H$ (?)
	113	$C_8D_5H_7$
ii	93	C_6H_7D
	91	C_6H_7
iii	79	C_6H_7
	78	C_6H_7 or -D
	77	C_6H_5 or -HD
iv	70	$C_5H_6D_2$
	69	$C_5H_5D_2$
	68	C_5H_6D or $C_5H_4D_2$
	67	C_5H_7
v	59	C_4HD_5
	58	$C_4H_2D_4$
	57	$C_4H_3D_3$
	56	
	55	
	54	Loss of H's or D's
	53	
	51	
vi	44	C_3D_4
	43	C_3D_3H
	39	C_3H_3
vii	27	C_2DH

The results basically indicate that there is a random scrambling of the deuterium.

Experimental

d_4 1,4-Dimethylene Cyclohexane, 32

A. Triphenylmethylphosphonium Iodide.[27] To a separate pressure bottle containing 37.7 g (.144 mole) of triphenylphosphine (Ph_3P) in dry benzene, 45 ml (102.6 g, 0.7 mole) of d_3 methyl iodide was added. The pressure bottle was sealed and allowed to react for 48 hours. Fifty-five grams (.136 mole) of Ph_3PCD_3I was isolated, m.p. 182°C. Yield 95 percent.

B. 1,4-Dimethylene Cyclohexane 32 in DMSO/NaH. A total of 4.8 g (.1 mole) of NaH, as a 50 percent dispersion in oil, was weighted in a three neck flask fitted with a reflux condenser, syringe cap, and thermometer. The flask was then purged with Helium gas. Fifty milliliters of dry dimethyl sulfoxide (DMSO) was added through a syringe while placing flask under partial vacuum. The mixture was stirred at 70-80°C until evolution of H_2 ceased, then cooled in an ice bath.

Eighty grams (.2 mole) of the Ph_3PCD_3I was added to the reaction flask. A dark red color was immediately observed. The reaction was stirred for 10 minutes at room temperature. A total of 10.8 g (.11 mole) of cyclohexanone (newly distilled) was added through the syringe fitting and stirred for 30 minutes. The mixture was then vacuum distilled at 42 C° and 5 mm pressure resulting in 10.5 g of product. NMR analysis showed substantial benzene present in product. Rotary evaporation resulted in 10.1 g (.09 mole) of product 32 remaining in the flask, 85 percent yield. Further purification of a portion of the residue by fractional distillation (20 mm) resulted in decomposition of the flask contents.

C. 32 in KtBuO/KtBuOH. The 1:1 equivalent complex was prepared by reacting 40 g (1.0 moles) potassium with 200 ml (157 g, 2.12 moles) of t-Butanol.

A solution of 100 ml of the butanol/butoxide complex and 200 ml of diethyl ether is introduced into a 500 ml round bottom flask fitted with a reflux condenser, an additional funnel, a mechanical stirrer, and a gas inlet tube. The flask is purged with N_2 and a gentle flow is maintained throughout the reaction. The solution is stirred and 36.38 g (0.09 mole) Ph_3PCD_3I is added over a 5-10 minute period.

Freshly distilled 1,4-cyclohexane dione, 36, (5.6 g, .05 mole) is added dropwise. The mixture is heated under reflux for 24 hours, cooled to room temperature, and the precipitate removed by suction filtration (suction bottle was kept in an ice bath). The precipitate was washed repeatedly with 10 ml portions of ether for a total of 100 ml. The combined ether filtrates are washed successively with 100 ml portions of water until water extracts are neutral to pH paper. The ether layer is dried with $CaCl_2$ and filtered. The ether is carefully distilled through a 10 cm Vigreaux column. Careful fractional distillation through the same column at 20 mm Hg, 30-60°C, yield 5 g (.04 4 mole) of 32 (88 percent yield). The boiling point of the isolated product was 122-123°C and compared favorably with reported data.[16b] NMR showed a single peak at δ = 2.22. Trace signals for residue of diethyl ether were also visible.

Alternative Synthesis for 32

1,4-Dimethanol Cyclohexane (d_4) 38

A three neck, round bottomed flask fitted with an additional funnel, a condenser nitrogen inlet, and an oil bubbler vent, was flushed with nitrogen gas and charged with 5 g (.12 mole) of $LiAlD_4$ in 100 ml of previously distilled tetrahydrofuran (THF) distilled over $LiAlH_4$. The mixture was stirred under positive gas pressure for 2 hours. A total 18.0 ml (19.8 g, .099 mole) of freshly distilled 1,4-cyclohexane dicarboxylate, 37, was dissolved in 50 ml of distilled THF and added to the reaction dropwise. It is absolutely necessary that stirring procedures be efficient. It has been observed that in the case where the stirring is poor, a ledge will form containing the gelatinous di-alcohol product on the bottom and unreacted ester on the surface. Any agitation will cause the ledge to turn over, introducing a large amount of ester into the reaction. This has already caused a serious accident in this laboratory. At the completion of the addition, the reaction was refluxed for 24 hours, quenched with 150 ml of methanol and allowed to stir for an additional 6 hours. The reaction mixture was filtered and the solvent removed leaving 11.5 g (.077 mole) of gelatinous product (m.p. 40-55°C, lit mp 30 C, cis 43°C, trans 67°C). Yield 78 percent. The product was verified by gas chromatography and IR using authentic nondeuterated product. GLC, 10 percent UCON, 10 ft, 200 C, ret time 54 sec. NMR (for H product) δ= 1.0-2.0, m, 8H; 3.33, d, 4H; 3.69, s, 2H; 4.65, s, -OH (absent in d form). IR, λ = 3.05, 3.4, 6.85, 7.25, 8.3w, 8.9w, 9.6w, 9.9w, 10.9w (IR compares favorably to authentic product).

1,4-Cyclohexane Dimethanol Tosyl Ester (d_4), 40

In a 500 ml round bottom flask, a solution consisting of 250 ml of dry pyridine (distilled over barium oxide) and 11.50 g (.077 mole) of the 1,4-tetradeutero dimethanol cyclohexane is prepared. The flask is cooled in a salt/ice bath and 45.0 g (0.23 M) of p-toluene sulfonyl chloride is added while swirling in ice. The flask is refrigerated for 48 hours. The reaction mixture was poured over approximately 500 ml of ice at which time a fine, white crystal formed. The solid was vacuum filtered, washed with water, and air dried. Additional drying was necessary. A total of 17.18 g (0.38 mole) of a white solid was having a melting point of 147-148°C. Yield 49 percent. NMR, δ = 1.23, t, 4H; 1.0-2.0, m, H; 2.47, s, 6H; 3.3-4.1, m, 2H; 7.33, d, 8H. IR, λ = 3.5s, 6.9m, 7.3w, 8.5w, 10.5w, 11.2w.

1,4-Cyclohexane Dimethyl Iodide (d_4), 41[31]

A total of 17.18 g (.038 mole) of the tosylate salt was dissolved in 300 ml of acetone with slight warning. Fifty-one grams (.34 mole) of NaI was dissolved in 125 ml of acetone (sat.) under reflux (solubility 39.9 g/100 cc).[25] The two solutions were mixed while hot and refluxed for 40 hours. The mixture was cooled prior to adding 400 ml of water. The aqueous reaction mixture was then extracted with three 200 ml portions of diethyl ether. The ether layers were combined and washed with a 10 percent solution of $NaHSO_3$. The ether layer was then dried anhydrous Na_2SO_4. The solvent was removed under vacuum yielding 11.7 g (0.32 mole) of a yellow solid (m.p.62-68°C). Yield 84 percent. NMR, δ = 1-2.2, m, 8H; 3.1, d, 4H.

1,4-Dimethylene Cyclohexane (d4), 32

The 11.7 g (.032 mole) of dimethyl iodide was placed in a round bottom flask fitted with a reflux condenser, additional funnel, and thermometer. A five-fold excess of K-OtBu (potassium tert-butoxide), 18 g (.16 mole) dissolved in 200 ml of butanol was introduced into the flask. The solution was refluxed for 24 hours (750 nm, 82°C). The reaction was cooled, placed in a large separatory funnel, and diluted with 300 ml of water. The aqueous solution was extracted 3x with 25 ml of pentane. The organic extracts were combined and washed with equal volumes of water until the t-BuOH odor was no longer detectable in the organic liquid. Two additional washes were performed. The pentane layer was dried with anhydrous sodium sulfate and suction filtered. The pentane was concentrated by rotary evacuation and finally removed by micro-distillation. Gas chromatography, (10 ft, 2 mm column, 10 percent UCONW98, 50-150°C at 15 /min, ret. time 20 sec) revealed 32 present as 33 percent of the components by triangulation. The remainder being pentane and trace impurities (~3 percent). Further micro-distillation resulted in 2.7 g (.024 moles) of 32 with trace pentane. The distillate was used for the irradiation experiments in this condition. NMR, = 2.21, s, 8H; 4.67, s, 4H (absent in d form).

Irradiation of 32, Mercury Sensitized

A solution of 0.5 g (4.5 mmoles) of 32 in 100 ml of diethyl ether was prepared and irradiated for hours in the identical manner as described in Chapter III. A 5.56 percent yield was calculated by triangulation of the GLC trace. The dibromide peak was verified by doping the sample with authentic 22.

CHAPTER IV

REFERENCES

(27) Greenwald, R.; Chaykovsky, M.; Corey, E. J. J. Org. Chem. 1963, 28, 1128.

(28a) Witting, G.; Schoellkopf, U. Org. Syn. 1940, 40, 66.

(28b) Schlosser, M.; Christmann, K. F. Ang. Chemie. Int. Ed. 1964, 3, 636.

(29a) Mori, A.; Tzuzuki, B. Bull. Chem. Soc. Jap. 1966, 39 (11), 2454-8.

(29b) Fridrich, I.; Gast, L. E. J. Amer. Oil Chem. Soc. 1967, 44 (2), 110-12.

(30) Lerman, L.; Liberman, M. Dokladu Aka. Nauk, SSR. 1971, 201 (1), 115.

(31) Gajewsky, J. J.; Hoffman, L. K.; Shih, C N. J. Amer. Chem. Soc. 1974, 96, 3705, and personal communications.

CHAPTER V

THEORETICAL TREATMENT OF ISOSTRUCTURAL ISOMERS

Introduction

Interest in the propellane systems was gaining momentum. Witness the fact that at the time the work described in previous chapters were published, an independent group published the synthesis of [2.2.2]propellane through the electrochemical reduction of the dibromide 35.[32,33] The dichloride derivative was trapped in the reaction process, similar to that described in Chapter II addressing our identification of a dibromo derivative. Just prior to this report, Phil Eaton had successfully synthesized a derivative of 2 and verified the mechanism of Grob fragmentation to the dimethylene cyclohexane.[34]

As the interest in the propellane systems was continuing to grow, our group was often approached by other researchers with ideas and suggestions for propellane related systems. One such suggestion came from Dr. Ed Wasserman of Bell Laboratories.[35] Dr. Wasserman, a noted ESR spectroscopist, had expressed an interest in studying a system which might be characterized by a one electron bond. He had in mind the generation of a propellyl cation, 43, having the same structural skeleton as 2 with a positive charge. Since the INDO open-shell calculations demonstrated a certain degree of success in predicting the synthesis of 2, it was of interest to Dr. Wasserman to have us perform calculations on 43 to calculate the hyperfine coupling constant as well as the relative energy and structural information.

Dewar and Olah were successful in generating the dication, 42, from 1,4-dichlorobicyclo[2.2.2]octane in SbF_5-SO_2ClF (SO_2) or "magic acid" at -78 C.[36] This group also reported results from MINDO/3 and molecular mechanical calculations of 42.[37] The authors comment that the MINDO/3 method defines the $r_{1,4}$ distances significantly shorter than that predicted by the molecular mechanics force field method. In fact, the $r_{1,4}$ distance is progressively shortened going from the neutral bicyclooctane, to the positive radical, to the dictation, despite the increasing effect of electrostatic repulsion. Only the dication can be compared to the calculations in this chapter as neither the bicyclooctane nor the positive radical were calculated to have a central bond. Although there is no reference of hydrogens being attached at the bridgehead positions, we assume that these are true bicyclootane structures. The authors indicate that this stability is due to the delocalization of a positive charge to the twelve hydrogen atoms, then suggest that there is an increased stability due to 42 being "aromatic." The aromaticity argument stems from 42 being isoconjugate with the cyclobutadiene dictation system.

Many of the above suggestions encouraged the research work presented in the remainder of this chapter. Even prior to Dewar's calculations we attempted to look at various isoelectronic species of the hydrocarbon propellanes as well as various propellanes containing heteroatoms such as nitrogen and boron as a complete set. In each case, we were able to generate comparison between isoelectronic, not necessarily isomeric structures. The calculations of the various charged molecules of each isomeric group would yield an understanding of the electron delocalization throughout the framework of the molecular skeleton. A comparison of isoelectronic species would indicate

the effects of altering the size and charge of nucleuses within the molecular framework. Rather than simply calculate the single molecular framework suggested in some of the above discussion, we undertook to treat all possible classes within each subgroup.

Theoretical Approach

Calculations were performed in a manner similar to that described in Chapter II. A D_{3h} symmetry was assumed for all configurations of the propellanes and the geometries optimized variationally. To the three propellane states calculated in Chapter II, we have added the propellyl dication, 42, the radical monocation, 43, the anion, 44, and the dianion, 45. The two carbons in the 1,4 bridgehead positions were substituted with nitrogens in the second category of compounds calculated, the diazo-bicyclo[2.2.2]octane, 46, group. In this group, both the cation, 47, and the dication, 48, were also calculated. Since the diazo-dication is isoelectronic with the propellane species, it was of interest to identify the structures for the unpaired singlet dication, 49, and the unpaired triplet dication, 50. A third group of compounds, substituting boron for the bridgehead carbons, were calculated. This included the diborobicyclo[2.2.2]octane, 51, and its analogous anion, 52, and the dianion, 53. As a comparison to the propellyl dication, a 1-boro,2-azobicyclo [2.2.2]octane cation, 54, was calculated. A comparison to the 44 electron system 1-azobicyclo[2.2.2]octane cation, 55, and 1-boro,2-azobicyclo[2.2.2] octane, 56, were also calculated.

For ease of reference, Table 13 presents the appropriate nomenclature for each of the molecules calculated, the assigned reference number, and a symbol associated with each molecule. Because of the large number of structures studied, we have chosen to use these symbols throughout the remainder of

the text as opposed to the normal numerical designation to avoid having the reader continuously refer back to the reference table. The symbol is designated as A^n where A refers to the identity of the atoms in the 1,4 position. In the case where those atoms differ, two letters will replace A. The superscript n defines the charge and state calculated, e.g., C^{+2} = 42, BN = 56, etc.

TABLE 13. NOMENCLATURE AND REFERENCE SYMBOLS FOR THE MOLECULES AND THE RELATED STATES STUDIED IN OUR CALCULATIONS

Nomenclature	Reference Number	Symbol	Number of Electrons
(2.2.2)Propellane Singlet Symmetric	2	C^s	44
(2.2.2)Propellane Singlet Assymetric	3	C^a	44
(2.2.2)Propellane Triplet	21	C^t	44
(2.2.2)Propellane dictation	42	C^{+2}	42
(2.2.2)Propellane cation	43	C^{+1}	43
(2.2.2)Propellane anion	44	C^{-1}	45
(2.2.2)Propellane dianion	45	C^{-2}	46
Diazo-bicyclo(2.2.2)octane	46	N^0	46
Diazo-bicyclo(2.2.2)cation	47	N^{+1}	45
Diazo-bicyclo(2.2.2)dication symmetric	48	N^{+2s}	44
Diazo-bicyclo(2.2.2)dication assymetric	49	N^{+2a}	44
Diazo-bicyclo(2.2.2)dication triplet	50	N^{+2t}	44
Diboro-bicyclo(2.2.2)octane	51	B^0	42
Diboro-bicyclo(2.2.2)anion	52	B^{-1}	43
Diboro-bicyclo(2.2.2)dianion	53	B^{-2}	44
1,boro-bicyclo(2.2.2)octane cation	54	BC^{+1}	42
1,azo-bicyclo(2.2.2)octane cation	55	NC^{+1}	44
1,boro-2,azo-bicyclooctane	56	BN^0	44

Results

Each of the geometries were optimized and selected values were extracted from the computer generated outputs. Table 14 provides a summary of the optimized bond distances for bonds $r_{1,4}$, $r_{1,2}$, as well as the CH bond distances. Angle data (<123) is also presented. When the optimized bond lengths for the 1,4 bond are plotted against the <214 (from Table 12) the result is a straight line as shown in Figure 29.

TABLE 14a. OPTIMIZED GEOMETRIES FOR D_{3h} SYMMETRY

State	$r_{1,4}$	$r_{1,2}$	$r_{2,3}$	< 123	C-H
C^{+2}	1.720	1.470	1.492	94.45	1.125
C^{+1}	1.615	1.485	1.491	92.40	1.125
C^{s}	1.560	1.505	1.484	94.45	1.125
C^{a}	2.450	1.450	1.524	108.62	1.125
C^{t}	2.090	1.475	1.487	101.80	1.125
C^{-1}	2.555	1.465	1.507	110.95	1.135
C^{-2}	2.650	1.480	1.493	113.0	1.145
N^{0}	2.495	1.430	1.491	110.55	1.130
N^{+1}	2.390	1.415	1.506	108.2	1.125
N^{+2s}	1.425	1.465	1.481	88.87	1.120
N^{+2a}	2.330	1.405	1.518	106.8	1.125
N^{+2t}	1.980	1.430	1.486	99.9	1.125
B^{0}	1.780	1.565	1.496	95.2	1.125
B^{-1}	1.780	1.585	1.487	95.3	1.130
B^{-2}	1.750	1.600	1.485	97.75	1.140

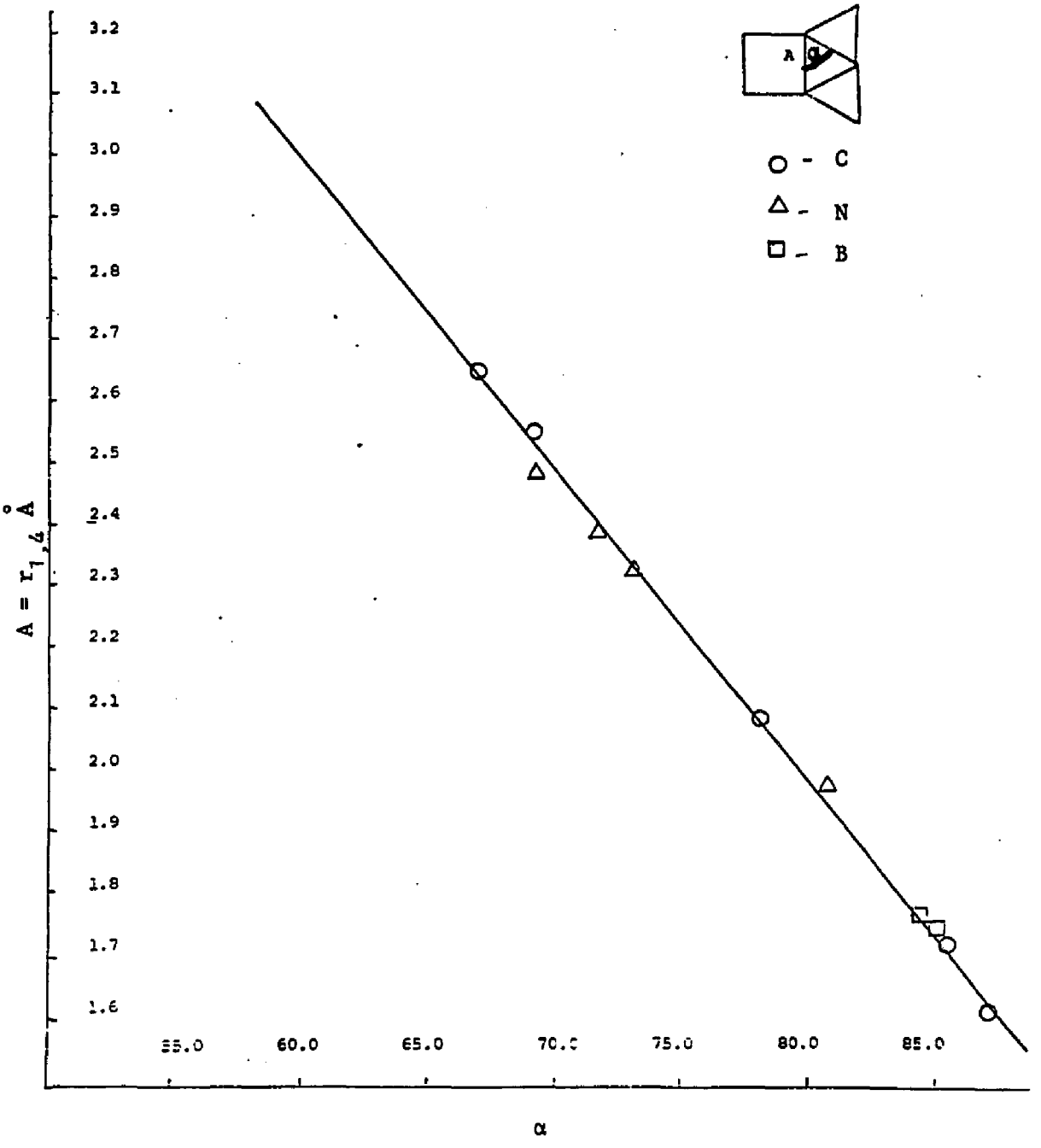

FIGURE 29. GRAPHIC COMPARISON OF THE RELATIONSHIP OF THE $r_{1,4}$ DISTANCE TO THE <214 OF THE BRIDGEHEAD CARBONS

TABLE 14b. OPTIMIZED GEOMETRIES FOR C_{3h} SYMMETRY

State	$r_{1,4}$	$r_{1,2}$	$r_{3,4}$	$r_{2,3}$	$r_{1,2H}$	$r_{4,3H}$	214	341
BN^0	1.665	1.595	1.450	1.490	1.120	1.125	89.80	82.95
BC^{+1}	1.750	1.560	1.475	1.480	1.125	1.125	85.05	84.75
NC^{+1}	1.720	1.440	1.475	1.481	1.125	1.125	82.60	87.90

Table 15 provides a comparative presentation of the total energies calculated for each state. The first column reflects the energy and atomic units extracted directly from the computer printout. In the second column the numbers have been normalized for each category of states (i.e., the lowest energy configuration within each category is reduced to 0 energy). Tables 16a and 16b present electron densities and hyperfine coupling constants respectively for the atoms of interest within each molecular state. Table 17 provides the reader with the extracted total bond orders and Px bond orders for each of the states.

Tables 18 through 29 present the orbital energy for orbital 10 through 24 for each molecule. The σ_h term describes the orbitals across the D_{3h} plane of symmetry and the point symmetry symbols identified in a manner similar to the method shown in Tables 3, 4, and 5; for simplicity the actual element of the symmetry operations is eliminated from these tables. An asterik is used to designate the HOMO for each set of orbitals.

Figures 27 through 37 were generated by using the optimized geometry of each molecule as the minimum energy geometry and increasing $r_{1,4}$ by 0.1 Å

TABLE 15. TOTAL ENERGIES CALCULATED FOR EACH MOLECULAR STATE

State	Calculated Energy, (Atomic Units)	Relative Energy
C^{+2}	-63.573 223	495
C^{+1}	-64.095 982	171
C^{s}	-64.371 624	0
C^{a}	-64.185 378	115
C^{t}	-64.249 602	76
C^{-1}	-64.193 156	110
C^{-2}	-63.942 422	266
N^{0}	-73.123 558	0
N^{+1}	-72.808 776	195
N^{+2s}	-72.353 964	477
N^{+2a}	-72.222 578	588
N^{+2t}	-72.271 365	528
B^{0}	-58.432 777	0
B^{-1}	-58.383 552	30
B^{-2}	-58.092 921	211
BN^{0}	-65.767 238	
BC^{+1}	-60.488 278	
NC^{+1}	-67.935 760	

symmetrically above and below the center of the molecule and plotting the total energy from $1.3 \leq r_{1,4} \leq 3.0$ Å. No attempt was made to optimize each individual geometry as in Chapter 2.

TABLE 16a. ELECTRON DENSITIES

State	C_1, C_4	Other C	H
C^{+2}	3.7008	3.9450	0.9107
C^{+1}	3.8544	3.9337	0.9741
C^{s}	4.0038	3.9925	1.0381
C^{a}	4.0982	3.8962	1.0354
C^{t}	4.0544	3.9078	1.0371
C^{-1}	4.2952	3.8636	1.1024
C^{-2}	4.5117	3.8211	1.1708
N^{+2s}	4.8462	3.8787	0.9196
N^{+2a}	4.8849	3.8692	0.9179
N^{+1}	5.0228	3.8615	0.9821
N^{o}	5.1878	3.8423	1.0475
N^{+2t}	4.8443	3.8822	0.9182
B^{o}	2.9117	3.9830	1.0232
B^{-1}	3.1143	3.9513	1.0886
B^{-2}	3.2952	3.9215	1.1567

TABLE 16b. HYPERFINE COUPLING CONSTANTS FOR SELECTED "OPEN SHELL" CALCULATIONS

State	C_1, C_4	Other C	H
C^{+1}	8.6029	2.4090	10.3150
C^{t}	52.5750	7.6866	9.5112
C^{-1}	67.1726	-6.1873	9.8076
N^{+1}	17.5826	-5.2336	6.0553
N^{+2t}	18.9998	2.2784	6.5479
B^{-1}	0.0134	8.2485	14.5351

TABLE 17. THE $r_{1,4}$ BOND DISTANCE VERSUS BOND ORDER FOR CALCULATED MOLECULES

State	$R_{1,4}$	Bond order
C^{+2}	1.720	.190
C^{+1}	1.615	.443
C^{s}	1.560	.867
C^{a}	2.450	-.193
C^{t}	2.090	.009
C^{-1}	2.555	-.074
C^{-2}	2.650	-.012
N^{+2s}	1.430	.949
N^{+2a}	2.330	-.304
N^{+1}	2.390	-.113
N^{o}	2.495	-.031
N^{+2t}	1.980	-.015
B^{o}	1.780	.199
B^{-1}	1.780	.340
B^{-2}	1.750	.671
BN^{o}	1.665	.406
BC^{+1}	1.750	.208
NC^{+1}	1.720	.210

TABLE 18. ORBITAL ENERGY CALCULATIONS FOR C^{+2} WITH ASSOCIATED D_{3h} SYMMETRY

Orbital	E (a.u.)	σ_h	Point Symmetry
24	- .2236	S	A_1'
23	- .2794	A	A_2''
22	- .4782	S	A_1'
21*	- .9153	A	
20	- .9153	A	
19	- .9736	A	A_1''
18	-1.0712	S	
17	-1.0712	S	
16	-1.1153	A	
15	-1.1153	A	
14	-1.1681	A	A_2''
13	-1.1742	S	
12	-1.1742	S	
11	-1.1940	S	A_2'
10	-1.4115	S	A_1'

*HOMO

TABLE 19. ORBITAL ENERGY CALCULATIONS FOR C^{+1}

Orbital	Alpha Spin E (a.u.)	Alpha Spin σ_h	Alpha Spin Point Symmetry	Beta Spin E (a.u.)	Beta Spin σ_h	Beta Spin Point Symmetry
24	.0146	S	A_1'	.0246	S	A_2''
23	- .0164	A	A_2''	.0119	A	A_2''
22*	- .5719	S	A_1'	- .2316	S	A_1'
21	- .6749	A		- .6701	A	
20	- .6749	A		- .6701	A	
19	- .7611	A	A_1''	- .7568	A	A_1''
18	- .8455	S		- .8336	S	
17	- .8455	S		- .8336	S	
16	- .8847	A		- .8806	A	
15	- .8847	A		- .8806	A	
14	- .9439	A	A_2''	- .9241	A	A_2''
13	- .9686	S		- .9540	S	
12	- .9686	S		- .9540	S	
11	- .9741	S	A_2'	- .9714	S	A_2'
10	-1.1741	S	A_1'	-1.1409	S	A_1'

TABLE 20a. ORBITAL ENERGY CALCULATIONS FOR C-1 [illegible] = 1.90 A

Orbital	Alpha Spin E (a.u.)	Alpha Spin σ_h	Alpha Spin Point Symmetry	Beta Spin E (a.u.)	Beta Spin σ_h	Beta Spin Point Symmetry
24	.4534	S		.4521	S	
23*	.0309	A	$A_2"$	.4322	A	$A_2"$
22	-.0588	S	A_1'	.0255	S	A_1'
21	-.2207	A		-.2174	A	
20	-.2207	A		-.2174	A	
19	-.3271	A	$A_1"$	-.3287	A	$A_1"$
18	-.3856	S		-.3842	S	
17	-.3856	S		-.3842	S	
16	-.4443	A		-.4445	A	
15	-.4443	A		-.4445	A	
14	-.4790	S		0.4735	A	$A_2"$
13	-.4790	S		-.4756	S	
12	-.4843	A	$A_2"$	-.4756	S	
11	-.5245	S	A_2'	-.5251	S	A_2'
10	-.7180	S	A_1'	-.6771	S	A_1'

*HOMO

TABLE 20b. ORBITAL ENERGY CALCULATIONS FOR C^{-1} r = 2.55 A

	Alpha Spin			Beta Spin		
Orbital	E (a.u.)	σ_h	Point Symmetry	E (a.u.)	σ_h	Point Symmetry
24	.4546	S		.4582	S	
23*	-.0499	S	A_1'	.2911	S	A_1'
22	-.1601	A	A_2''	-.0307	A	A_2''
21	-.2212	A		-.2153	A	
20	-.2212	A		-.2153	A	
19	-.3185	A	A_1''	-.3141	A	A_1''
18	-.3793	S		-.3756	S	
17	-.3793	S		-.3756	S	
16	-.4270	S		-.4092	S	
15	-.4270	S		-.4092	S	
14	-.4464	A		-.4425	A	
13	-.4464	A		-.4425	A	
12	-.5122	S	A_2'	-.5061	A	A_2''
11	-.5122	A	A_2''	-.5093	S	A_2'
10	-.7237	S	A_1'	-.6863	S	A_1'

*HOMO

TABLE 21. ORBITAL ENERGY LEVELS FOR C^{-2}

Orbital	E (a.u.)	σ_h	Point Symmetry
24	.6614	S	
23*	.2092	S	A_1'
22	.1129	A	A_2''
21	.0095	A	
20	.0095	A	
19	-.1048	A	A_1'
18	-.1445	S	
17	-.1445	S	
16	-.2031	S	
15	-.2031	S	
14	-.2222	A	
13	-.2222	A	
12	-.2859	A	A_2''
11	-.2993	S	A_2'
10	-.4626	S	A_1'

*HOMO

TABLE 22. ORBITAL ENERGY LEVELS FOR N^{+2}, r = 1.425 and 2.330

Orbital	r = 1.425 A E (a.u.)	σ_h	Point Symmetry	r = 2.333 A E (a.u.)	σ_h	Point Symmetry
24	- .2857	A	A_2''	- .2470	S	A_1'
23	- .3201	S	A_1'	- .5398	S	A_1'
22*	- .9462	S	A_1'	- .9394	A	A_2''
21	- .9670	A		- .9655	A	
20	- .9670	A		- .9655	A	
19	- .9796	A	A_1'	- .9680	A	A_1''
18	-1.0960	S		-1.0944	S	
17	-1.0960	S		-1.0944	S	
16	-1.1368	A		-1.1493	S	
15	-1.1368	A		-1.1493	S	
14	-1.1999	S	A_2'	-1.1556	A	
13	-1.2476	S		-1.1556	A	
12	-1.2476	S		-1.1711	S	A_2'
11	-1.2857	A	A_2''	-1.2867	A	A_2''
10	-1.4607	S	A_1'	-1.4842	S	

*HOMO

TABLE 23. ORBITAL ENERGY LEVELS FOR $N^{+2}t$

Orbital	Alpha Spin E (a.u.)	Alpha Spin σ_h	Alpha Spin Point Symmetry	Beta Spin E (a.u.)	Beta Spin σ_h	Beta Spin Point Symmetry
24	- .3107	S	A_1'	- .2636	S	A_1'
23*	- .9216	S	A_1'	- .4008	A	A_2''
22	- .9729	S	A_1''	- .4348	S	
21	- .9771	A		- .9684	A	
20	- .9771	A		- .9684	A	
19	-1.0220	A	A_2''	- .9703	A	A_1''
18	-1.1247	S		-1.1030	S	
17	-1.1247	S		-1.1030	S	
16	-1.1596	A		-1.1516	A	
15	-1.1596	A		-1.1516	A	
14	-1.1858	S		-1.1776	S	
13	-1.1858	S		-1.1776	S	
12	-1.1911	S	A_2'	-1.1891	S	A_2'
11	-1.2980	A	A_2''	-1.2703	A	A_2''
10	-1.4847	S		-1.4047	S	A_1'

*HOMO

TABLE 24. ORBITAL ENERGY LEVELS FOR N+1

Orbital	Alpha Spin E (a.u.)	Alpha Spin σ_h	Alpha Spin Point Symmetry	Beta Spin E (a.u.)	Beta Spin σ_h	Beta Spin Point Symmetry
24	- .0079	S	A_1'	.0034	S	A_1'
23*	- .6293	S	A_1'	- .2642	S	A_1'
22	- .7314	A		- .6383	A	A_2''
21	- .7314	A		- .7260	A	
20	- .7314	A	A_1''	- .7260	A	
19	- .7962	A	A_2''	- .7457	A	A_1''
18	- .8762	S		- .8609	S	
17	- .8762	S		- .8609	S	
16	- .9186	S		- .9050	S	
15	- .9186	S		- .9050	S	
14	- .9200	A		- .9163	A	
13	- .9200	A		- .9163	A	
12	- .9501	S	A_2'	- .9484	S	A_2'
11	-1.0559	A	A_2''	-1.0482	A	A_2''
10	-1.2542	S		-1.2160	S	A_1'

*HOMO

TABLE 25. ORBITAL ENERGY LEVELS FOR NO

Orbital	E (a.u.)	σ_h	Point Symmetry
24	.2250	A	A_2''
23*	-.3604	S	A_1'
22	-.4885	A	
21	-.4885	A	
20	-.5039	A	A_2''
19	-.5264	A	A_1''
18	-.6317	S	
17	-.6317	S	
16	-.6791	S	
15	-.6791	S	
14	-.6796	A	
13	-.6796	A	
12	-.7294	S	A_2'
11	-.8154	A	A_2''
10	-.9900	S	A_1'

*HOMO

TABLE 26. ORBITAL ENERGY LEVELS FOR B^{o}

Orbital	E (a.u.)	σ_h	Point Symmetry
24	.2452	S	
23	.2383	A	$A_2"$
22	.0790	S	A_1'
21*	-.3798	A	
20	-.3798	A	
19	-.5483	A	$A_1"$
18	-.5483	A	$A_2"$
17	-.5852	S	
16	-.5852	S	
15	-.6363	A	
14	-.6363	A	
13	-.6952	S	
12	-.6952	S	
11	-.7626	S	A_2'
10	-.8335	S	A_1'

*HOMO

TABLE 27. ORBITAL ENERGY LEVELS FOR B^{-1}

Orbital	Alpha Spin E (a.u.)	Alpha Spin σ_h	Alpha Spin Point Symmetry	Beta Spin E (a.u.)	Beta Spin σ_h	Beta Spin Point Symmetry
24	.4484	S		-.4548	S	
23	.4484	S		-.4548	S	
22*	.0185	S	A_1'	-.3215	S	A_1'
21	-.1562	A		-.1535	A	
20	-.1562	A		-.1535	A	
19	-.3461	A	A_1''	-.3392	A	A_1''
18	-.3692	A	A_2''	-.3502	A	A_2''
17	-.3699	S		-.3660	S	
16	-.3699	S		-.3660	S	
15	-.4242	A		-.4181	A	
14	-.4242	A		-.4181	A	
13	-.4936	S		-.4803	S	
12	-.4936	S		-.4803	S	
11	-.5975	S	A_2'	-.5530	S	A_2'
10	-.6051	S	A_1'	-.5884	S	A_1'

*HOMO

TABLE 28. ORBITAL ENERGY LEVELS FOR B^{-2}

Orbital	E (a.u.)	σ_h	Point Symmetry
24	.6523	S	
23	.6523	S	
22*	.2597	S	A_1'
21	.0668	A	
20	.0668	A	
19	-1.404	A	A_2''
18	- .1412	A	A_1''
17	- .1512	S	
16	- .1512	S	
15	- .2123	A	
14	- .2123	A	
13	- .2821	S	
12	- .2821	S	
11	- .3479	S	A_2'
10	- .3670	S	A_1'

*HOMO

TABLE 29. ORBITAL ENERGY LEVELS FOR BN°

Orbital	E (a.u.)	Point Symmetry
24	.2323	
23	.1975	A_1
22*	-.3974	A_1
21	-.4064	
20	-.4064	
19	-.5458	A_2
18	-.6086	
17	-.6086	
16	-.6509	A_1
15	-.6758	
14	-.6758	
13	-.7275	
12	-.7275	
11	-.7589	A_2
10	-.9231	A_1

*HOMO

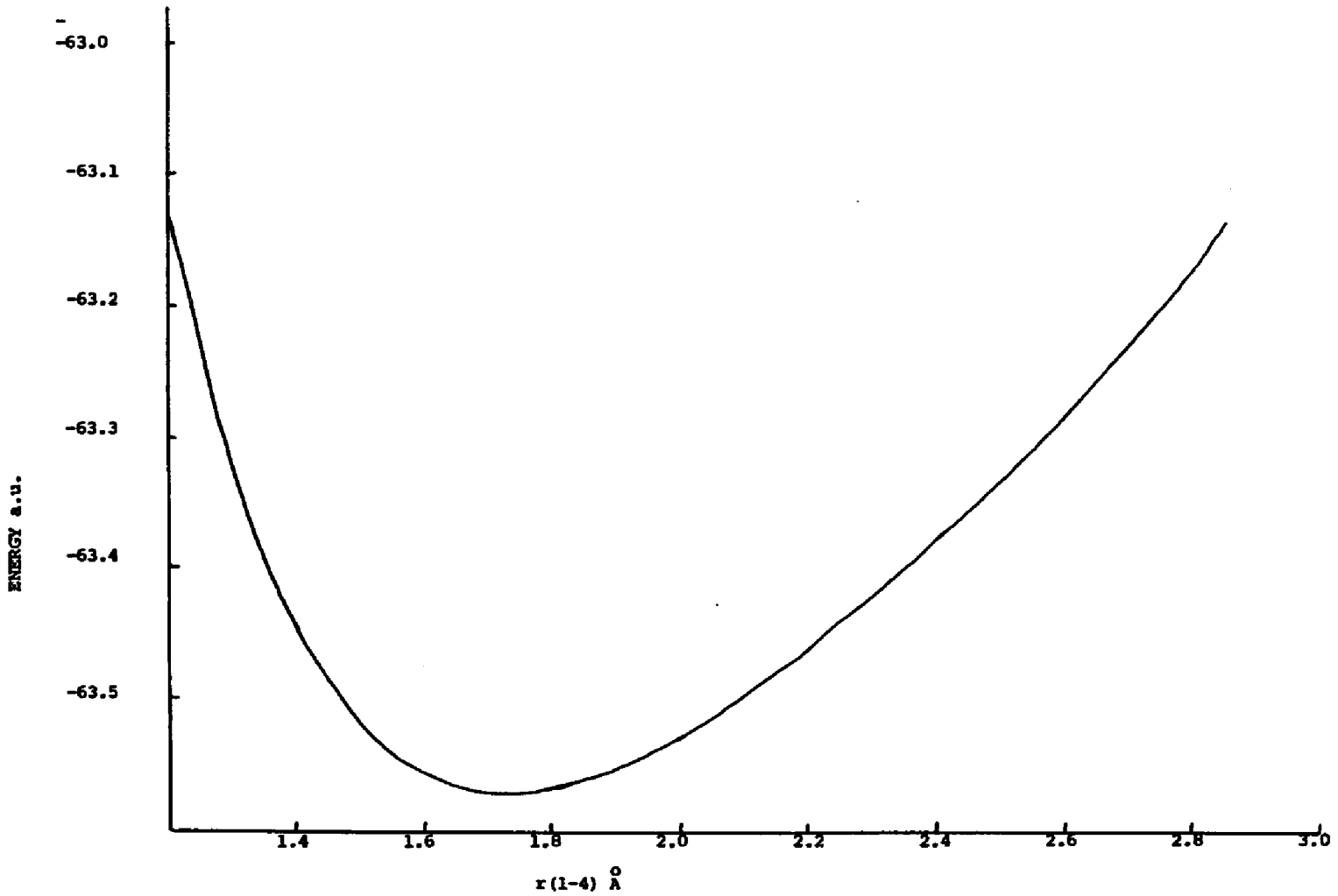

FIGURE 30. ENERGY SURFACE SEGMENT FOR $r_{1,4}$ STRETCH IN C^{+2}, 42 ELECTRON SYSTEM

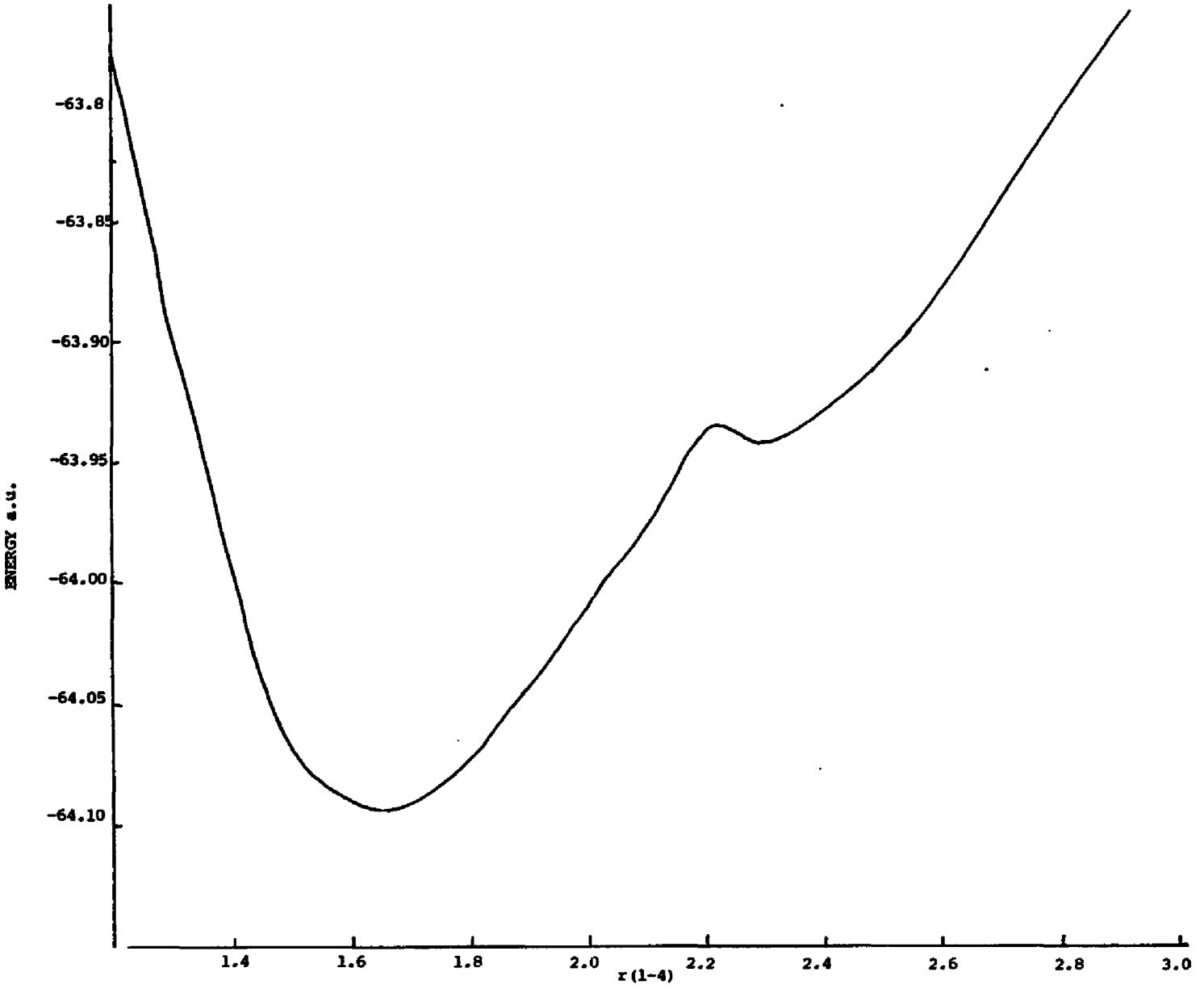

FIGURE 31. ENERGY SURFACE SEGMENT FOR C^{+1}, 43 ELECTRONS

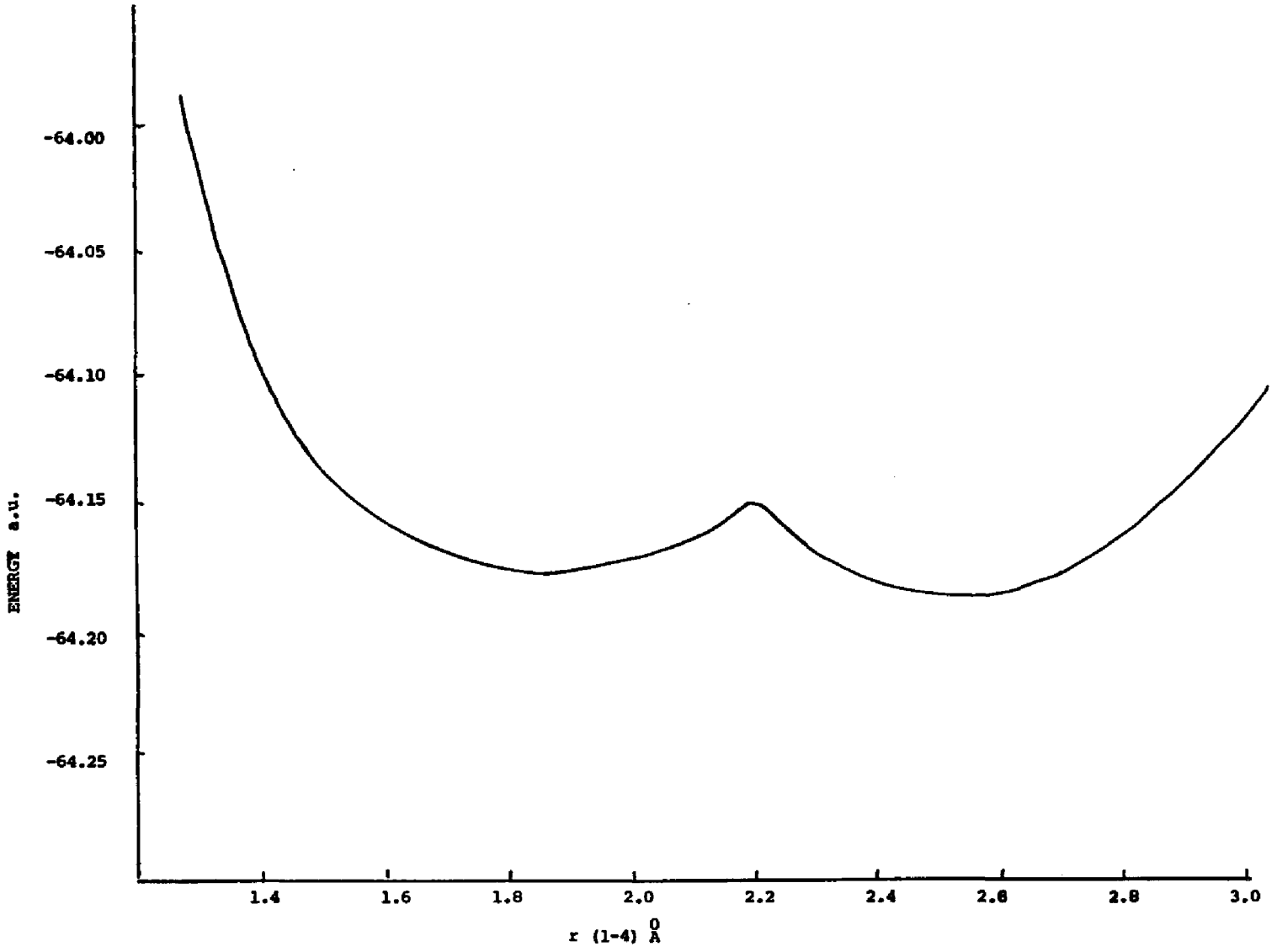

FIGURE 32. ENERGY SURFACE SEGMENT FOR C^{-1}, 45 ELECTRONS

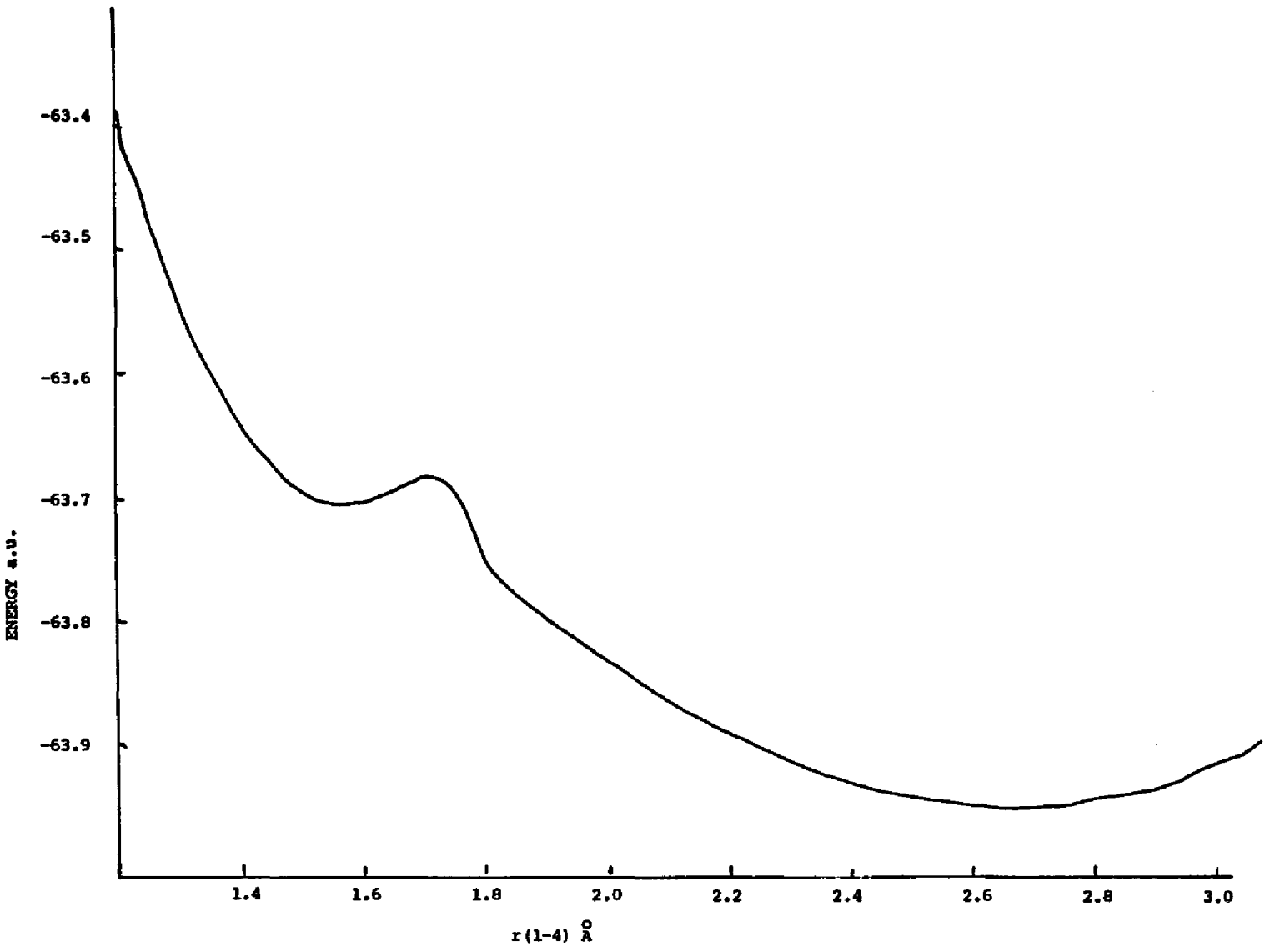

FIGURE 33. ENERGY SURFACE SEGMENT FOR C^{-2}, 46 ELECTRONS

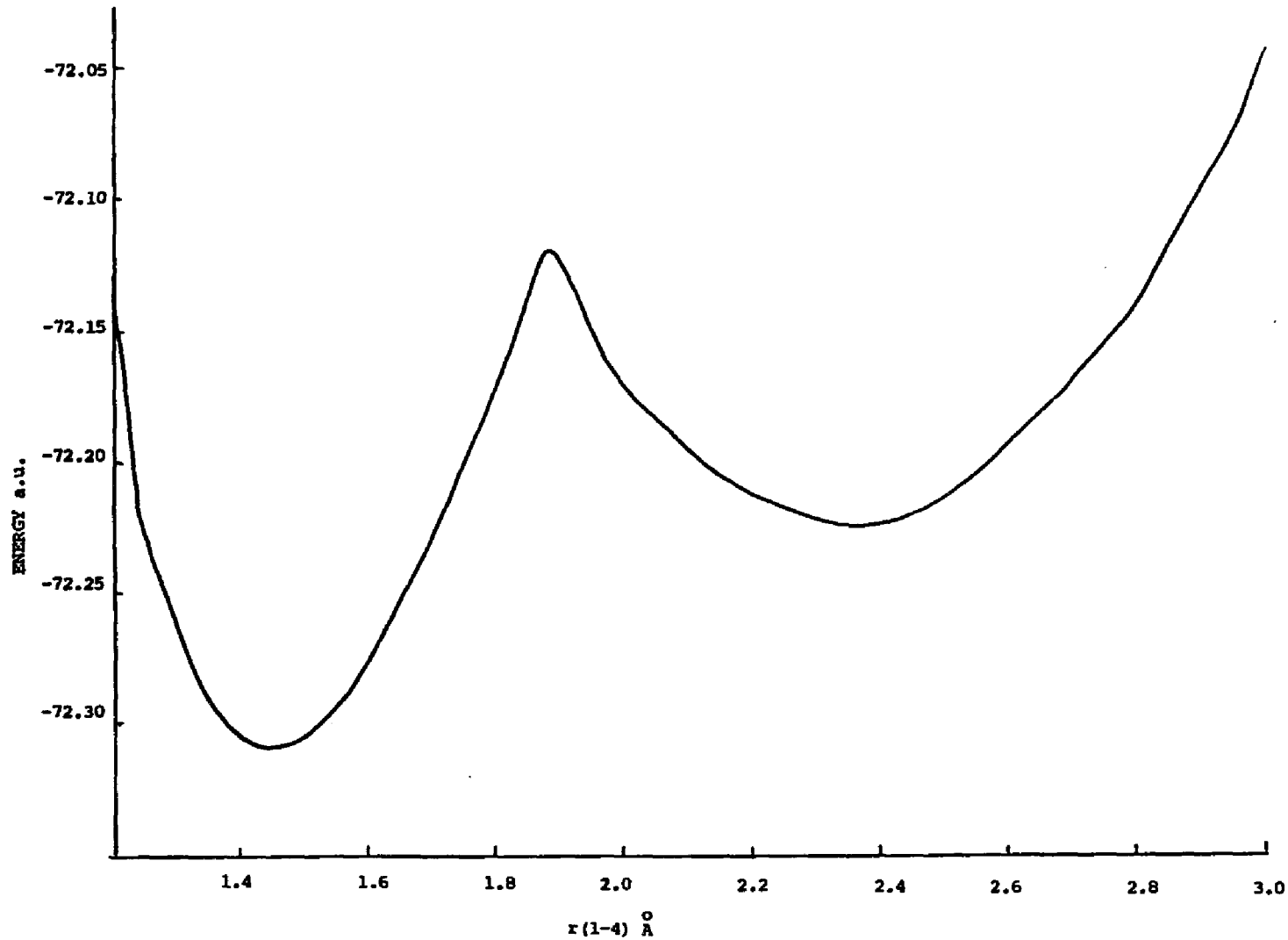

FIGURE 34. ENERGY SURFACE SEGMENT FOR N^{+2}, 44 ELECTRONS

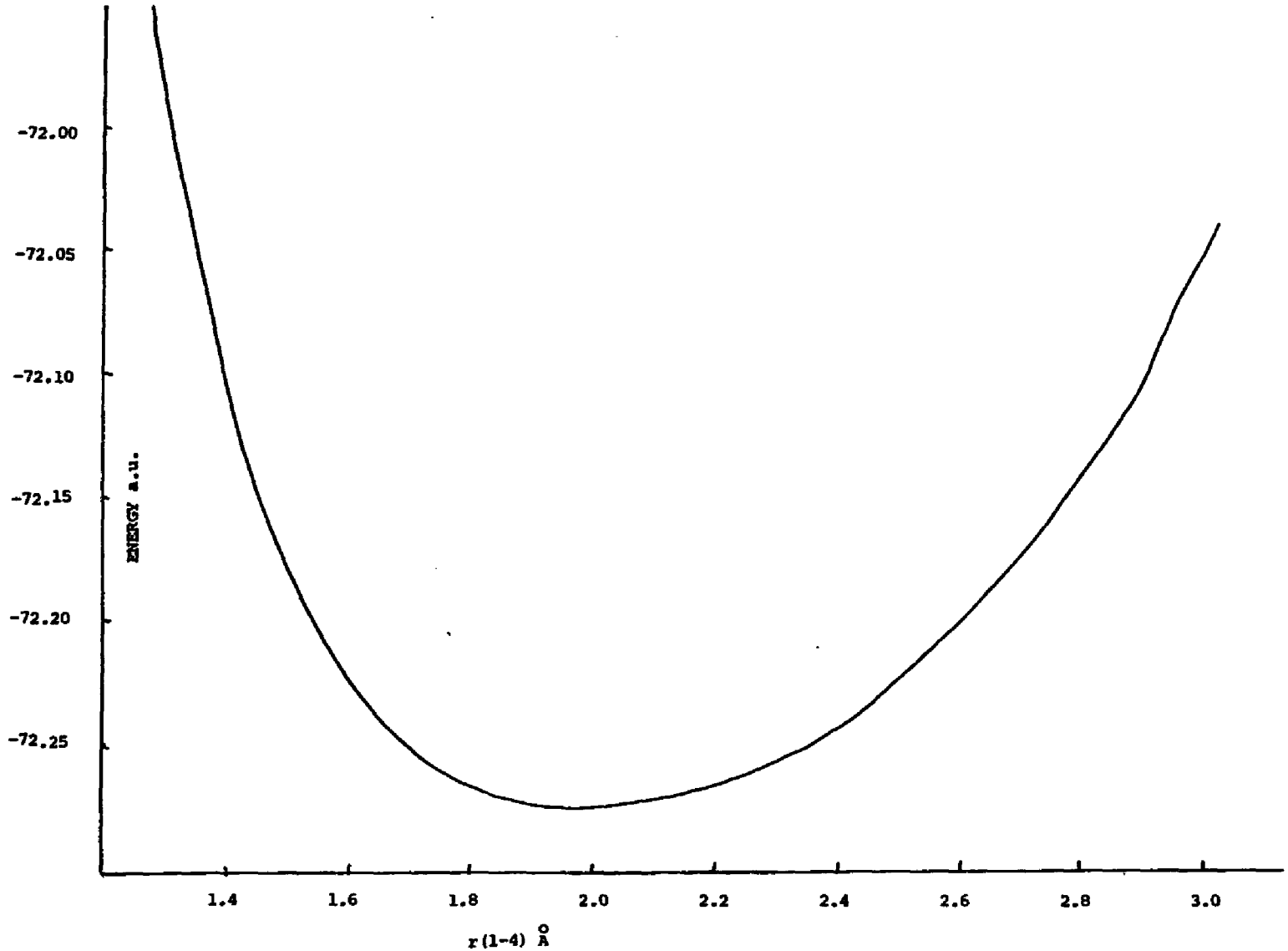

FIGURE 35. ENERGY SURFACE SEGMENT FOR N^{+2t}, (OPEN SHELL TRIPLET) 44 ELECTRONS

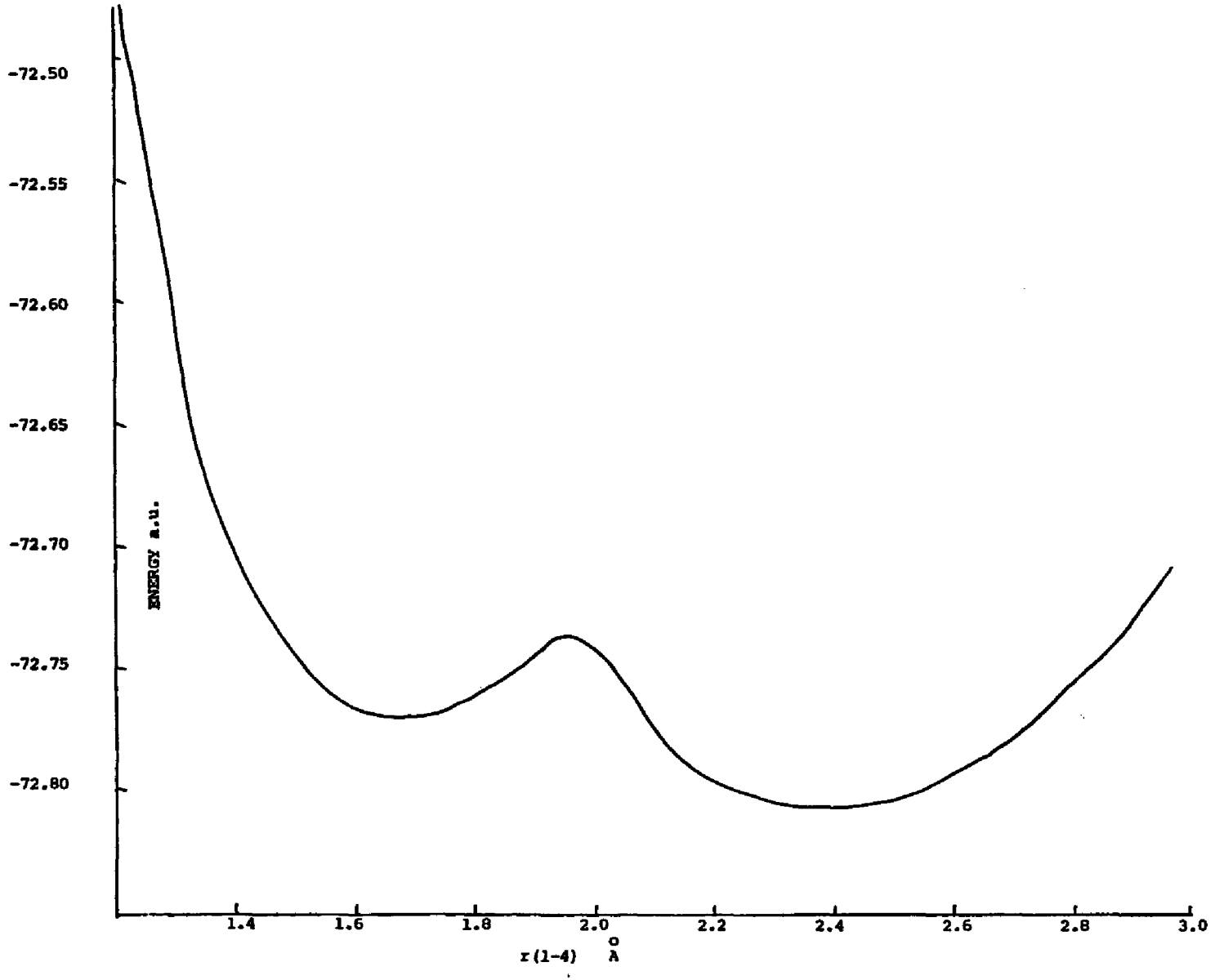

FIGURE 36. ENERGY SURFACE SEGMENT FOR N^{-1}, 45 ELECTRONS

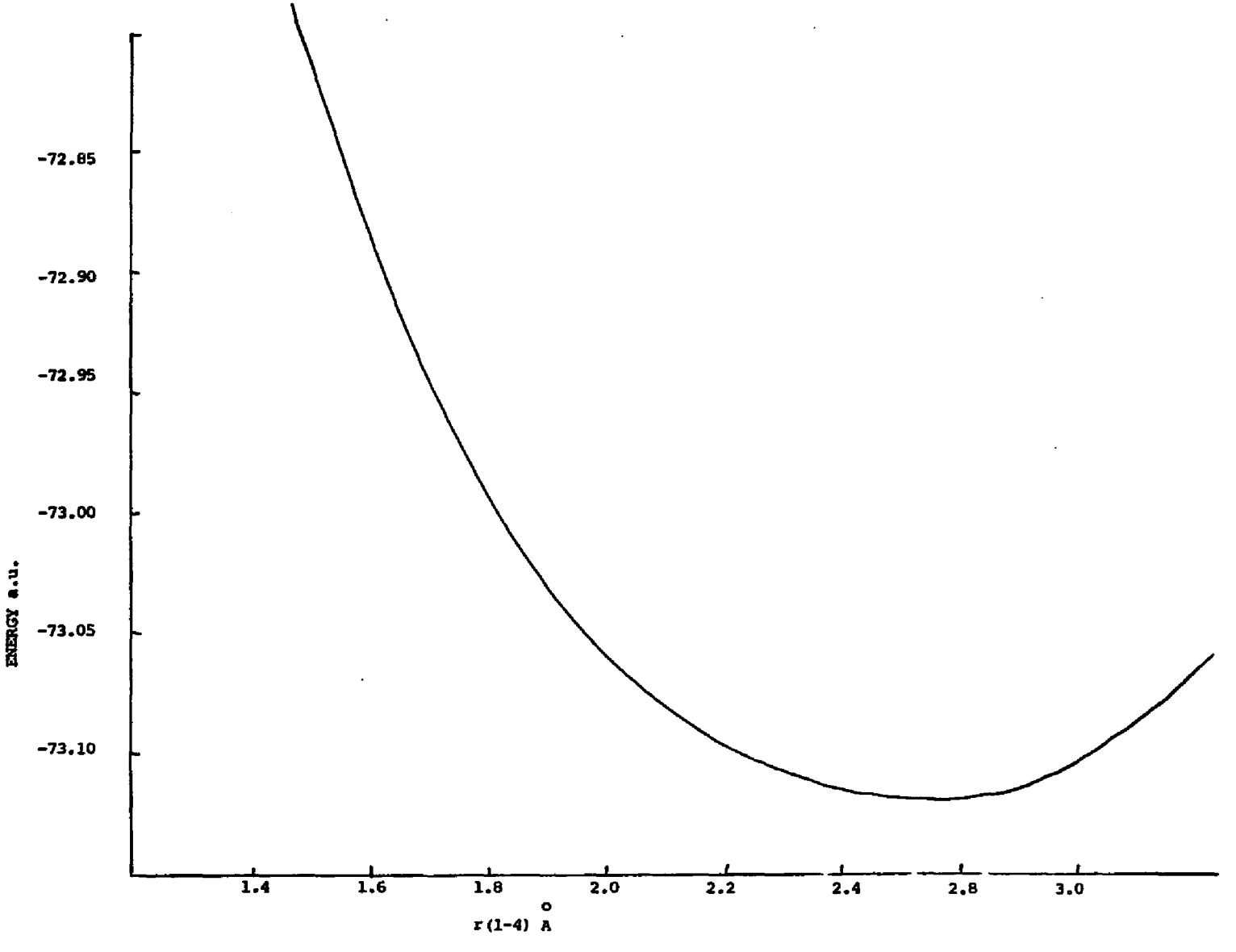

FIGURE 37. ENERGY SURFACE SEGMENT FOR N°, 46 ELECTRONS

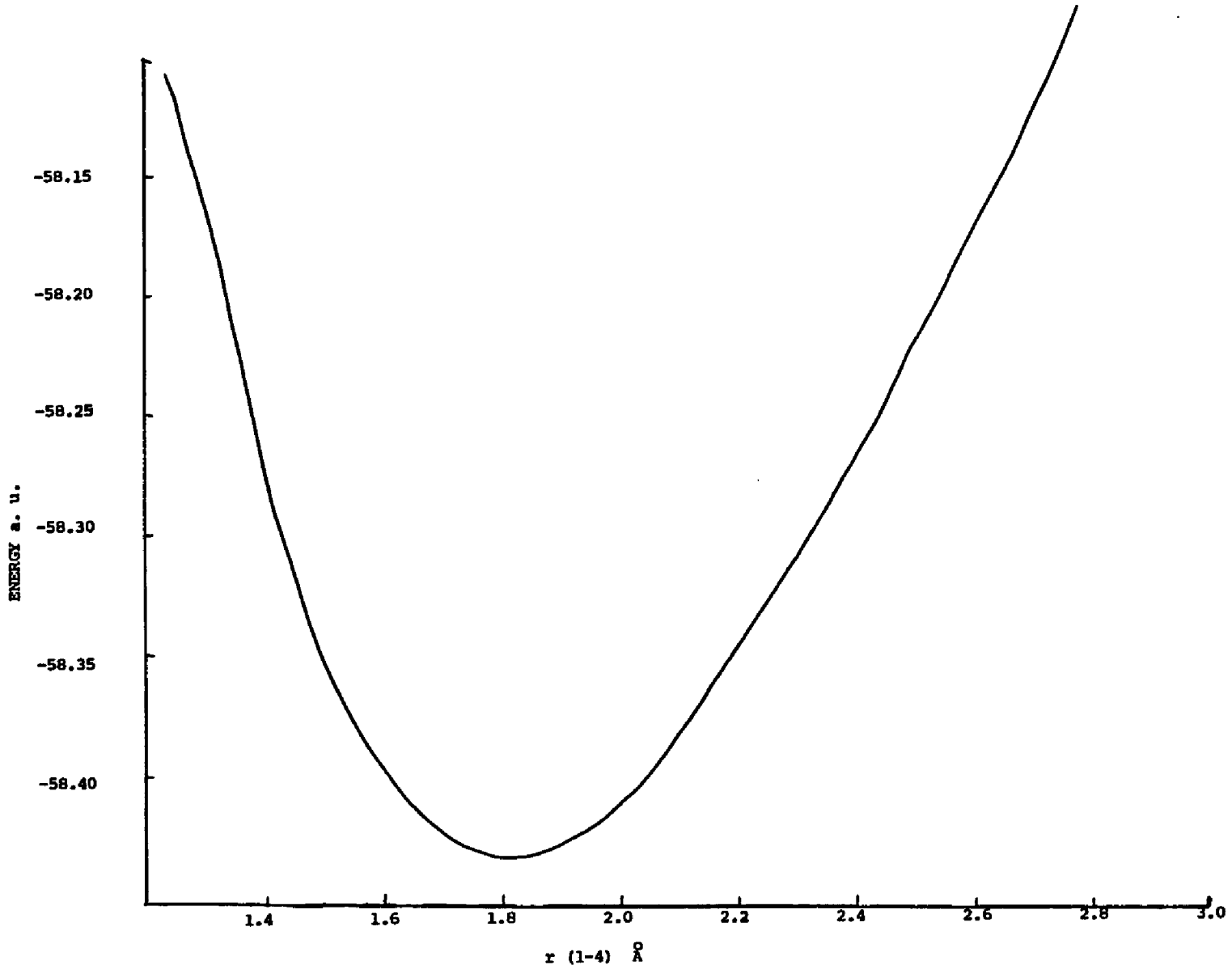

FIGURE 38. ENERGY SURFACE SEGMENT FOR B^{o}, 42 ELECTRONS

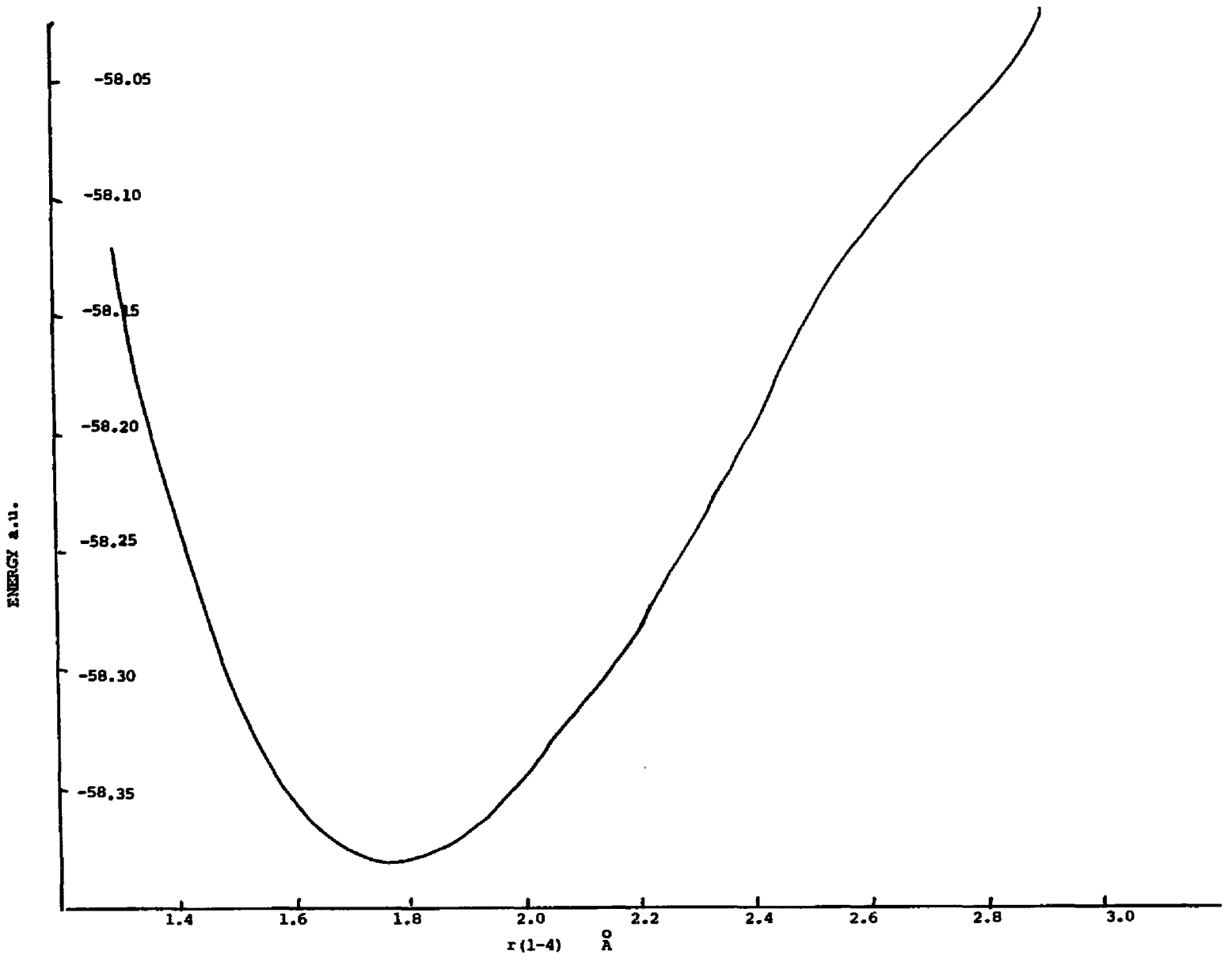

FIGURE 39. ENERGY SURFACE SEGMENT FOR B^{-1}, 43 ELECTRONS

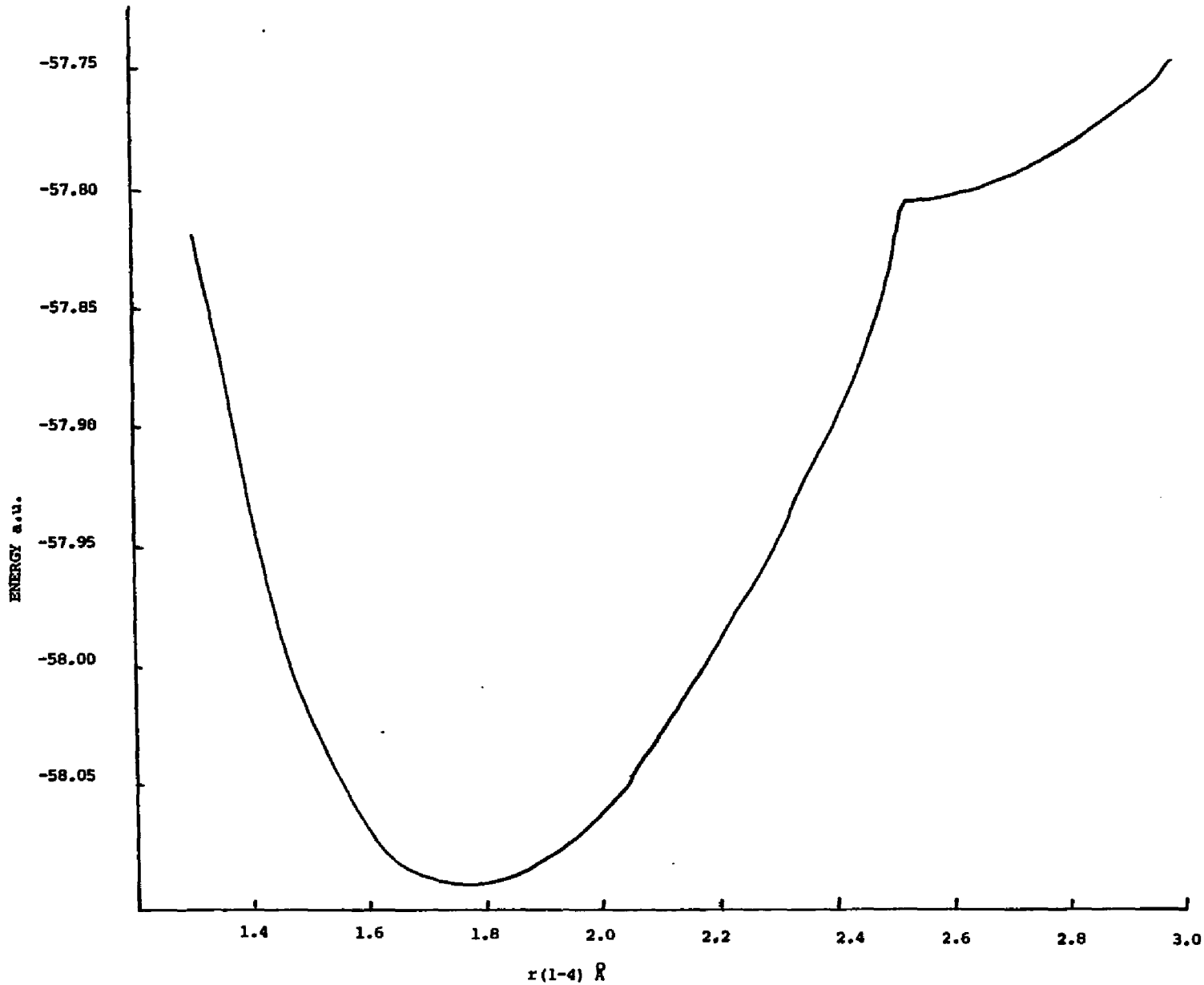

FIGURE 40. ENERGY SURFACE SEGMENT FOR B^{-2}, 44 ELECTRONS

DISCUSSION

In the exercise described in the earlier portion of this chapter, considerable data was collected and in some cases calculated from the INDO treatment of fourteen additional molecules. The sections following will deal with selected observations of interest regarding comparison of the isostructional isomers to the propellyl molecules calculated and reported in Chapter II. Because of the large volume of data, discussions will be channeled to topics related to the stability of the [2.2.2] propellane and some of its isomers.

The $r_{1,4}$ Bond Distance

A tabular comparison of the $r_{1,4}$ bond distance versus the appropriate isoelectronic grouping is compiled in Table 30. One observation of note is the consistence within class in the bond distances for the 44 electron group. As the size of the 1,4 atoms decreases (B > C > N) the central bond distance decreases as expected.

With each isomeric group the 44 electron system is always the shortest bond distance calculated. In the propellyl category as electrons are added to the C^{+2} structure, there is first a gradual decrease in the distance due to simply reducing the nuclear repulsion of the C^{+2} molecule. Addition of the first electron to the C^{s} molecule however increases the distance abruptly, whereas final addition of the second electron to C^{-1} increases $r_{1,4}$ only slightly. This abrupt increase is due to a large change in the net electron density of the C_1 and C_4 carbons (Table 16a). Rather than observing the extra electrons being increasingly diffused to the other carbons, the calculation

indicated a migration away from the outer carbons with increasing density in the C_1, C_4, and hydrogen atoms. Table 20a indicates that the added electron is lying in an antibonding orbital and thus may explain the abrupt increase in $r_{1,4}$ distance.

TABLE 30. A COMPARISON OF $r_{1,2}$ VALUES TO VARIOUS ISOELECTRONIC GROUPINGS

	$r_{1,4}$				
#Electrons	42	43	44	45	46
Molecule					
C^{+2}	1.72				
C^{+1}		1.62			
C^{S}			1.56		
C^{A}			2.45		
C^{T}			2.09		
C_{-1}				2.56	
C^{-2}					2.65
N^{+2s}			1.43		
N^{+2A}			2.33		
N^{2T}			1.98		
N^{+1}				2.39	
N^{0}					2.50
B^{0}	1.78				
B^{-1}			1.78		
B^{-2}			1.75		
B-N			1.67		
NC^{+1}			1.72		
BC^{+1}	1.75				

As in the neutral propellane the monoanion also appears to have a second minimum at an $r_{1,4}$ distance of 1.90 Å (Figure 32). This structure does have a bonding HOMO (Table 20b) and is only 10 Kcal higher in energy than the isolectionic isomer having an $r_{1,4}$ = 2.55 Å. It is difficult from this calculation to predict which of the two structures is the preferred lower

energy state. The bond order for the bonded structure is calculated to be 0.189 thus confirming the presence of a bonding HOMO. Electron densities for $C_{1,4}$, $C_{2,3}$ and H are 4.2193 and 1.1075 respectively having little variation from that calculated for the r = 2.55 Å structure. A similar case is observed in the isoelectronic calculation (Figure 36) however in this case the HOMO is found to be a bonding orbital (Table 24).

C^{+2} Dication

The C^{+2} dication was calculated to be approximately 500 K cal higher in energy than the neutral propellane. The optimized geometrical parameters were found to be essentially the same as those calculated for the isolectronic B^0 molecule (Table 14).

Dewar's calculation[36] of the $r_{1,4}$ bond distance using MINDO/3 yielded a value of 1.99 Å compared to the 1.72 Å predicted by INDO. Although Dewar attributes an "unusual" stability to C^{+2} in comparison to the bicyclo [2.2.2.] octane 57 and its monocation, 58, ($r_{1,4}$ = 2.59 and 2.35 respectively) no such effect is obvious when calculating the same molecular system in context with the propellane isomers. Figure 41 depicts the electronic energy levels 24 to 10 and their expected population. Removal of an electron from the C^0 molecule destablizes the symmetric HOMO as expected. Removal of the second electron leaves the HOMO as part of a degenerate assymetric pair. The fact that this is a 42 electron system with a degenerate HOMO may imply "aromaticity", our calculation could not demonstrate any unusual stabilization effects. A simplified comparison of C^{+2} and C^0 orbitals is shown in Figure 42. No unusual orbital stabilization effects are obvious on analysis, with the possible exception of 300 K cal decrease in energy in

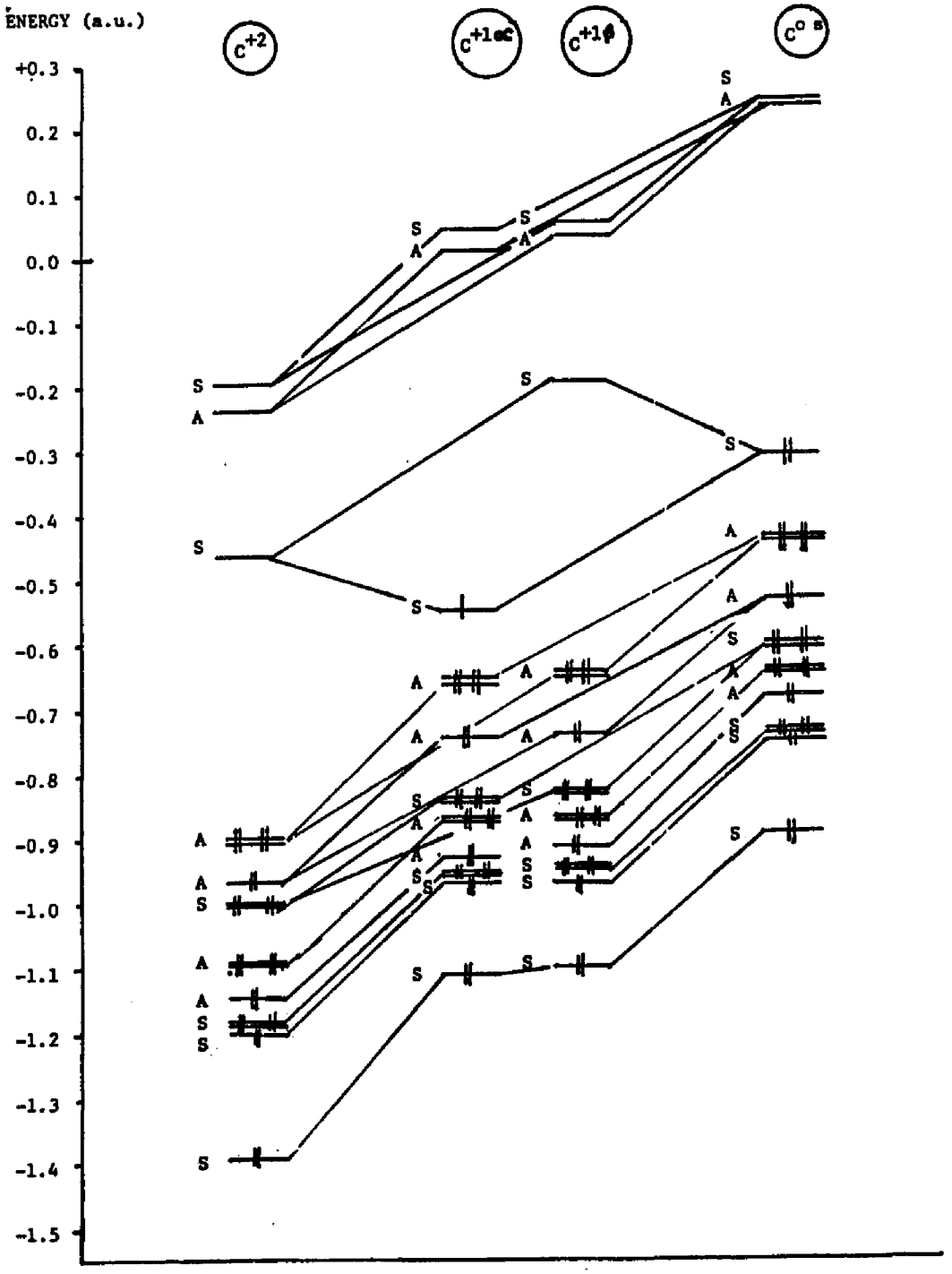

FIGURE 41. ELECTRON ORBITAL ENERGY LEVELS FOR C°, C^{+1}, AND C^{+2}

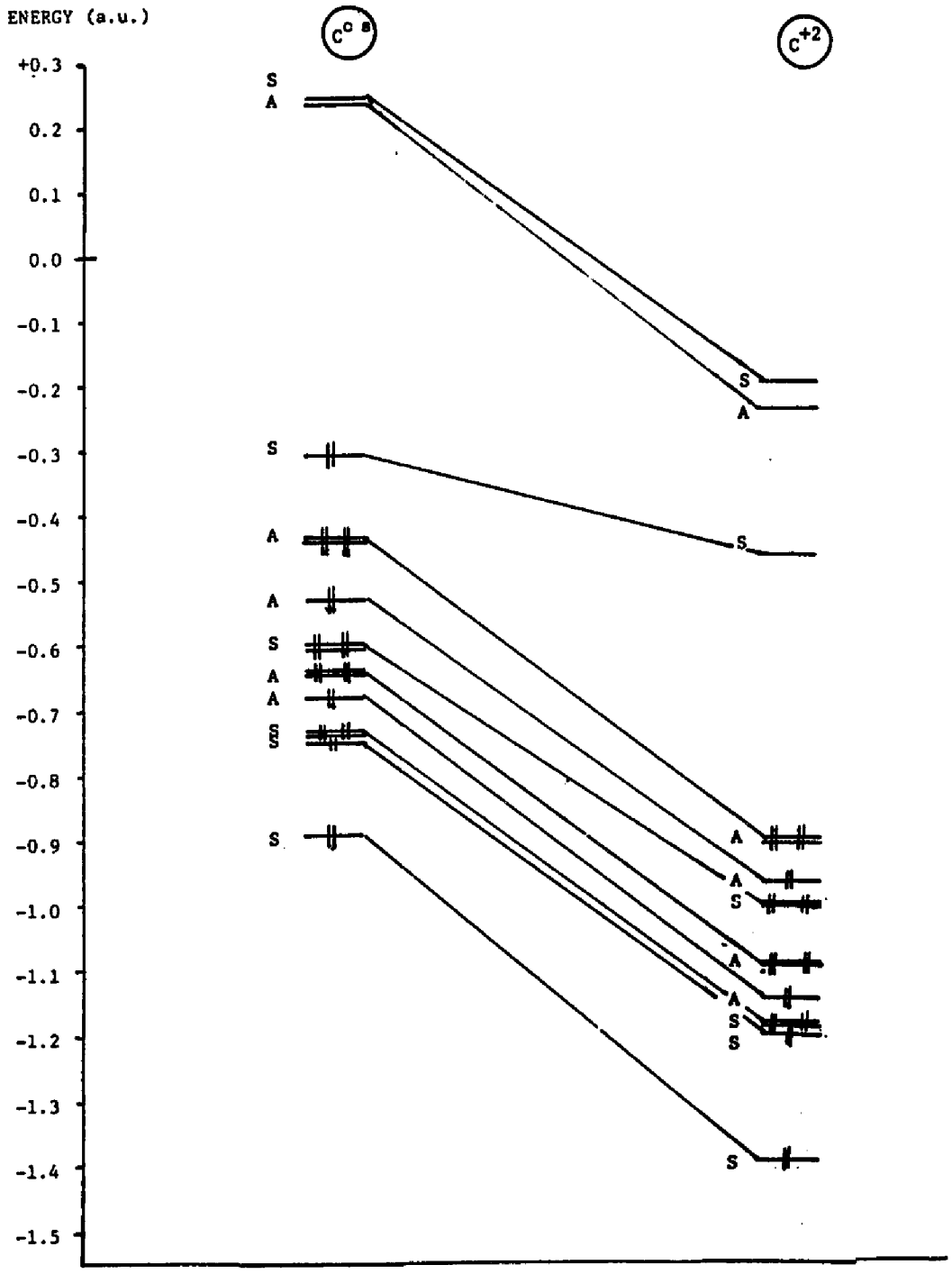

FIGURE 42. ENERGY LEVELS COMPARED FOR C^{+2} AND C°

orbital 10. This orbital is important to all of the propellane calculations as it transforms in a bonding manner (A_1) for all D_{3h} symmetry operations and contributes to the stability of all of the molecules calculated.

In comparing the C^{+2} case to the isoelectronic neutral B^0 in (Figure 43) orbitals 18 and 19 appear to be degenerate in energy however transform as $A_1"$ and $A_2"$ in symmetry. In correlation to the orbitals in the C^{+2} case the orbitals are lowered in energy unequally. (264 K cal and 385 K cal) resulting in a net stabilization of 121 K cal. Orbital 10 is likewise lowered by a large amount, 365 K cal.

Dewar also predicts an increased distribution of electrons to the methylene hydrogens in the MINDO/3 calculation. No such stabilization effect is evident in this INDO calculation as the electronic charge appears to be evenly distributed throughout the carbon-hydrogen skeleton.

DABCO and Isomers

The DABCO isomers also prove most interesting. The shortest bond distance is found in the N^{+2} symmetric dictation (44 electrons) despite the charge repulsion. Figure 44 depicts the orbital energy levels of N^o and their relative positions to the symmetric dictation N^{+2} and the monocation N^{+1}. Note that in the removal of electrons from the neutral species, there is a drop in the relative orbital energies while still maintaining a symmetric or bonding HOMO. Removing electrons from the neutral propellane likewise reduces the relative energy of the HOMO; however, in the case of the C^{+2} dication the last four electrons are placed in a set of degenerate antibonding orbitals.

The N^{+2} molecule is isoelectronically similar to the C^o propellane in (44 electrons) and can also boast of a double well minimum on

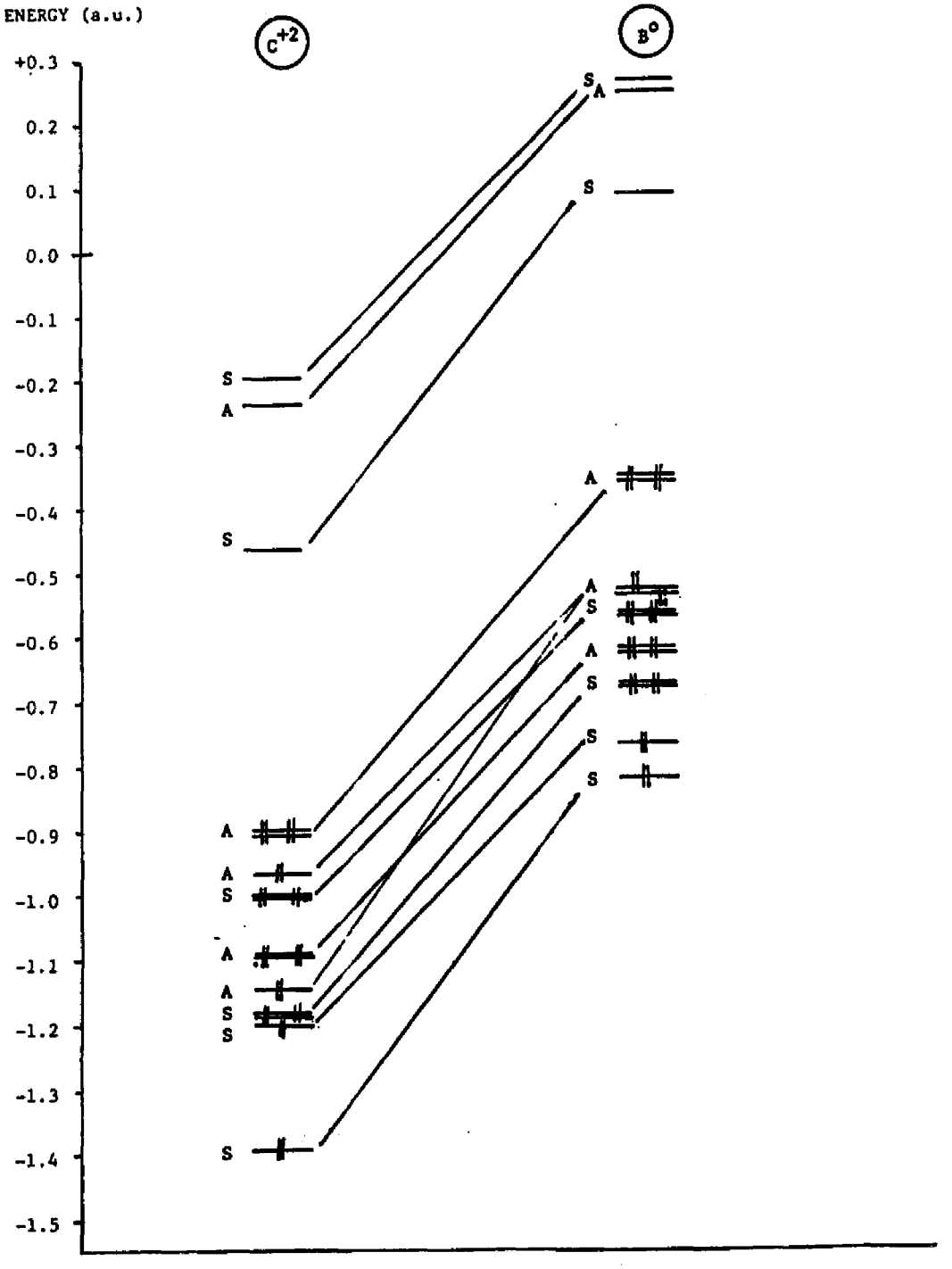

FIGURE 43. ENERGY LEVELS COMPARED FOR C^{+2} AND B°

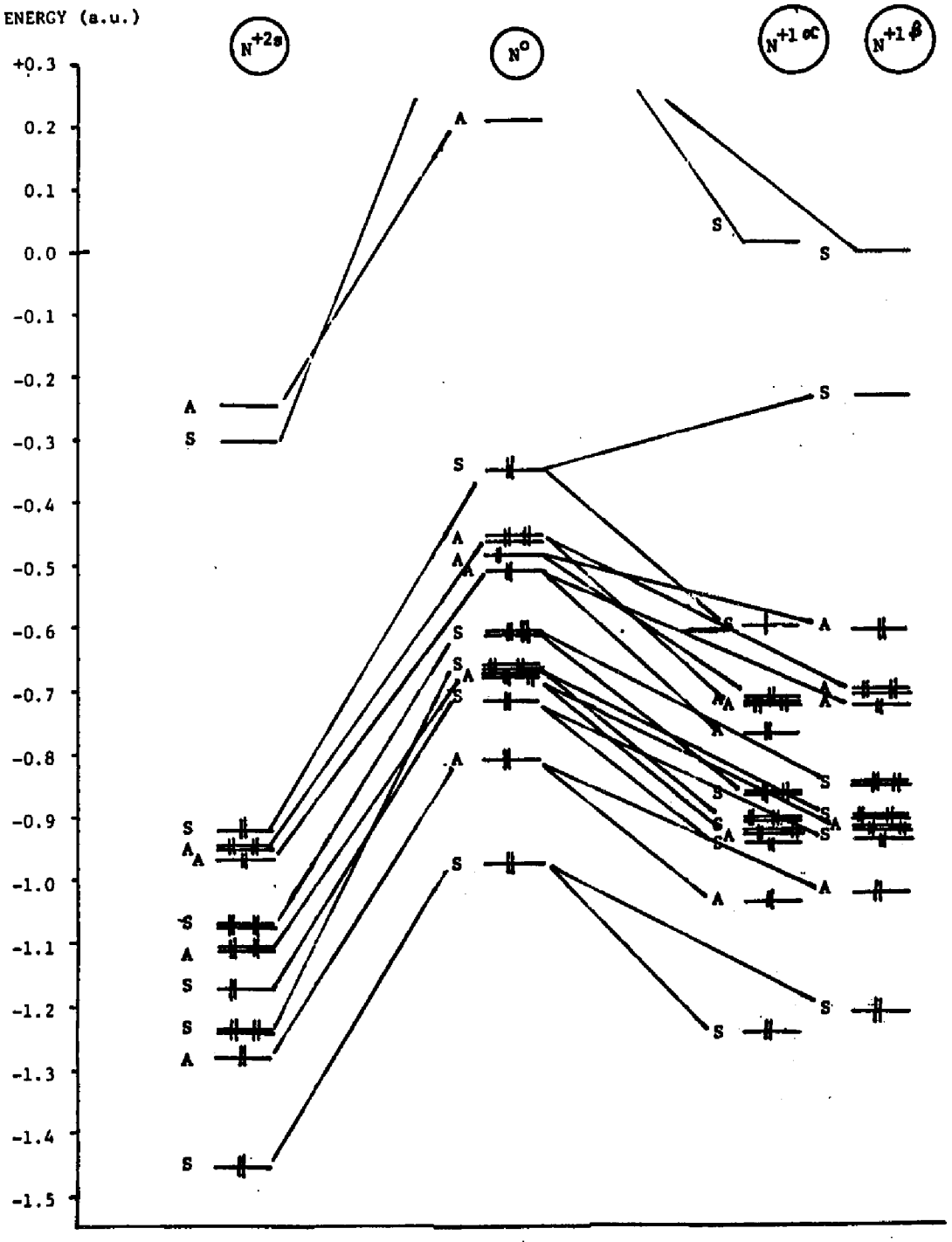

FIGURE 44. ENERGY LEVELS COMPARED FOR DABCO AND ISOMERS

the same segment of the potential energy, Figure 34. In fact, a triple state analogous to C^t has also been calculated (Figure 35). A comparison of orbital energies of N^{+2s} to N^{+2a} indicates the same HOMO-LUMO crossing (Figure 45) as observed in the propellyl case (Figure 12) and both molecules possess a low lying triplet state capable of being populated. Two questions come to mind in the above discussion:

- Is the higher energy minimum of N^{+2a} real or is it also a saddlepoint on an analogous Cope type surface?
- Is there a dicationic molecule which can be suitably excited to populate this low-lying triplet state to form the DABCO dication?

The answer to both questions should ideally be contained in the same species, however, this author knows of no dispositive, diradical species. This, however could be the the subject of further research.

<u>B^o Isomers</u>

B^o has its HOMO as part of a degenerate pair of assymetric orbitals similar to the C^{+2} case. The addition of a single electron to B^o populates a symmetric bonding orbital (Figure 46). The second electron likewise enters this orbital forming a pair occupying a symmetric (bonding) orbital. This bonding effect is evident in the dramatic increase of p_x bond order on the addition of electrons, (.1608 to .4590 to .7391 for B^o, B^{-1} and B^{-2} respectively). The electrons are increasingly directed to the 1,4 positions although there is an obvious increase in the hydrogen electron density in the B^{-2} case also.

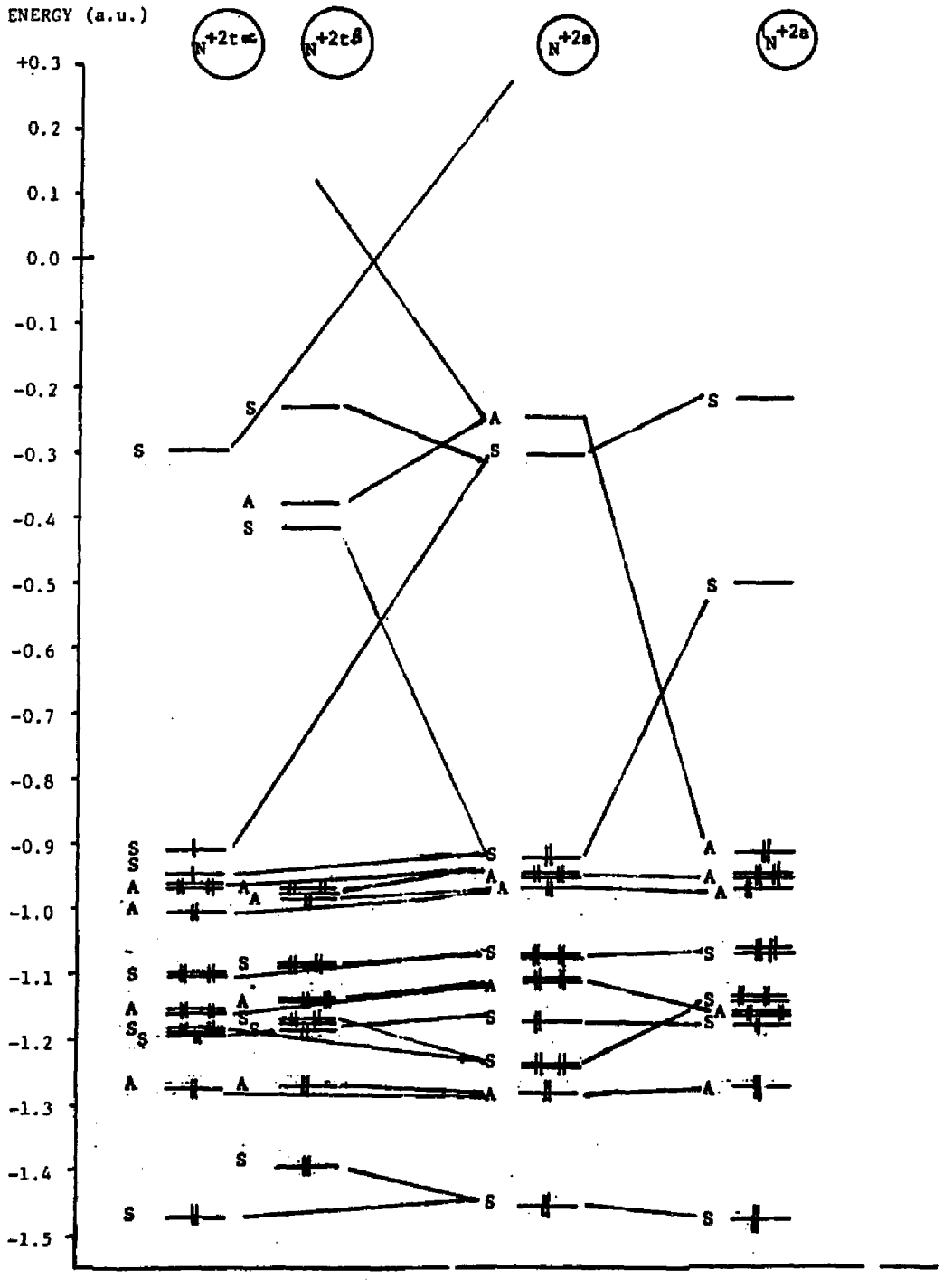

FIGURE 45. ENERGY LEVELS COMPARED FOR DABCO DICATIONS

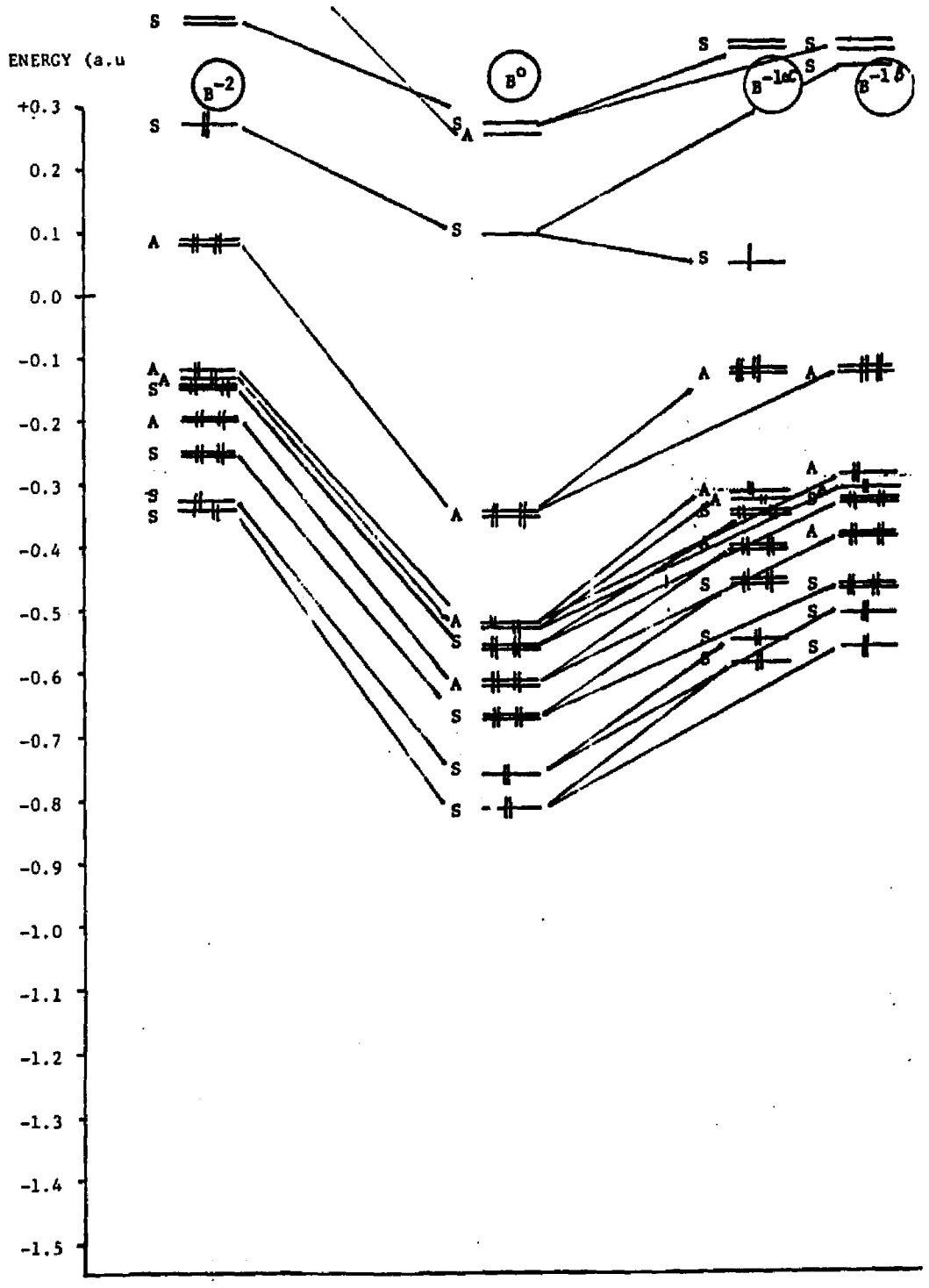

FIGURE 46. ORBITAL POPULATION AND RELATIVE ENERGIES OF B° ISOMERS

The calculation indicates the possibility of forming a tetra-coordinate Boron bond in this type of system. This effect would have to be proven by experiement

44 Electron System

Figure 47 depicts a comparison of population and orbital emerges. Each of the molecules calculated exhibit a symmetric bonding HOMO and each configuration purports to be a stabile species. C^{OS} and N^{+2s} both have definitively exhibited dual miniman, the B^{-2a} case however has not been optimized in this study. A deflection at longer $r_{1,4}$ is observed when calculating a segment of the energy surface which describes an increase in the 1,4 distance (Figure 40). Perhaps optimization in this region would result in a second variationally stable species.

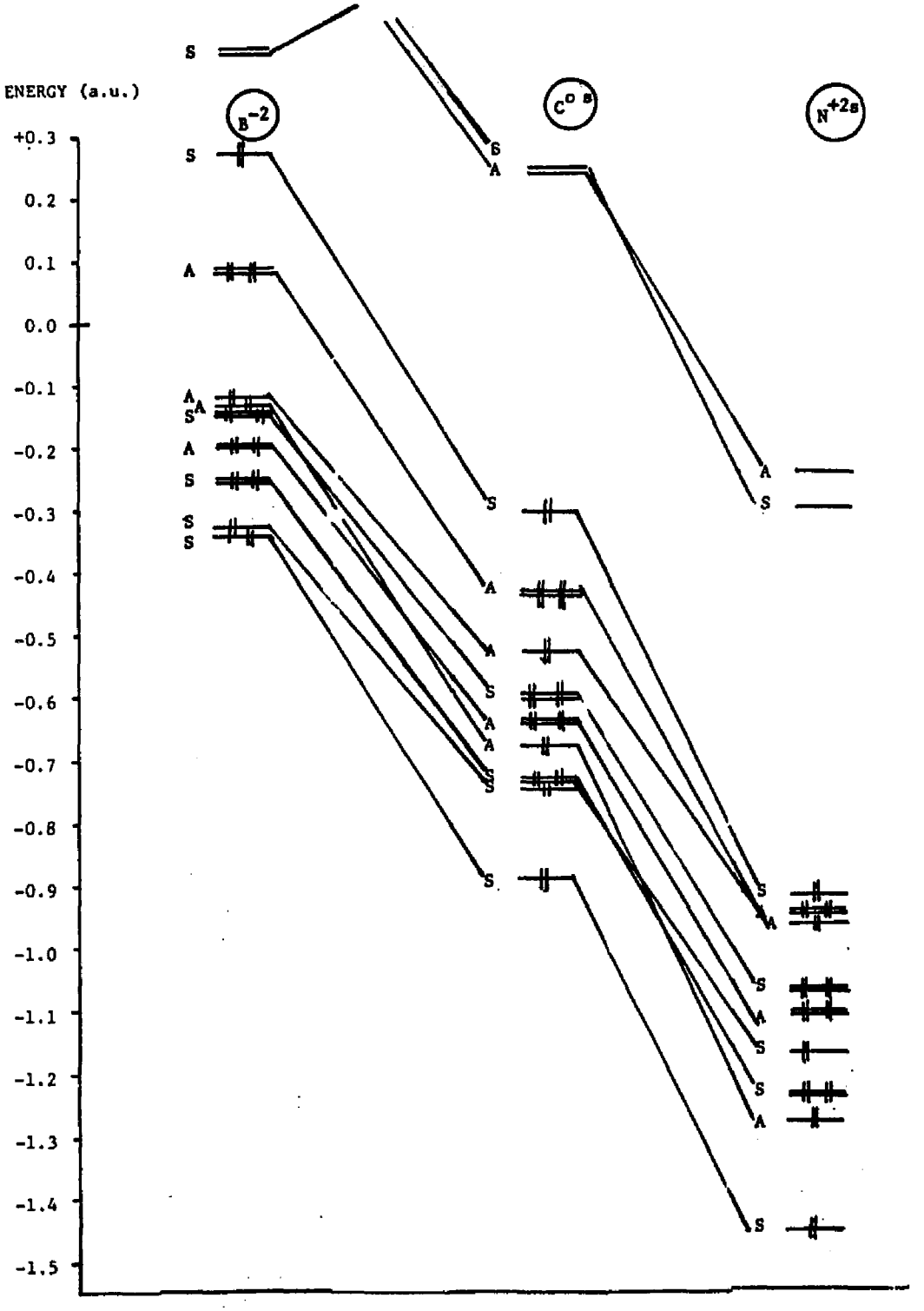

FIGURE 47. ORBITAL POPULATIONS AND ENERGIES OF THE 44 ELECTRON SYSTEMS

CHAPTER V

REFERENCES

(32) Dannenberg, J. J.; Prooiv, T. M. J. Am. Chem. Soc. 1974, 96, 913.

(33) Wiberg, K. B.; Burgmaier, G. J. J. Amer. Chem. Soc. 1976, 94, 7396.

(34) Eaton, P. E.; Temme, G. H., III Ibid. 1973, 95, 7508.

(35) Wasserman, E. Bell Laboratories, personal communication.

(36) Olah, G.; Schleyer, P.v.R.; Dewar, M.J.S. J. Am. Chem. Soc. 1973, 95, 6829.

(37) Bingham, R.; Dewar, M.J.S.; Lo, D. H. Ibid. 1975, 97, 1285.

(38) Fry, J. L.; Engler, E. M.; Schleyer, P.v.R. Ibid. 1972, 94, 4628.

CHAPTER VI

CONCLUSIONS

This will be the final and most welcomed chapter of this dissertation. In the following sections I've attempted to summarize the various highlights of the research work as well as make some recommendations for potential extension of this work.

[2.2.2.] Propellane

The successful synthesis of 2 resulting from this research work has clearly demonstrated that semiempirical, particularly the INDO method, was very useful in predicting a synthesis pathway, which would most likely not have been tried, had not these calculations been performed. Molecule 2 had been the subject of numerous investigations prior to the beginning of this thesis research. In every case attempts at synthesis of the molecule had culminated unsuccessfully. The INDO calculations confirmed that the molecule 2 did have an unusual energy surface and exhibited two minimal energy wells on the segment described by streching the $r_{1,4}$ bond distance. The calculation when used in the "open shell" triplet mode indicated that a triplet state of 2 might possibly exist which has been an intermediate energy between the two possible structures predicted in the singlet state as well as an intermediate $r_{1,4}$ bond distance. It seemed that the triplet state would be an ideal electronic configuration to achieve if one were interested in synthesizing 2.

The calculation by Newton and Schulman indicated that 2 would have a very short, however, finite life and may be difficult to isolate. Therefore

in order to prove that 2 had been present in the reaction it became important to select a derivative method which produced a stable product and unquestionably proved the presence of 2 in the synthesis. This, of course, could be complicated by the fact that with two energy minima there may possibly be two different reactions occuring in the derivation reaction. However, investigation by Gajewsky and Dewar indicate that the second minima is more than likely a "saddle point" on a secondary energy surface. In other words, what appears to be a minimum energy on the $r_{1,4}$ stretch segment may be a maximum energy on a Cope rearrangement involving 1,4 dimethylene-cyclohexane, 4. The degenerate Cope rearrangement proceeds in a concerted manner and therefore, what appears to be a second stable minima, is merely a transition state on the secondary surface. Therefore, it is not considered competitive with any reaction process.

Compound 4 seemed a likely candidate as a starting material for this synthesis. On inspection 4 had the appropriate geometry to form 2 through an apparent forbidden 2 + 2 addition. Compound 4 could also be excited through a triplet energy structure which would geometrically rearrangement to the triplet state of 2 or compound 19. If 19 was achieved, the compound could merely decay to the potential energy well represented by 2 Any of 4 which may have entered on the right side of the energy surface depicted in Figure 10 would merely follow the very rapid Cope rearrangement to one of the preferred configurations of 4 thus reestablishing starting material.

The above summary should convince the reader of the worth of the INDO calculations in a system requiring unpaired electron systems. This is not to say that INDO will be the panacea for all reactions involving synthesis or possibly even diradicals. Each specific calculation method has its own

merits and its own applications. It is only to the user to decide which system will give him the appropriate leading information without taxing his time for his research project. With little knowledge of the intricacies of quantum mechanics, the experimental chemist can use the various semiempirical programs in a manner not unlike the test tube. I might add also that even though INDO calculations have fallen out of common use and better systems such MINDO/3 and MNDO are available, it is not clear that any more sophisticated or refined system would have given a better lead into a synthetic method for 2.

An additional benefit of this research was a relatively unique method of synthesizing 1,4 dibromobicyclooctane, 23. A combination of steps used although complicated did produce acceptable yields of the required compound for characterization and comparison to our reaction product mixes.

Other Propellanes

The different sequences of isomers to the propellane were calculated primarily to indicate trends associated with substituting different atoms in the 1,4 positions of the propellane. Similarities in isoelectronic species were consistent with effects expected.

The true value of the exercise was the validation of the INDO method for predicting geometrical changes in the molecules studied, consistent with physical theory. Other interesting phenomena could also be extrapolated from the series of calculations. These are as follows:

- A double minimum Potential Energy slice is predicted for all 43, 44 and 45 electron containing propellane systems.
- The DABCO Dication has a shorter $r_{1,4}$ bond distance than the neutral species, despite the charge repulsion.

- The DABCO dication surface is similar in shape to the surface of the propellane 2. It also possesses a triplet state intermediate in both energy and bond distance when compared to the symmetric and assymetric geometries. If in fact a DABCO dication were achieved, the triplet state intersystem crossing would require little energy (See Figure 45). The consequence of the decay of a relaxed triplet would be of interest to examine. Whether the decay would proceed to the DABCO minimum or the secondary minimum (right side of Figure 34.) would be as unpredictable as in the propellane case.
- The neutral propellane may by synthesized from [2.2.2.0.] bicyclooctane dication (generated in "magic acid"). This dication is identical in structure and state to C^{+2}. Subsequent electrolytic reduction with two electrons could produce C^{o} or 2 in better yield.
- The propellyl dication has a degenerate, assymmetric HOMO and a symmetric LUMO. The reduction of the species with one electron will stabilize the symmetric orbital by almost 60 K cal. This structure would represent the one-electron bonded (C^{+1}) propellane. Hyperfine coupling constants can be measured in an electron spin resonance (ESR) spectrometer and compared to the predicted values presented on Table 16b.

Perhaps the reader can identify a number of other predictions resulting from the calculations. The power of the semi-empirical computations is in their ability to generate considerable data. The value of this form of

computational chemistry lies in the ability of the researcher to extract the appropriate information from the computed model and use that information to predict a process, surface or geometry. The success of the calculation is always measured in the experiment as in the case of this study; the synthesis of [2.2.2] Propellane.

ACKNOWLEDGEMENTS

My thanks has to extend first to Professor J. J. Dannenberg for his patience and efforts on my behalf, to my committee, Professors R. Odum, L. Massa, and J. Howell, who have also patiently awaited this dissertation. Thanks also to Professor Angelo Santoro for his special help.

Special thanks goes to JoAnn Prociv (my wife) for her moral and sometimes physical support in the preparation of this work.

Thanks to Al Adelman, Richard Nathan, and Joseph Pizzuto of Battelle for not letting up.

And lastly for the able efforts of Cheryl Noblick without whom this thesis would have never been organized and typed.

APPENDIX A

$(C\text{-}C)^S$

ORBITAL	E (a.u)	1-4 Character	C_3	C'_3	C_2	C'_2	C''_2	σ_h	σ_v	σ_v'	σ_v''	S	S'	Point Symmetry
24	.2383	N	0	0	0	0	1	1	0	0	1	0	0	
23	.2360	A	1	1	-1	-1	-1	-1	1	1	1	-1	-1	A_2''
22	-.3226	B	1	1	1	1	1	1	1	1	1	1	1	A_1'
21	-.4279	N	0	0	0	-1	0	-1	0	1	0	0	0	
20	-.4279	N	0	0	-1	0	0	-1	1	0	0	0	0	
19	-.5461	N	1	1	1	1	1	-1	-1	-1	-1	-1	-1	A_1''
18	-.6103	N	0	0	-1	0	0	1	-1	0	0	0	0	
17	-.6103	N	0	0	0	-1	0	1	0	-1	0	0	0	
16	-.6532	N	0	0	0	-1	0	-1	0	1	0	0	0	
15	-.6532	N	0	0	0	0	-1	-1	0	0	1	0	0	
14	-.6998	A	1	1	-1	-1	-1	-1	1	1	1	-1	-1	A_2''
13	-.7470	N	0	0	0	1	0	1	0	1	0	0	0	
12	-.7470	N	0	0	0	-1	0	1	0	-1	0	0	0	
11	-.7567	N	1	1	-1	-1	-1	1	-1	-1	-1	1	1	A_2'
10	-.9031	B	1	1	1	1	1	1	1	1	1	1	1	A_1''

Table II. Symmetry character table for II.

$(C\text{-}C)^A$

ORBITAL	E (a.u.)	1-4 Character	C_3	C'_3	C_2	C'_2	C''_2	σ_h	σ_v	σ_v'	σ_v''	S	S'	Point Symmetry
24	.2482	N	0	0	1	0	0	1	1	0	0	0	0	
23	-.0335	B	1	1	1	1	1	1	1	1	1	1	1	A_1'
22	-.3053	A	1	1	-1	-1	-1	-1	1	1	1	-1	-1	A_2''
21	-.4493	N	0	0	0	0	1	-1	0	0	-1	0	0	
20	-.4493	N	0	0	0	0	-1	-1	0	0	1	0	0	
19	-.5325	N	1	1	1	1	1	-1	-1	-1	-1	-1	-1	A_1''
18	-.6139	N	0	0	1	0	0	1	1	0	0	0	0	
17	-.6139	N	0	0	-1	0	0	1	-1	0	0	0	0	
16	-.6320	N	0	0	0	0	-1	1	0	0	-1	0	0	
15	-.6320	N	0	0	0	0	1	1	0	0	1	0	0	
14	-.6723	N	0	0	0	0	-1	-1	0	0	1	0	0	
13	-.6723	N	0	0	-1	0	0	-1	1	0	0	0	0	
12	-.7259	N	1	1	-1	-1	-1	1	-1	-1	-1	1	1	A_2'
11	-.7359	A	1	1	-1	-1	-1	-1	1	1	1	-1	-1	A_2''
10	-.9509	B	1	1	1	1	1	1	1	1	1	1	1	A_1'

Table III. Symmetry character table for XVIII.

$(\Theta\text{-}C)^T$ α Spin

ORBITAL	E (a.u.)	1-4 Character	C_3	C'_3	C_2	C'_2	C''_2	σ_h	σ_v	σ_v'	σ_v''	S	S'	Point Symmetry
24	.2424	N	0	0	1	0	0	1	1	0	0	0	0	
23	-.3207	B	1	1	1	1	1	1	1	1	1	1	1	A_1'
22	-.3214	A	1	1	-1	-1	-1	-1	1	1	1	-1	-1	A_2''
21	-.4574	N	0	0	-1	0	0	-1	1	0	0	0	0	
20	-.4574	N	0	0	0	-1	0	-1	0	1	0	0	0	
19	-.5404	N	1	1	1	1	1	-1	-1	-1	-1	-1	-1	A_1''
18	-.6318	N	0	0	-1	0	0	1	-1	0	0	0	0	
17	-.6318	N	0	0	1	0	0	1	1	0	0	0	0	
16	-.6667	N	0	0	0	-1	0	-1	0	1	0	0	0	
15	-.6667	N	0	0	-1	0	0	-1	1	0	0	0	0	
14	-.6871	N	0	0	0	-1	0	1	0	-1	0	0	0	
13	-.6871	N	0	0	-1	0	0	1	-1	0	0	0	0	
12	-.7257	A	1	1	-1	-1	-1	-1	1	1	1	-1	-1	A_2''
11	-.7503	N	1	1	-1	-1	-1	1	-1	-1	-1	1	1	A_2'
10	-.9753	B	1	1	1	1	1	1	1	1	1	1	1	A_1'

Table IVa. Character table for the triplet state configuration, α spin.

$(C\text{-}C)^{T}_{\beta}$ Spin

ORBITAL	E (a.u.)	1-4 Character	C_3	C'_3	C_2	C'_2	C''_2	σ_h	σ_v	$\sigma_{v'}$	$\sigma_{v''}$	s	s'	Point Symmetry
24	.2468	N	0	0	1	0	0	1	1	0	0	0	0	
23	.1721	B	1	1	-1	-1	-1	-1	1	1	1	-1	-1	A_2''
22	.1090	A	1	1	1	1	1	1	1	1	1	1	1	A_1'
21	-.4488	N	0	0	0	-1	0	-1	0	1	0	0	0	
20	-.4488	N	0	0	0	0	-1	-1	0	0	1	0	0	
19	-.5358	N	1	1	1	1	1	-1	-1	-1	-1	-1	-1	A_1''
18	-.6190	N	0	0	-1	0	0	1	-1	0	0	0	0	
17	-.6190	N	0	0	1	0	0	1	1	0	0	0	0	
16	-.6615	N	0	0	0	-1	0	-1	0	1	0	0	0	
15	-.6615	N	0	0	0	0	-1	-1	0	0	1	0	0	
14	-.6755	N	0	0	0	1	0	1	0	1	0	0	0	
13	-.6755	N	0	0	0	-1	0	1	0	-1	0	0	0	
12	-.7007	A	1	1	-1	-1	-1	-1	1	1	1	-1	-1	A_2''
11	-.7471	N	1	1	-1	-1	-1	1	-1	-1	-1	1	1	A_2'
10	-.8843	B	1	1	1	1	1	1	1	1	1	1	1	A_1'

Table IVb. Character table for the triplet state configuration, β spin.

$(C_{3v})^{+2}$

ORBITAL	E (a.u.)	1-4 Character	C_3	C'_3	C_2	C'_2	C''_2	σ_h	σ_v	σ_v'	σ_v''	S	S'	Point Symmetry
24	-.2236	B	1	1	1	1	1	1	1	1	1	1	1	A_1'
23	-.2794	A	1	1	-1	-1	-1	-1	1	1	1	-1	-1	A_2''
22	-.4782	B	1	1	1	1	1	1	1	1	1	1	1	A_1'
21	-.9153	N	0	0	-1	0	0	-1	0	1	0	0	0	
20	-.9153	N	0	0	0	0	-1	-1	0	0	1	0	0	
19	-.9736	N	1	1	1	1	1	-1	-1	-1	-1	-1	-1	A_1''
18	-1.0712	N	0	0	0	0	1	1	0	0	1	0	0	
17	-1.0712	N	0	0	0	0	-1	1	0	0	-1	0	0	
16	-1.1153	N	0	0	0	-1	0	-1	0	1	0	0	0	
15	-1.1153	N	0	0	-1	0	0	-1	1	0	0	0	0	
14	-1.1681	A	1	1	-1	-1	-1	-1	1	1	1	-1	-1	A_2''
13	-1.1742	N	0	0	0	1	0	1	0	1	0	0	0	
12	-1.1742	N	0	0	0	-1	0	1	0	-1	0	0	0	
11	-1.1940	N	1	1	-1	-1	-1	1	-1	-1	-1	1	1	A_2'
10	-1.4115	B	1	1	1	1	1	1	1	1	1	1	1	A_1'

$(C\text{-}C)^{+1}$ α Spin

ORBITAL	E (a.u.)	1-4 Character	C_3	C'_3	C_2	C'_2	C''_2	σ_h	σ_v	$\sigma_{v'}$	$\sigma_{v''}$	S	S'	Point Symmetry
24	.0146	B	1	1	1	1	1	1	1	1	1	1	1	A_1'
23	- .0164	A	1	1	-1	-1	-1	-1	1	1	1	-1	-1	A_2''
22	- .5719	B	1	1	1	1	1	1	1	1	1	1	1	A_1'
21	- .6749	N	0	0	0	-1	0	-1	0	1	0	0	0	
20	- .6749	N	0	0	-1	0	0	-1	1	0	0	0	0	
19	- .7611	N	1	1	1	1	1	-1	-1	-1	-1	-1	-1	A_1''
18	- .8455	N	0	0	-1	0	0	1	-1	0	0	0	0	
17	- .8455	N	0	0	1	0	0	1	1	0	0	0	0	
16	- .8847	N	0	0	-1	0	0	-1	1	0	0	0	0	
15	- .8847	N	0	0	0	0	-1	-1	0	0	1	0	0	
14	- .9439	A	1	1	-1	-1	-1	-1	1	1	1	-1	-1	A_2''
13	- .9686	N	0	0	0	1	0	1	0	1	0	0	0	
12	- .9686	N	0	0	0	-1	0	1	0	-1	0	0	0	
11	- .9741	N	1	1	-1	-1	-1	1	-1	-1	-1	1	1	A_2'
10	-1.1741	B	1	1	1	1	1	1	1	1	1	1	1	A_1'

$(C\text{-}C)^{+1}$ β Spin

ORBITAL	E (a.u.)	1-4 Character	C_3	C'_3	C_2	C'_2	C''_2	σ_h	σ_v	σ_v'	σ_v''	S	S'	Point Symmetry
24	.0246	B	0	0	-1	0	0	1	-1	0	0	0	0	
23	.0119	A	1	1	-1	-1	-1	-1	1	1	1	-1	-1	A_2''
22	-.2316	B	1	1	1	1	1	1	1	1	1	1	1	A_1'
21	-.6701	N	0	0	1	0	0	-1	-1	0	0	0	0	
20	-.6701	N	0	0	-1	0	0	-1	1	0	0	0	0	
19	-.7568	N	1	1	1	1	1	-1	-1	-1	-1	-1	-1	A_1''
18	-.8336	N	0	0	0	-1	0	1	0	-1	0	0	0	
17	-.8336	N	0	0	0	0	-1	1	0	0	-1	0	0	
16	-.8806	N	0	0	-1	0	0	-1	1	0	0	0	0	
15	-.8806	N	0	0	0	-1	0	-1	0	1	0	0	0	
14	-.9241	A	1	1	-1	-1	-1	-1	1	1	1	-1	-1	A_2''
13	-.9540	N	0	0	-1	0	0	1	-1	0	0	0	0	
12	-.9540	N	0	0	1	0	0	1	1	0	0	0	0	
11	-.9714	N	1	1	-1	-1	-1	1	-1	-1	-1	1	1	A_2'
10	-1.1409	B	1	1	1	1	1	1	1	1	1	1	1	A_1'

$(C-C)^{-1}2.555\alpha$ Spin

ORBITAL	E (a.u.)	1-4 Character	C_3	C'_3	C_2	C'_2	C''_2	σ_h	σ_v	σ_v'	σ_v''	S	S'	Point Symmetry
24	.4546	N	0	0	0	0	1	1	0	0	1	0	0	
23	-.0499	B	1	1	1	1	1	1	1	1	1	1	1	A_1'
22	-.1601	A	1	1	-1	-1	-1	-1	1	1	1	-1	-1	A_2''
21	-.2212	N	0	0	-1	0	0	-1	1	0	0	0	0	
20	-.2212	N	0	0	1	0	0	-1	-1	0	0	0	0	
19	-.3185	N	1	1	1	1	1	-1	-1	-1	-1	-1	-1	A_1''
18	-.3793	N	0	0	0	0	-1	1	0	0	-1	0	0	
17	-.3793	N	0	0	0	0	1	1	0	0	1	0	0	
16	-.4270	N	0	0	0	-1	0	1	0	-1	0	0	0	
15	-.4270	N	0	0	0	0	-1	1	0	0	-1	0	0	
14	-.4464	N	0	0	0	-1	0	-1	0	1	0	0	0	
13	-.4464	N	0	0	0	0	-1	-1	0	0	1	0	0	
12	-.5122	N	1	1	-1	-1	-1	1	-1	-1	-1	1	1	A_2'
11	-.5122	A	1	1	-1	-1	-1	-1	1	1	1	-1	-1	A_2''
10	-.7237	B	1	1	1	1	1	1	1	1	1	1	1	A_1'

$(C\text{-}C)^{-1}_{2.555}$ β Spin

ORBITAL	E (a.u.)	1-4 Character	C_3	C'_3	C_2	C'_2	C''_2	σ_h	σ_v	σ_v'	σ_v''	S	S'	Point Symmetry
24	.4582	N	0	0	0	0	1	1	0	0	1	0	0	
23	.2911	B	1	1	1	1	1	1	1	1	1	1	1	A_1'
22	-.0307	A	1	1	-1	-1	-1	-1	1	1	1	-1	-1	A_2''
21	-.2153	N	0	0	0	0	-1	-1	0	0	1	0	0	
20	-.2153	N	0	0	0	0	1	-1	0	0	-1	0	0	
19	-.3141	N	1	1	1	1	1	-1	-1	-1	-1	-1	-1	A_1''
18	-.3756	N	0	0	0	0	1	1	0	0	1	0	0	
17	-.3756	N	0	0	1	0	0	1	1	0	0	0	0	
16	-.4092	N	0	0	0	-1	0	1	0	-1	0	0	0	
15	-.4092	N	0	0	0	1	0	1	0	1	0	0	0	
14	-.4425	N	0	0	0	-1	0	-1	0	1	0	0	0	
13	-.4425	N	0	0	0	0	-1	-1	0	0	1	0	0	
12	-.5061	N	1	1	-1	-1	-1	-1	1	1	1	-1	-1	A_2''
11	-.5093	A	1	1	-1	-1	-1	1	-1	-1	-1	1	1	A_2'
10	-.6863	B	1	1	1	1	1	1	1	1	1	1	1	A_1'

$(C\text{-}C)^{-1}_{1.90}$ α Spin

ORBITAL	E (a.u.)	1-4 Character	C_3	C'_3	C_2	C'_2	C''_2	σ_h	σ_v	$\sigma_{v'}$	$\sigma_{v''}$	S	S'	Point Symmetry
24	.4534	N	0	0	-1	0	0	1	1	0	0	0	0	
23	.0309	A	1	1	-1	-1	-1	-1	1	1	1	-1	-1	A_2''
22	-.0588	B	1	1	1	1	1	1	1	1	1	1	1	A_1'
21	-.2207	N	0	0	0	0	1	-1	0	0	-1	0	0	
20	-.2207	N	0	0	0	0	-1	-1	0	0	1	0	0	
19	-.3271	N	1	1	1	1	1	-1	-1	-1	-1	-1	-1	A_1''
18	-.3856	N	0	0	-1	0	0	1	-1	0	0	0	0	
17	-.3856	N	0	0	1	0	0	1	1	0	0	0	0	
16	-.4443	N	0	0	0	0	-1	-1	0	0	1	0	0	
15	-.4443	N	0	0	0	0	1	-1	0	0	-1	0	0	
14	-.4790	N	0	0	0	0	-1	1	0	0	-1	0	0	
13	-.4790	N	0	0	0	-1	0	1	0	-1	0	0	0	
12	-.4843	A	1	1	-1	-1	-1	-1	1	1	1	-1	-1	A_2''
11	-.5245	N	1	1	-1	-1	-1	1	-1	-1	-1	1	1	A_2'
10	-.7180	B	1	1	1	1	1	1	1	1	1	1	1	A_1'

$(C\text{-}C)^{-1}$ β Spin

ORBITAL	E (a.u.)	1-4 Character	C_3	C'_3	C_2	C'_2	C''_2	σ_h	σ_v	σ_v'	σ_v''	S	S'	Point Symmetry
24	.4521	N	0	0	1	0	0	1	1	0	0	0	0	
23	.4322	A	1	1	-1	-1	-1	-1	1	1	1	-1	-1	A_2''
22	.0255	B	1	1	1	1	1	1	1	1	1	1	1	A_1'
21	-.2174	N	0	0	0	-1	0	-1	0	1	0	0	0	
20	-.2174	N	0	0	1	0	0	-1	0	-1	0	0	0	
19	-.3287	N	1	1	1	1	1	-1	-1	-1	-1	-1	-1	A_1''
18	-.3842	N	0	0	1	0	0	1	1	0	0	0	0	
17	-.3842	N	0	0	0	0	1	1	0	0	1	0	0	
16	-.4445	N	1	1	0	1	0	-1	0	-1	0	0	0	
15	-.4445	N	0	0	0	-1	0	-1	0	1	0	0	0	
14	-.4735	N	1	1	-1	-1	-1	-1	1	1	1	-1	-1	A_2''
13	-.4756	N	0	0	1	0	0	1	1	0	0	0	0	
12	-.4756	A	0	0	-1	0	0	1	-1	0	0	0	0	
11	-.5251	N	1	1	-1	-1	-1	1	-1	-1	-1	1	1	A_2'
10	-.6771	B	1	1	1	1	1	1	1	1	1	1	1	A_1'

$(C\text{-}C)^{-1}$ α Spin

r = 1.55

ORBITAL	E (a.u.)	1-4 Character	C_3	C'_3	C_2	C'_2	C''_2	σ_h	σ_v	σ_v'	σ_v''	S	S'	Point Symmetry
24	.4160	B	0	0	-1	0	0	1	-1	0	0	0	0	
23	.1915	B	0	0	1	0	0	1	1	0	0	0	0	
22	-.0952	B	1	1	1	1	1	1	1	1	1	1	1	A_1'
21	-.2147	A	0	0	0	0	-1	-1	0	0	1	0	0	
20	-.2285	A	0	0	0	0	1	-1	0	0	-1	0	0	
19	-.3366	A	1	1	1	1	1	-1	-1	-1	-1	-1	-1	A_1''
18	-.3691	B	0	0	0	0	1	1	0	0	1	0	0	
17	-.4035	B	0	0	0	0	-1	1	0	0	-1	0	0	
16	-.4519	A	0	0	0	0	1	-1	0	0	-1	0	0	
15	-.4642	A	0	0	0	0	-1	-1	0	0	1	0	0	
14	-.4999	A	1	1	-1	-1	-1	-1	1	1	1	-1	-1	A_2''
13	-.5223	B	0	0	-1	0	0	1	-1	0	0	0	0	
12	-.5250	B	0	0	0	-1	0	1	0	-1	0	0	0	
11	-.5511	B	1	1	-1	-1	-1	1	-1	-1	-1	1	1	A_2'
10	-.7093	B	0	0	0	0	1	1	0	0	1	0	0	

$(C\text{-}C)^{-1}$ β Spin

r- 1.55

ORBITAL	E (a.u.)	1-4 Character	C_3	C'_3	C_2	C'_2	C''_2	σ_h	σ_v	σ_v'	σ_v''	S	S'	Point Symmetry
24	.4267	B	1	1	-1	-1	-1	-1	1	1	1	-1	-1	A_2''
23	.4252	B	0	0	-1	0	0	1	-1	0	0	0	0	
22	-.0900	B	1	1	1	1	1	1	1	1	1	1	1	A_1'
21	-.2062	A	0	0	0	0	-1	-1	0	0	1	0	0	
20	-.2133	A	0	0	-1	0	0	-1	1	0	0	0	0	
19	-.3193	A	1	1	1	1	1	-1	-1	-1	-1	-1	-1	A_1''
18	-.3658	B	0	0	0	0	1	1	0	0	1	0	0	
17	-.3935	B	0	0	0	0	-1	1	0	0	-1	0	0	
16	-.4397	A	0	0	0	0	1	-1	0	0	-1	0	0	
15	-.4574	A	0	0	1	0	0	-1	-1	0	0	0	0	
14	-.4957	A	1	1	-1	-1	-1	-1	1	1	1	-1	-1	A_2''
13	-.5037	B	0	0	0	0	0	1	0	0	0	0	0	
12	-.5142	B	0	0	0	0	1	1	0	0	1	0	0	
11	-.5478	B	0	0	0	0	0	1	0	0	0	0	0	
10	-.7085	B	0	0	0	0	1	1	0	0	1	0	0	

$(C\text{-}C)^{-2}$

ORBITAL	E (a.u.)	1-4 Character	C_3	C'_3	C_2	C'_2	C''_2	σ_h	σ_v	σ_v'	σ_v''	S	S'	Point Symmetry
24	.6614	N	0	0	0	0	1	1	0	0	1	0	0	
23	.2092	B	1	1	1	1	1	1	1	1	1	1	1	A_1'
22	.1129	A	1	1	-1	-1	-1	-1	1	1	1	-1	-1	A_2''
21	.0095	N	0	0	1	0	0	-1	0	-1	0	0	0	
20	.0095	N	0	0	0	-1	0	-1	0	1	0	0	0	
19	-.1048	N	1	1	1	1	1	-1	-1	-1	-1	-1	-1	A_1'
18	-.1445	N	0	0	0	0	1	1	0	0	1	0	0	
17	-.1445	N	0	0	0	1	0	1	0	1	0	0	0	
16	-.2031	N	0	0	-1	0	0	1	-1	0	0	0	0	
15	-.2031	N	0	0	1	0	0	1	1	0	0	0	0	
14	-.2222	N	0	0	-1	0	0	-1	1	0	0	0	0	
13	-.2222	N	0	0	0	-1	0	-1	0	1	0	0	0	
12	-.2859	A	1	1	-1	-1	-1	-1	1	1	1	-1	-1	A_2''
11	-.2993	N	1	1	-1	-1	-1	1	-1	-1	-1	1	1	A_2'
10	-.4626	B	1	1	1	1	1	1	1	1	1	1	1	A_1'

$(N\text{-}N)^{+2}$
1.425

ORBITAL	E (a.u.)	1-4 Character	C_3	C'_3	C_2	C'_2	C''_2	σ_h	σ_v	σ_v'	σ_v''	S	S'	Point Symmetry
24	-.2857	A	1	1	-1	-1	-1	-1	1	1	1	-1	-1	A_2''
23	-.3201	B	1	1	1	1	1	1	1	1	1	1	1	A_1'
22	-.9462	B	1	1	1	1	1	1	1	1	1	1	1	A_1'
21	-.9670	N	0	0	0	0	-1	-1	0	0	1	0	0	
20	-.9670	N	0	0	-1	0	0	-1	1	0	0	0	0	
19	-.9796	N	1	1	1	1	1	-1	-1	-1	-1	-1	-1	A_1'
18	-1.0960	N	0	0	0	0	1	1	0	0	1	0	0	
17	-1.0960	N	0	0	0	0	-1	1	0	0	-1	0	0	
16	-1.1368	N	0	0	-1	0	0	-1	1	0	0	0	0	
15	-1.1368	N	0	0	0	0	-1	-1	0	0	1	0	0	
14	-1.1999	N	1	1	-1	-1	-1	1	-1	-1	-1	1	1	A_2'
13	-1.2476	N	0	0	1	0	0	1	1	0	0	0	0	
12	-1.2476	N	0	0	-1	0	0	1	-1	0	0	0	0	
11	-1.2857	A	1	1	-1	-1	-1	-1	1	1	1	-1	-1	A_2''
10	-1.4607	B	1	1	1	1	1	1	1	1	1	1	1	A_1'

$(N\text{-}N)^{+2}$
2.330

ORBITAL	E (a.u.)	1-4 Character	C_3	C'_3	C_2	C'_2	C''_2	σ_h	σ_v	σ_v'	σ_v''	S	S'	Point Symmetry
24	-.2470	B	1	1	1	1	1	1	1	1	1	1	1	A_1'
23	-.5398	B	1	1	1	1	1	1	1	1	1	1	1	A_1'
22	-.9394	A	1	1	-1	-1	-1	-1	1	1	1	-1	-1	A_2''
21	-.9655	N	0	0	0	-1	0	-1	0	1	0	0	0	
20	-.9655	N	0	0	0	0	-1	-1	0	0	1	0	0	
19	-.9680	N	1	1	1	1	1	-1	-1	-1	-1	-1	-1	A_1''
18	-1.0944	N	0	0	0	0	1	1	0	0	1	0	0	
17	-1.0944	N	0	0	0	0	-1	1	0	0	-1	0	0	
16	-1.1493	N	0	0	-1	0	0	1	-1	0	0	0	0	
15	-1.1493	N	0	0	0	-1	0	1	0	-1	0	0	0	
14	-1.1556	N	0	0	0	0	-1	-1	0	0	1	0	0	
13	-1.1556	N	0	0	0	0	1	-1	0	0	-1	0	0	
12	-1.1711	N	1	1	-1	-1	-1	1	-1	-1	-1	1	1	A_2'
11	-1.2867	A	1	1	-1	-1	-1	-1	1	1	1	-1	-1	A_2''
10	-1.4842	N	0	0	0	0	1	1	0	0	1	0	0	

$(N\text{-}N)^{+2t}$ α Spin

ORBITAL	E (a.u.)	1-4 Character	C_3	C'_3	C_2	C'_2	C''_2	σ_h	σ_v	σ_v'	σ_v''	S	S'	Point Symmetry
24	-.3107	B	1	1	1	1	1	1	1	1	1	1	1	A_1'
23	-.9216	B	1	1	1	1	1	1	1	1	1	1	1	A_1'
22	-.9729	N	1	1	1	1	1	1	-1	-1	-1	-1	-1	A_1''
21	-.9771	N	0	0	0	0	-1	-1	0	0	1	0	0	
20	-.9771	N	0	0	0	0	1	-1	0	0	-1	0	0	
19	-1.0220	A	1	1	-1	-1	-1	-1	1	1	1	-1	-1	A_2''
18	-1.1247	N	0	0	-1	0	0	1	-1	0	0	0	0	
17	-1.1247	N	0	0	1	0	0	1	1	0	0	0	0	
16	-1.1596	N	0	0	1	0	0	-1	-1	0	0	0	0	
15	-1.1596	N	0	0	-1	0	0	-1	1	0	0	0	0	
14	-1.1858	N	0	0	1	0	0	1	1	0	0	0	0	
13	-1.1858	N	0	0	0	1	0	1	0	1	0	0	0	
12	-1.1911	N	1	1	-1	-1	-1	1	-1	-1	-1	1	1	A_2'
11	-1.2980	A	1	1	-1	-1	-1	-1	1	1	1	-1	-1	A_2''
10	-1.4847	N	0	0	1	0	0	1	1	0	0	0	0	

$(N-N)^{+1}$ α Spin

ORBITAL	E (a.u.)	1-4 Character	C_3	C'_3	C_2	C'_2	C''_2	σ_h	σ_v	$\sigma_{v'}$	$\sigma_{v''}$	S	S'	Point Symmetey
24	-.0079	B	1	1	1	1	1	1	1	1	1	1	1	A_1'
23	-.6293	B	1	1	1	1	1	1	1	1	1	1	1	A_1'
22	-.7314	N	0	0	0	0	-1	-1	0	0	1	0	0	
21	-.7314	N	0	0	0	-1	0	-1	0	1	0	0	0	
20	-.7482	N	1	1	1	1	1	-1	-1	-1	-1	-1	-1	A_1''
19	-.7962	A	1	1	-1	-1	-1	-1	1	1	1	-1	-1	A_2''
18	-.8762	N	0	0	0	-1	0	1	0	-1	0	0	0	
17	-.8762	N	0	0	0	0	-1	1	0	0	-1	0	0	
16	-.9186	N	0	0	0	-1	0	1	0	-1	0	0	0	
15	-.9186	N	0	0	-1	0	0	1	-1	0	0	0	0	
14	-.9200	N	0	0	0	-1	0	-1	0	1	0	0	0	
13	-.9200	N	0	0	0	0	-1	-1	0	0	1	0	0	
12	-.9501	N	1	1	-1	-1	-1	1	-1	-1	-1	1	1	A_2'
11	-1.0559	A	1	1	-1	-1	-1	-1	1	1	1	-1	-1	A_2''
10	-1.2542	N	0	0	-1	0	0	1	-1	0	0	0	0	

$(N-N)^{+1}$ β Spin

ORBITAL	E (a.u.)	1-4 Character	C_3	C'_3	C_2	C'_2	C''_2	σ_h	σ_v	σ_v'	σ_v''	S	S'	Point Symmetry
24	.0034	B	1	1	1	1	1	1	1	1	1	1	1	A_1'
23	-.2642	B	1	1	1	1	1	1	1	1	1	1	1	A_1'
22	-.6383	N	1	1	-1	-1	-1	-1	1	1	1	-1	-1	A_2''
21	-.7260	N	0	0	0	-1	0	-1	0	1	0	0	0	
20	-.7260	N	0	0	-1	0	0	-1	1	0	0	0	0	
19	-.7457	A	1	1	1	1	1	-1	-1	-1	-1	-1	-1	A_1''
18	-.8609	N	0	0	0	0	1	1	0	0	1	0	0	
17	-.8609	N	0	0	0	0	-1	1	0	0	-1	0	0	
16	-.9050	N	0	0	0	1	0	1	0	1	0	0	0	
15	-.9050	N	0	0	-1	0	0	1	-1	0	0	0	0	
14	-.9163	N	0	0	0	0	-1	-1	0	0	1	0	0	
13	-.9163	N	0	0	0	0	1	-1	0	0	-1	0	0	
12	-.9484	N	1	1	-1	-1	-1	1	-1	-1	-1	1	1	A_2'
11	-1.0482	A	1	1	-1	-1	-1	-1	1	1	1	-1	-1	A_2''
10	-1.2160	S	1	1	1	1	1	1	1	1	1	1	1	A_1'

$(N\text{-}N)^0$

ORBITAL	E (a.u.)	1-4 Character	C_3	C'_3	C_2	C'_2	C''_2	σ_h	σ_v	σ_v'	σ_v''	S	S'	Point Symmetry
24	.2250	A	1	1	-1	-1	-1	-1	1	1	1	-1	-1	A_2''
23	-.3604	B	1	1	1	1	1	1	1	1	1	1	1	A_1'
22	-.4885	N	1	1	0	1	0	-1	0	-1	0	0	0	
21	-.4885	N	0	0	0	-1	0	-1	0	1	0	0	0	
20	-.5039	A	1	1	-1	-1	-1	-1	1	1	1	-1	-1	A_2''
19	-.5264	N	1	1	1	1	1	-1	-1	-1	-1	-1	-1	A_1''
18	-.6317	N	0	0	-1	0	0	1	-1	0	0	0	0	
17	-.6317	N	0	0	0	-1	0	1	0	-1	0	0	0	
16	-.6791	N	0	0	-1	0	0	1	-1	0	0	0	0	
15	-.6791	N	0	0	0	0	1	1	0	0	1	0	0	
14	-.6796	N	0	0	0	-1	0	-1	0	1	0	0	0	
13	-.6796	N	0	0	0	0	-1	-1	0	0	1	0	0	
12	-.7294	N	1	1	-1	-1	-1	1	-1	-1	-1	1	1	A_2'
11	-.8154	A	1	1	-1	-1	-1	-1	1	1	1	-1	-1	A_2''
10	-.9900	B	1	1	1	1	1	1	1	1	1	1	1	A_1'

$(B\text{-}B)^{-2}$

ORBITAL	E (a.u.)	1-4 Character	C_3	C'_3	C_2	C'_2	C''_2	σ_h	σ_v	σ_v'	σ_v''	S	S'	Point Symmetry
24	.6523	N	0	0	-1	0	0	1	-1	0	0	0	0	
23	.6523	N	0	0	1	0	0	1	1	0	0	0	0	
22	.2597	B	1	1	1	1	1	1	1	1	1	1	1	A_1'
21	.0668	N	0	0	0	-1	0	-1	0	1	0	0	0	
20	.0668	N	0	0	1	0	0	-1	0	-1	0	0	0	
19	-1.404	A	1	1	-1	-1	-1	-1	1	1	1	-1	-1	A_2''
18	-.1412	N	1	1	1	1	1	-1	-1	-1	-1	-1	-1	A_1''
17	-.1512	N	0	0	0	0	1	1	0	0	1	0	0	
16	-.1512	N	0	0	-1	0	0	1	-1	0	0	0	0	
15	-.2123	N	0	0	0	-1	0	-1	0	1	0	0	0	
14	-.2123	N	1	1	0	1	0	-1	0	-1	0	0	0	
13	-.2821	N	0	0	0	0	-1	1	0	0	-1	0	0	
12	-.2821	N	0	0	0	-1	0	1	0	-1	0	0	0	
11	-.3479	N	1	1	-1	-1	-1	1	-1	-1	-1	1	1	A_2'
10	-.3670	B	1	1	1	1	1	1	1	1	1	1	1	A_1'

$(N\text{-}N)^{+2t}$ β Spin

ORBITAL	E (a.u.)	1-4 Character	C_3	C'_3	C_2	C'_2	C''_2	σ_h	σ_v	σ_v'	σ_v''	S	S'	Point Symmetry
24	-.2636	B	1	1	1	1	1	1	1	1	1	1	1	A_1'
23	-.4008	A	1	1	-1	-1	-1	-1	1	1	1	-1	-1	A_2''
22	-.4348	B	1	1	1	1	1	1	1	1	1	1	1	
21	-.9684	N	0	0	1	0	0	-1	-1	0	0	0	0	
20	-.9684	N	0	0	-1	0	0	-1	1	0	0	0	0	
19	-.9703	A	1	1	1	1	1	-1	-1	-1	-1	-1	-1	A_1''
18	-1.1030	N	0	0	0	1	0	1	0	1	0	0	0	
17	-1.1030	N	0	0	0	-1	0	1	0	-1	0	0	0	
16	-1.1516	N	0	0	0	-1	0	-1	0	1	0	0	0	
15	-1.1516	N	0	0	0	1	0	-1	0	-1	0	0	0	
14	-1.776	N	0	0	0	1	0	1	0	1	0	0	0	
13	-1.776	N	0	0	1	0	0	1	1	0	0	0	0	
12	-1.1891	N	1	1	-1	-1	-1	1	-1	-1	-1	1	1	A_2'
11	-1.2703	A	1	1	-1	-1	-1	-1	1	1	1	-1	-1	A_2''
10	-1.4047	N	1	1	1	1	1	1	1	1	1	1	1	A_1'

$(B\text{-}B)^{-1}$ α Spin

ORBITAL	E (a.u.)	1-4 Character	C_3	C'_3	C_2	C'_2	C''_2	σ_h	σ_v	σ_v'	σ_v''	S	S'	Point Symmetry
24	.4484	N	0	0	-1	0	0	1	-1	0	0	0	0	
23	.4484	N	0	0	1	0	0	1	1	0	0	0	0	
22	.0185	B	1	1	1	1	1	1	1	1	1	1	1	A_1'
21	-.1562	N	0	0	0	0	1	-1	0	0	-1	0	0	
20	-.1562	N	0	0	1	0	0	-1	-1	0	0	0	0	
19	-.3461	N	1	1	1	1	1	-1	-1	-1	-1	-1	-1	A_1''
18	-.3692	A	1	1	-1	-1	-1	-1	1	1	1	-1	-1	A_2''
17	-.3699	N	0	0	-1	0	0	1	-1	0	0	0	0	
16	-.3699	N	0	0	0	0	1	1	0	0	1	0	0	
15	-.4242	N	0	0	0	0	-1	-1	0	0	1	0	0	
14	-.4242	N	0	0	0	0	1	-1	0	0	-1	0	0	
13	-.4936	N	0	0	0	0	-1	1	0	0	-1	0	0	
12	-.4936	N	0	0	-1	0	0	1	-1	0	0	0	0	
11	-.5975	N	1	1	-1	-1	-1	1	-1	-1	-1	1	1	A_2'
10	-.6051	B	1	1	1	1	1	1	1	1	1	1	1	A_1'

$(B\text{-}B)^{-1}$ β Spin

ORBITAL	E (a.u.)	1-4 Character	C_3	C'_3	C_2	C'_2	C''_2	σ_h	σ_v	σ_v'	σ_v''	$'s$	s'	Point Symmetry
24	-.4548	N	0	0	0	1	0	1	0	1	0	0	0	
23	-.4548	N	0	0	1	0	0	1	1	0	0	0	0	
22	-.3215	B	1	1	1	1	1	1	1	1	1	1	1	A_1'
21	-.1535	N	0	0	0	0	1	-1	0	0	-1	0	0	
20	-.1535	N	0	0	0	0	-1	-1	0	0	1	0	0	
19	-.3392	N	1	1	1	1	1	-1	-1	-1	-1	-1	-1	A_1''
18	-.3502	A	1	1	-1	-1	-1	-1	1	1	1	-1	-1	A_2''
17	-.3660	N	0	0	1	0	0	1	1	0	0	0	0	
16	-.3660	N	0	0	-1	0	0	1	-1	0	0	0	0	
15	-.4181	N	0	0	0	0	-1	-1	0	0	1	0	0	
14	-.4181	N	0	0	0	0	1	-1	0	0	-1	0	0	
13	-.4803	N	0	0	0	0	-1	1	0	0	-1	0	0	
12	-.4803	N	0	0	-1	0	0	1	-1	0	0	0	0	
11	-.5530	N	1	1	-1	-1	-1	1	-1	-1	-1	1	1	A_2'
10	-.5884	B	1	1	1	1	1	1	1	1	1	1	1	A_1'

$(B\text{-}B)^0$

ORBITAL	E (a.u.)	1-4 Character	C_3	C'_3	C_2	C'_2	C''_2	σ_h	σ_v	σ_v'	σ_v''	S	S'	Point Symmetry
24	.2452	N	0	0	-1	0	0	1	-1	0	0	0	0	
23	.2383	A	1	1	-1	-1	-1	-1	1	1	1	-1	-1	A_2''
22	.0790	B	1	1	1	1	1	1	1	1	1	1	1	A_1'
21	-.3798	N	0	0	0	-1	1	-1	0	1	0	0	0	
20	-.3798	N	0	0	1	0	0	-1	0	-1	0	0	0	
19	-.5483	N	1	1	1	1	1	-1	-1	-1	-1	-1	-1	A_1''
18	-.5483	A	1	1	-1	-1	-1	-1	1	1	1	-1	-1	A_2''
17	-.5852	N	0	0	-1	0	0	1	-1	0	0	0	0	
16	-.5852	N	0	0	1	0	0	1	1	0	0	0	0	
15	-.6363	N	0	0	-1	0	0	-1	1	0	0	0	0	
14	-.6363	N	0	0	0	-1	0	-1	0	1	0	0	0	
13	-.6952	N	0	0	0	1	0	1	0	1	0	0	0	
12	-.6952	N	0	0	0	-1	0	1	0	-1	0	0	0	
11	-.7626	N	1	1	-1	-1	-1	1	-1	-1	-1	1	1	A_2'
10	-.8335	B	1	1	1	1	1	1	1	1	1	1	1	A_1'

$(B\text{-}N)^0$

ORBITAL	E (a.u.)	1-4 Character	C_3	C'_3	C_2	C'_2	C''_2	σ_h	σ_v	σ_v'	σ_v''	S	S'	Point Symmetry
24	.2323	N	0	0					0	0	-1			
23	.1975	A	1	1					1	1	1			A_1
22	-.3974	B	1	1					1	1	1			A_1
21	-.4064	N	0	0					-1	0	0			
20	-.4064	N	0	0					0	0	0			
19	-.5458	N	1	1					-1	-1	-1			A_2
18	-.6086	N	0	0					0	-1	0			
17	-.6086	N	0	0					0	1	0			
16	-.6509	B	1	1					1	1	1			A_1
15	-.6758	N	0	0					1	0	0			
14	-.6758	N	0	0					-1	0	0			
13	-.7275	N	0	0					0	-1	0			
12	-.7275	N	0	0					0	1	0			
11	-.7589	N	1	1					-1	-1	-1			A_2
10	-.9231	B	1	1					1	1	1			A_1

$(C\text{-}N)^{+1}$ α Spin

ORBITAL	E (a.u.)	1-4 Character	C_3	C'_3	C_2	C'_2	C''_2	σ_h	σ_v	σ_v'	σ_v''	S	S'	Point Symmetry
24	-.2941	A	1	1					1	1	1			A_1
23	-.3414	A	1	1					1	1	1			A_1
22	-.9396	N_B	0	0					-1	0	0			
21	-.9396	N	0	0					0	0	1			
20	-.9436	B	1	1					1	1	1			A_1
19	-.9740	N	1	1					-1	-1	-1			A_2
18	-1.0885	N	0	0					0	1	0			
17	-1.0885	N	0	0					0	0	1			
16	-1.1463	N	0	0					0	0	0			
15	-1.1463	N	0	0					0	0	0			
14	-1.1977	N	1	1					-1	-1	-1			A_2
13	-1.2004	N	0	0					0	0	0			
12	-1.2004	N	0	0					0	0	1			
11	-1.2213	N	1	1					1	1	1			A_1
10	-1.4719	N_B	0	0					0	0	0			

$(C\text{-}N)^{+1}$ β Spin

ORBITAL	E (a.u.)	1-4 Character	C_3	C'_3	C_2	C'_2	C''_2	σ_h	σ_v	σ_v'	σ_v''	S	S'	Point Symmetry
24	-.2706	A	1	1					1	1	1			A_1
23	-.2908	A	1	1					1	1	1			A_1
22	-.4911	B	1	1					1	1	1			A_1
21	-.9347	N	0	0					0	1	0			
20	-.9347	B	0	0					0	0	0			
19	-.9718	N	1	1					-1	-1	-1			A_2
18	-1.0774	N	0	0					0	0	1			
17	-1.0774	N	0	0					0	0	-1			
16	-1.1368	N	0	0					0	0	0			
15	-1.1368	N	0	0					0	0	0			
14	-1.1916	N	0	0					1	0	0			
13	-1.1916	N	0	0					0	0	0			
12	-1.1963	N	1	1					-1	-1	-1			A_2
11	-1.2077	N	1	1					1	1	1			A_1
10	-1.4179	B	1	1					1	1	1			

$(B\text{-}C)^{+1}$ α Spin

ORBITAL	E (a.u.)	1-4 Character	C_3	C'_3	C_2	C'_2	C''_2	σ_h	σ_v	σ_v'	σ_v''	S	S'	Point Symmetry
24	-.2138	A	1	1					1	1	1			A_1
23	-.2328	A	1	1					1	1	1			A_1
22	-.4500	B	1	1					1	1	1			A_1
21	-.8599	A	0	0					0	0	1			
20	-.8753	A	0	0					0	0	-1			
19	-.9716	A	1	1					-1	-1	-1			A_2
18	-1.0488	B	0	0					0	0	0			
17	-1.0571	A	0	0					0	0	-1			
16	-1.0855	A	0	0					0	0	0			
15	-1.0953	A	0	0					0	0	0			
14	-1.1000	A	0	0					0	0	1			
13	-1.1555	B	0	0					0	0	0			
12	-1.1641	B	0	0					0	0	-1			
11	-1.2020	B	1	1					-1	-1	-1			A_2
10	-1.3570	B	0	0					0	0	1			

$(B\text{-}C)^{+1}$ β Spin

ORBITAL	E (a.u.)	1-4 Character	C_3	C'_3	C_2	C'_2	C''_2	σ_h	σ_v	σ_v'	σ_v''	S	S'	Point Symmetry
24	-.2062	A	1	1					1	1	1			A_1
23	-.2232	A	1	1					1	1	1			A_1
22	-.4459	B	1	1					1	1	1			A_1
21	-.5867	A	0	0					0	0	0			
20	-.8520	A	0	0					0	0	1			
19	-.9548	A	1	1					-1	-1	-1			A_2
18	-1.0310	B	0	0					0	0	0			
17	-1.0395	A	0	0					0	0	0			
16	-1.0567	A	0	0					0	0	0			
15	-1.0818	A	0	0					0	0	-1			
14	-1.0858	A	0	0					0	0	1			
13	-1.1346	B	0	0					0	0	-1			
12	-1.1533	B	0	0					0	0	0			
11	-1.1930	B	1	1					-1	-1	-1			A_2
10	-1.3533	B	0	0					0	0	1			

BIBLIOGRAPHY

Allinger, N. L.; Freiberg, L. A. J. Amer. Chem. Soc. 1960, 82, 2393; 1966, 88, 2999.

Altman, J.; Babad, E.; Itzchaki, J.; Ginsburg, D. Tetrahedron Suppl. 1966, Part 1, 8, 279.

Baker, F. W.; Holtz, H. D.; Stock, L. M. J. Org. Chem. 1963, 28, 514.

Bingham, R.; Dewar, M.J.S.; Lo, D. H. Ibid. 1975, 97, 1285.

Borden, W. T.; Reich, I. L.; Sharpe, L. A.; Reich, H. J. J. Amer. Chem. Soc. 1970, 92, 3808.

Bulkin, B. J.; Dill, K.; Dannenberg, J. J. Anal. Chem. 1971, 43, 974.

Castaneda, F. F. Ph.D Thesis, University of California, Berkeley, 1970.

Chatt, J.; Venazi, L. M. J. Chem. Soc. 1957, 4735.

Dannenberg, J. J.; Prociv, T. M. J.C.S. Chem. Comm. 1973, 291.

Dannenberg, J. J.; Prociv, T. M. J. Am. Chem. Soc. 1974, 96, 913.

Dewar, M.J.S.; Wade, L. E Ibid. 1973, 95, 5121.

Dewar, M.J.S.; et al. J. Amer. Chem. Soc. 1974, 96, 5242.

Dewar, M.J.S.; Gordberg, R. S. Ibid. 1970, 92, 1582.

Eaton, P. E. 155th National Meeting of the American Chemical Society, San Francisco, CA, April, 1968, p. 1.

Eaton, P. E.; Temme, G. H., III Ibid. 1973, 95, 7508.

Franklin, J. L. Ind. Eng. Chem. 1949, 41, 1070.

Fridrich, I.; Gast, L. E. J. Amer. Oil Chem. Soc. 1967, 44 (2), 110-12.

Fry, J. L.; Engler, E. M.; Schleyer, P.v.R. Ibid. 1972, 94, 4628.

Gajewsky, J. J.; Hoffman, L. K.; Shih, C. N. J. Amer. Chem. Soc. 1974, 96, 3705, and personal communications.

Ginsberg, D. Accts. Chem. Res. 1972, 5, 249.

Ginsberg, D. Accts. Chem. Res. 1969, 2, 121.

Goldstein, M. J.; Benzon, M. S. Ibid. 1972, 94, 5119; 1972, 94, 7147

Greenwald, R.; Chaykovsky, M.; Corey, E. J. J. Org. Chem. 1963, 28, 1128.

Grob, C. A.; Schiess, P. W. Agnew Chem., 1967, 79, 1.

Grob, C. A. Ibid. 1969, 81, 543.

Hoffman, R. Accts. Chem. Res. 1971, 4, 1.

Hoffman, R.; Swaminathan, S.; Odell, B. G.; Gleiter, R. J. Amer. Chem. Soc. 1970, 92, 7091.

Hoffman, R.; Stohrer, W. J. Amer. Chem. Soc. 1972, 94, 779.

Hoffman, R.; Stohrer, W. XXIII International Congress of Pure and Applied Chemistry, Special Lecture; Butterworth, London.

Holtz, H. D.; Stock, L. M. J. Amer. Chem. Soc. 1963, 86, 5183.

Lambert, A. J. Amer. Chem. Soc. 1967, 89, 1836.

Lantenshlaeger, F., Wright, C. F. Can. J. Chem. 1963, 41, 1972.

Lerman, L.; Liberman, M. Dokladu Aka. Nauk, SSR. 1971, 201 (1), 115.

Maciel, G. E.; Dorn, H. C. J. Amer. Chem. Soc. 1971, 93, 1268.

Mori, A.; Tzuzuki, B. Bull. Chem. Soc. Jap. 1966, 39 (11), 2454-8.

Newton, M. D.; Schulman, J. M. J. Amer. Chem. Soc. 1972, 94, 4391.

Olah, G.; Schleyer, P.v.R.; Dewar, M.J.S. J. Am. Chem. Soc. 1973, 95, 6829.

Pople, J. A.; Beveridge, D. L.; Dobosch, P. A. J. Chem. Phys. 1967, 47, 2026.

Roberts, J. D.; Moreland, W. T., Jr.; Frazer, W. Ibid. 1953, 75, 637.

Schlosser, M.; Christmann, K. F. Ang. Chemie. Int. Ed. 1964, 3, 636.

Snyder, E. I. J. Amer. Chem. Soc. 1970, 92, 7529.

Srinivasan, R. J. Amer. Chem. Soc. 1964, 86, 3318.

Turro, N. J. Molecular Photochemistry, W. A. Benjamin, Inc., New York, 1965, p. 119.

Wasserman, E. Bell Laboratories, personal communication.

Wiberg, K. B.; Burgmaier, G. J. J. Amer. Chem. Soc. 1976, 94, 7396.

Wiberg, K. B.; Burgmaier, G. J. Tet. Letters 1969, 317.

Wiberg, K. B.; Epling, G. A.; Jason, M. Ibid. 1974, 96, 912.

Witting, G.; Schoellkopf, U. Org. Syn. 1940, 40, 66.